ADDIS ABABA UNIVERSITY
ADDIS ABABA INSTITUTE OF TECHNOLOGY
SCHOOL OF CIVIL AND ENVIRONMENTAL ENGINEERING

Application of a Rigorous Subgrade Model in the Analysis of Rectangular Plates on an Elastic Foundation Using Finite Difference Method

By:

Tofik Seid Habib

2019

Addis Ababa, Ethiopia

ADDIS ABABA UNIVERSITY
ADDIS ABABA INSTITUTE OF TECHNOLOGY
SCHOOL OF CIVIL AND ENVIRONMENTAL ENGINEERING

Application of a Rigorous Subgrade Model in the Analysis of Rectangular Plates on an Elastic Foundation Using Finite Difference Method

By:

Tofik Seid Habib

Advisor: **Dr.-Ing Asrat Worku**

A Thesis Submitted to Addis Ababa Institute of Technology in partial fulfillment of the requirements for the Degree of Master of Science in Geotechnical Engineering

2019

Addis Ababa, Ethiopia

The undersigned have examined the thesis entitled '**Application of a Rigorous Subgrade Model in the Analysis of Rectangular Plates on an Elastic Foundation Using Finite Difference Method**' presented by **Tofik Seid**, a candidate for the degree of Master of Science and hereby certify that it is worthy of acceptance.

____________________	____________________	____________________
Advisor	Signature	Date
____________________	____________________	____________________
External Examiner	Signature	Date
____________________	____________________	____________________
Internal Examiner	Signature	Date
____________________	____________________	____________________
Chairman	Signature	Date

UNDERTAKING

I certify that the research work titled **"Application of a Rigorous Subgrade Model in the Analysis of Rectangular Plates on an Elastic Foundation Using Finite Difference Method "** is my own work. The work has not been presented elsewhere for assessment. Where material has been used from other sources, it has been properly acknowledged.

Name: Tofik Seid

Signature: ___________________

Advisor: Dr-Ing Asrat Worku

Signature: ___________________

Acknowledgment

First, I would like to give my thanks to the Ethiopian Roads Authority (ERA) Scholarship Program for granting me a scholarship to pursue the Master's Program in Addis Ababa Institute of Technology. Secondly, I would like to pay owed gratitude to my advisor, Dr-Ing. Asrat Worku for his excellent tuition, valuable advice, constructive comments, productive guidance, and endless patience throughout the study. I would also like to thank all my friends for their assistance and encouragement throughout my work. Finally, yet importantly, I wish to express my appreciation to my wife Dr. Semira and my family for their understanding and patience during my study.

TABLE OF CONTENTS

LIST OF FIGURES

LIST OF TABLES

LIST OF SYMBOLS AND ABBREVIATION

AAU: Addis Ababa University

B: Plate width

D: Flexural rigidity of a plate

DE: Differential equation

E_p : Modulus of elasticity of a plate

E_s : Modulus of elasticity of a soil

FDM: Finite difference method

FE: Finite element

FEM: Finite element method

G_s : Shear modulus of an elastic medium

G : Shear modulus of a plate

G_k : Kerr's shear layer constant with units of kN/m

G_p : Pasternak's shear layer constant with units of kN/m

H: Thickness of a stratum

h_p : Plate thickness

L: Plate length

k_p : Spring coefficient in Pasternak's model with units of kN/m^3

k_{Kl} : Kerr's lower spring layer constant with units of kN/m^3

k_{Ku} : Kerr's upper spring layer constant with units of kN/m^3

k_w : Modulus of subgrade reaction with units of kN/m^3

M_x, M_y : Moment about y and x-axis, respectively

ODE: Ordinary differential equation

P: Applied concentrated vertical load

$p(x, y)$: Distributed bearing pressure on the plate

PDE: Partial differential equation

PEF: Plate on elastic foundation

$q(x, y)$: Applied distributed load

T: Applied tension force on a Filonenko-Borodich model

Kr: Relative rigidity of the soil-plate system

R_x, R_y: Fictitious edge reactions, due to interactions in foundation and plate

R_{xy}: Fictitious plate corner reaction due to interaction in the foundation

SSI: Soil-structure interaction

w_c: Deflection of plate corner

$w_F(x, y)$: Vertical displacement of foundation surface beyond plate edges

$w_{m,n}$: Nodal deflection of the plate

w_L, w_B : Deflections of the plate along long and short edges, respectively

x, y, z: Cartesian coordinate system

u: Displacement in the x-direction

V_x, V_y: Shear force per unit length in the x and y-axis, respectively

Q_x, Q_y: Transverse shear force per unit length of the plate in the x and y-axis, respectively

N_x, N_y: Shear forces per unit length of the soil medium in the x and y-axis, respectively

v : Displacement in the y-direction

w : Displacement in the z-direction

σ : Normal stress

τ : Shear stress

ε : Strain

χ : Adjustment factor

ν_p : Poisson's ratio of a soil

ν_s : Poisson's ratio of a plate

$[C]$: Coefficient matrix of the plate

$\{q\}_{m,n}$: Vector of nodal loads

$\{q\}$: Vector of nodal loads on the whole system

$\{\ \}$: Column matrix

$[\ ]$: Matrix

ABSTRACT

Plate on elastic foundation establishes an adequate idealization in the analysis of shallow foundations, which includes isolated footings, combined footings, mat foundations, and flexible pavement. The important issue in the analysis is modeling the contact between the plate and the soil medium that is a soil-structure interaction (SSI) problem. The primary difficulty in the analysis of the soil–structure interaction lies in the determination of the contact pressure. The simplest subgrade model is the single parameter Winkler mechanical model, which represents the foundation soil by a series of independent springs. Winkler model is widely used and practiced in spite of its deficiency in representing the continuous behavior of real soils. Later, many advanced mechanical subgrade models have been proposed in order to improve on the inherent lack of shear interaction among the individual springs. However, these models still have their drawbacks in that they do not represent the subgrade shear interaction adequately. With the objective to improve on such drawbacks, a generalized continuum-based model has been recently proposed by Worku. This generalized subgrade model satisfies the fundamental elastic laws and all the boundary conditions since it is derived by considering all stress, strain and displacement components.

The main objective of this work is to implement and calibrate the generalized continuum based subgrade model for the analysis of rectangular plates on an elastic foundation. The governing differential equation of a rectangular plate that incorporates Pasternak type subgrade model is formulated. Thus, an ordinary finite difference method is developed to solve the partial differential equations. Code based on MATLAB® programming language is written for determining deflections and internal actions of the plate. Finite Element based software is used as a tool to determine an adjustment factor for the generalized model. Finally, the proposed method has been validated by comparing the results with other numerical models for selected loading conditions. The results of the comparison show that the generalized model shows an excellent agreement with the FE outputs and capable of predicting the behavior of the rectangular plates on elastic foundations.

1. Introduction

1.1. Background

Shallow foundations are the most economical and popular structures that are used to transfer the load of the superstructure to the soil on which it is resting. Shallow foundations are usually idealized as beams (one dimensional in a plan such as spread footings, combined footings, strap footings, wall footings, etc.) or plates (two-dimensional in plan supporting several loads from columns and walls of footings such as mat foundation). One of the important and difficult issues in the analysis is modeling the contact between the structural and soil elements, which is a typical soil-structure interaction (SSI) problem. Numerous efforts have been made to improve the design and analysis of such foundations to optimize both the modeling of the soil media as well as the simulation of the interaction between soil and foundation (Wang, 2005).

Different subgrade models have been developed to account for soil-structure interaction (SSI) effect in the analysis of the foundation. Two approaches have been widely used: continuum and mechanical representations. Winkler (1867) subgrade model is the first classical mechanical model, which represents the subgrade using mutually independent mechanical elastic spring elements with spring constant k_w. One of the drawbacks of this model is that the deflection of the soil medium at any point on the surface is directly proportional to the load applied at that point and independent of the deflection at other locations (Wang, 2005). To overcome such shortcoming, multiple-parameter models introducing additional elements to ensure interaction among the springs were proposed (Filonenko-Borodich, 1950; Hetenyi, 1950; Pasternak, 1954; Kerr, 1964). Difficulty in determining the model parameter is the major drawback of mechanical models in general, for they cannot be directly determined from model tests.

In contrast, elastic continuum models idealize the subgrade as a homogeneous isotropic layer of linear-elastic material of finite thickness overlying a rigid base (Reissner, 1958; Kerr, 1964; Vlasov and Leont'ev, 1966; Kerr and Rhines, 1967; Selvadurai, 1979; Horvath, 2002; Worku, 2010). Continuum subgrade model development involves three parameters consisting of the elastic modulus and the Poisson's ratio, which are easily determined from tests, and the layer thickness. Most continuum models make arbitrary simplifying assumptions to ease the mathematical work involved. In general, the key drawbacks of such models include the sensitivity of the results to the layer thickness and the difficulty to implement using available commercial software.

Synthesis of the two approaches has the advantage of using the strengths of both subgrade models. It involves quantifying the mechanical model parameters in terms of the known parameters of the continuum model by directly equating corresponding terms of compatible models (Horvath, 2002; Worku, 2013).

Recently Worku (2010) proposed a generalized continuum subgrade model. The model approaches the problem by addressing the shortcomings of the previous continuum subgrade models. Without making simplifying assumptions, all stress, strain, and displacement components are fully accounted for. The proposed model has application in the analysis of beams and plates on elastic foundations. Further studies have been conducted on the adjustment of parameters and analysis of beams, strip plates, and circular plates using the generalized continuum subgrade model.

Based on this same model, the present study attempts to analyze the bending of rectangular plates resting on a Kerr-equivalent Pasternak type model using the finite difference method (FDM). Parameters for the Kerr-equivalent Pasternak-type model estimated with the use of the devolved generalized continuum subgrade model are employed. The study provides adjustment factor for the model and compares results with the particular finite element (FE) based modeling software selected for this purposes.

1.2. Objective

1.2.1. General Objective

The main objective of this study is to make use of a newly developed generalized continuum based subgrade model in the analysis of rectangular plates on an elastic foundation. The finite difference method (FDM) is employed since analytical solutions are too difficult and cumbersome. Moreover, the work aims at using finite element (FE) based software analysis results to adjust and compare the results with the new subgrade model.

1.2.2. Specific objectives

The specific objective of this study is

- To provide a complete analysis of a rectangular plate, which includes deflection, bending moments, and shear forces for various loading cases by employing the new Kerr-equivalent Pasternak-type model.
- To develop a finite difference method (FDM) program package using MATLAB®.
- To adjust the model parameters sensitivity to the stratum thickness for the various factors influencing the response such as aspect ratio, relative rigidity, and loading type, etc.
- To verify the results using the finite element (Plaxis 3D) results.

1.3. Scope of the study

The study is limited to the analysis of rectangular thin plate of constant thickness subjected to selected common and practical loadings. This work does not include analysis of a plate with holes and some irregularities, and shapes like circular, annular, and skew plates. The foundation is also assumed as a homogeneous elastic stratum.

1.4. Methodology

This thesis has been divided into three parts. The first part comprises a pertinent literature review including the latest studies conducted on both mechanical and continuum based subgrade models. In addition, theories and computational methods of elastic plates are briefly presented.

The second part of the study contains formulation and analysis of the differential equations of rectangular plate on an elastic foundation. Numerical and analytical methods are used to solve the partial differential equations. Furthermore, computer code is written to provide a fast and timesaving method of solution. The MATLAB® package is created for the purpose of determining deflections, bending moments, shear forces, and subgrade reaction.

The last part deals with adjusting Worku's generalized continuum-based subgrade models. FE based software, Plaxis 3D, is employed to adjust the model and evaluate the results of the solution method developed. Subsequently, the numerical results obtained for rectangular plates are compared with finite element method results.

1.5. Organization

This document is organized into five chapters. The first chapter deals with the background of the study, objective, scope, and methodology employed. The second chapter briefly reviews the major literature works related to existing subgrade models, plate theories and the computational techniques. The third chapter deals with the analysis of rectangular plates on an elastic foundation. In this part of the study, both the formulation and solution of the governing differential equations of the plate using a two-parameter subgrade model are discussed. In the fourth chapter, Worku's generalized continuum-based subgrade model is adjusted using the FE-based software results and comparison of results between the calibrated model and Plaxis 3D is made. Finally, the fifth chapter presents the conclusions drawn and the recommendations for further study.

2. Literature review

2.1. Introduction

The analysis of the interaction between structural elements such as beams, plates, or shells and the elastic foundation is of great importance to several geotechnical problems including, the analysis foundations of buildings, geotechnical, highway, airport runways, and railway structures. One of the functional requirements is to reduce the deflection and stresses of such plates, which is achieved by using appropriate models.

The problem of a plate on an elastic foundation may be viewed as composed of three components:

1. the soil medium
2. the plate, and
3. the interaction between the two media.

2.2. The soil medium

Every engineering structure, whether it is a building, bridge, highway pavement or railway track are designed to be supported by the soil or rock below as the case may be. Within a limited degree of uncertainty, the foundation structure can be characterized relatively well in comparison with that of the underlying soil or rock. This is because the properties of structural materials are well known (Fai, 1988).

In contrast, the nature and distribution of the underlying soil and rock cannot be represented precisely. However, since of interest here is the response of the soil medium at the contact area and not the stresses or displacements inside the soil medium, the problem reduces to finding a relatively simple mathematical expression, which should describe the response of the subgrade at the contact area with a reasonable degree of accuracy (Kerr, 1964).

Because of the complexity of soil behavior, the subgrade in soil-foundation interaction problems is replaced by a much simpler system called subgrade model (Sadrekarimi and Ghamari, 2008). Subgrade models are physically close and mathematically simple but sufficiently accurate models to represent the soil media in the soil–structure interaction problems (Dutta and Roy, 2002).

Assuming a linear elastic, homogeneous and isotropic behavior of the soil subgrade models are commonly developed following two approaches:

1. Mechanical approach, and

2. Continuum approach.

2.2.1. Mechanical Models

Mechanical foundation models are devised by assembling a few mechanical elements like spring beds and shear elements such as pure-shear plates, pure-flexural plates, or membranes under uniform tension in various arrangements to simulate the subgrade behavior. The development of these models starts with the simplest mechanical model, the Winkler model, and assumes various kinds of interaction between the independent springs in order to bring it closer to reality. Depending on the number of parameters used to describe the foundation behavior, mechanical models may be categorized as single-parameter, two-parameter, and three-parameter (Worku, 2010).

2.2.1.1. Winkler Single Parameter Model

The simplest and most frequently used mechanical model is the one devised by Winkler (1867), in which the subgrade is modeled as a series of closely spaced, mutually independent, linear elastic vertical springs. In this model, the properties of the soil are described only by the parameter k_w, which represents the stiffness of the vertical spring.

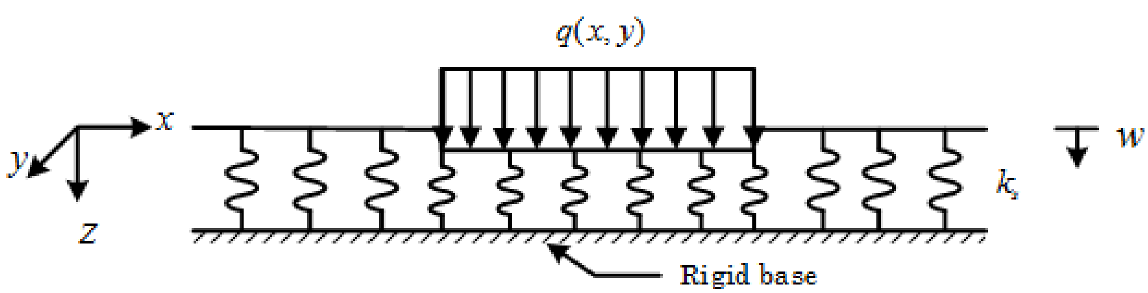

Figure 2.1: Winkler's foundation model

Winkler assumes that the contact pressure at any point is proportional to the deflection of the soil medium at that point and independent of the deflection at other locations. Mathematically, it can be written as

$$p(x,y)=k_w w(x,y) \tag{2.1}$$

Where $p(x,y)$ is the contact pressure, $w(x,y)$ is the vertical surface deflection, and k_w is coefficient or modulus of subgrade reaction with units of force per length cubed.

Because of its simple mathematical formulation, Winkler model can be easily employed in a variety of problems and readily incorporated into standard computer programs for structural analysis. However, it has drawbacks that this type of soil model has the discontinuous behavior of the surface displacement and the effect of interaction (shear coupling) between springs is not considered.

The other fundamental problem associated with the use of this model is the difficulty in the determination of the stiffness of the elastic springs. This is because the modulus of subgrade reaction is not a fundamental soil property but also varies with the foundation type, foundation dimension, and type of loading (Poulos, 2018).

2.2.1.2. Two-Parameter Models

Recognizing the inherent problems with the Winkler model, several researchers attempted to make the model more realistic by introducing some form of interaction among the spring elements that represent the soil continuum. This can be achieved by adding a second element that interacts with the spring elements in the form of elastic membranes, elastic beams, or elastic layers capable of transferring pure shearing deformation. These elements bring about another parameter to the subgrade model in addition to the coefficient of subgrade reaction.

Filonenko-Borodich (1945) developed a model, which achieves continuity between the individual spring elements in the Winkler model by connecting the springs by a thin elastic membrane under constant tension, T (Figure 2.2). In this model, the subgrade reaction is given by

$$p(x,y)=k_p w(x,y)-T\nabla^2 w(x,y) \tag{2.2}$$

Where ∇^2 is Laplace operator in x and y-direction.

The two elastic constants necessary to characterize the model are k_p and T; however, no method is provided for the computation of k_p or T.

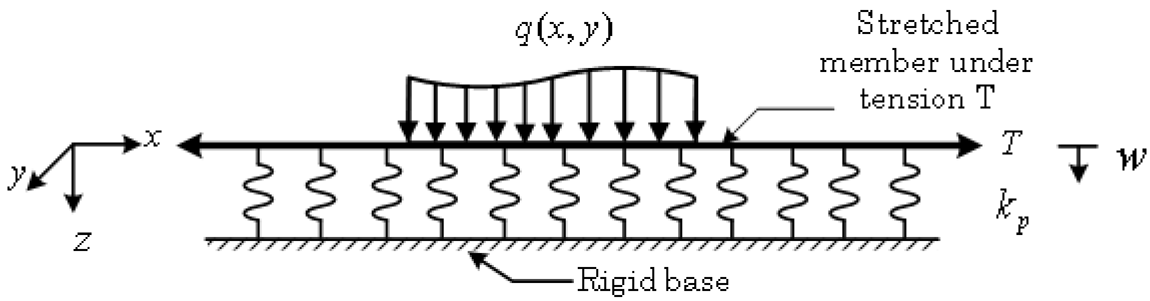

Figure 2.2: Filonenko-Borodich's model

Hetenyi (1946) proposed a model incorporating a purely flexural elastic plate with flexural rigidity, D, to represent the interaction between the independent, linear spring elements. According to this model, the subgrade reaction is given by:

$$p(x,y)=k_p w(x,y)-D\bar{\nabla}^4 w(x,y) \tag{2.3}$$

Where D is the flexural rigidity of the elastic plate

$\bar{\nabla}^4=\frac{\partial^4}{\partial x^4}+\frac{\partial^4}{\partial y^4}$; Note that this operator is different from the bi-harmonic operator, which is

$$\nabla^4(*)=\nabla^2\nabla^2(*)=\frac{\partial^4(*)}{\partial x^4}+\frac{\partial^4(*)}{\partial x^2\partial y^2}+\frac{\partial^4(*)}{\partial y^4}.$$

Pasternak (1954) improved the Winkler model by connecting the ends of the springs to a shear layer consisting of incompressible, vertical elements, which can deform only by transverse shear (Figure 2.3). According to this model, the subgrade reaction is given by:

$$p(x,y)=k_p w(x,y)-G_p\nabla^2 w(x,y) \tag{2.4}$$

Where G_p is the shear parameter of the layer. It can be seen that this equation is identical with Equation (2.2) if T is replaced by G_p.

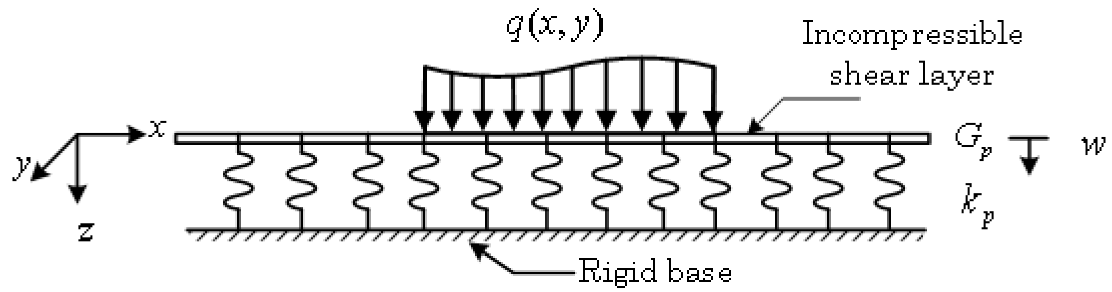

Figure 2.3: Pasternak's model

2.2.1.3. Three-Parameter Models

The three-parameter models constitute a generalization of two-parameter models; the third parameter is introduced with the intention of making them more realistic. Among the three parameter model, the Kerr model is the most widely known. Kerr modified Pasternak's model by introducing the second bed of springs on top of the shear layer as shown in (Figure 2.4), with the intention of representing an improved shear interaction among the springs (Worku, 2013).

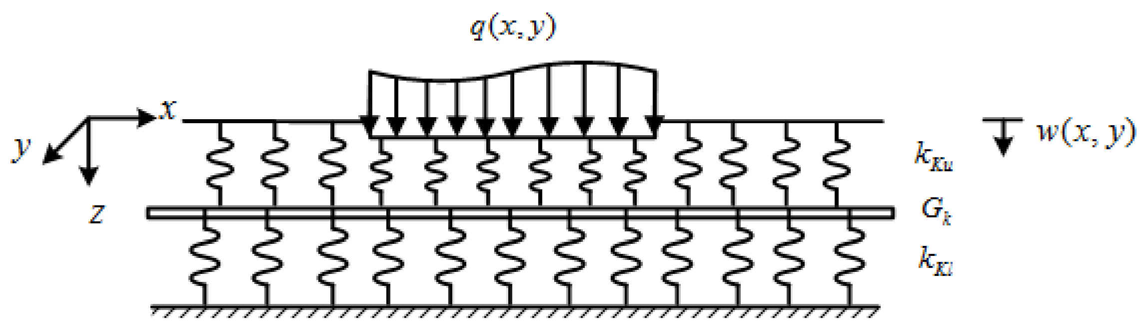

Figure 2.4: Kerr's (or modified Pasternak) model

Kerr derived the mathematical relationship that describes his model as

$$p(x,y)-\frac{G_K}{(k_{Ku}+k_{Kl})}\nabla^2 p(x,y)=\frac{k_{Ku}k_{Kl}}{(k_{Ku}+k_{Kl})}w(x,y)-\frac{G_K k_{Kl}}{(k_{Ku}+k_{Kl})}\nabla^2 w(x,y) \tag{2.5}$$

Where k_{Ku} and k_{Kl} are stiffness per unit area of the upper and lower spring beds, respectively; G_K is the coefficient of the shear element in the model with the dimension of force per unit length.

2.2.2. Continuum models

On soil media surface deflection is not only occurring immediately under the loaded region but also within certain limited zones beyond the loaded region. Elastic continuum models typically idealize the subgrade as a layer overlying a rigid base which involves elastic modulus, Poisson's ratio, and layer thickness parameters. In most continuum models, arbitrary assumptions are made concerning selected stress, strain, and displacement parameters as well as compatibility to produce a material with behavioral approximations built into it.

Reissner (1958) proposed a subgrade model derived by introducing displacement and stress constraints and making certain simplifying assumptions concerning the stress developed within an isotropic, homogeneous, linear-elastic continuum of finite thickness as a result of applied surface stress. Assuming the in-plane stresses (in the x, y plane) throughout a soil layer of thickness H are zero, Reissner derived the resulting second order differential equation as

$$p-\frac{H^2 G_s}{12 E_s}\nabla^2 p=\frac{E_s}{H}w-\frac{G_s H}{3}\nabla^2 w \tag{2.6}$$

Where G_s is the shear modulus of the elastic continuum, E_s is Young's modulus of the subgrade, p is the load intensity at the interface, and H is the subgrade thickness.

Vlasov and Leont'ev (1966) proposed a model of soil response, which is a type of two-parameter elastic model derived by introducing displacement constraints that simplify the basic equations for linear elastic isotropic continuum. In addition to neglecting the horizontal deformations, this model further imposes a deformation mode shape, $\phi(z)$, which is determined by applying the principle of minimum potential energy in the foundation-soil system. The resulting differential equation is given by

$$p(x,y)=k_v w(x,y)-G_v\nabla^2 w(x,y) \tag{2.7}$$

Where,

$$\begin{aligned} k_v &= \bar{E}\int_0^H \phi^2 dz \\ G_v &= G_s\int_0^H \phi^2 dz \end{aligned} \tag{2.8a}$$

$$\bar{E} = \frac{1-\nu_s}{(1+\nu_s)(1-2\nu_s)} E_s$$
$$G_s = \frac{E_s}{2(1+\nu_s)} \tag{2.8b}$$

Where G_s is the shear modulus of the elastic continuum, E_s is Young's modulus of the subgrade, p is the load intensity at the interface, and H is the subgrade thickness.

The vertical deformation mode shape, $\phi(z)$, as determined by applying variational principles is given by

$$\phi(z) = \frac{sinh\gamma\left(1-\dfrac{z}{H}\right)}{sinh\gamma} \tag{2.9a}$$

Where γ is a dimensionless parameter.

Since Equation (2.9a) becomes indeterminate for $\gamma = 0$, the following relation as obtained using L'Hospital's rule is used.

$$\phi(z) = 1 - \frac{z}{H} \tag{2.9b}$$

The parameter γ is given by the following expression:

$$\left(\frac{\gamma}{H}\right)^2 = \frac{G_s \int_{-\infty}^{+\infty}\int_{-\infty}^{+\infty} (\nabla w)^2\, dxdy}{\bar{E}\int_{-\infty}^{+\infty}\int_{-\infty}^{+\infty} w^2 dxdy} \tag{2.10}$$

2.2.2.1. Generalized Continuum Model

Worku (2009) also idealized the subgrade as a homogeneous, isotropic elastic layer of thickness H overlying a firm stratum (Figure 2.5) in the same way as Reissner's idealization. Worku assumed that the elasticity modulus, E_s and the shear modulus, G_s, vary with depth. Unlike Reissner's model, he did not neglect any of the stress, strain, or displacement components.

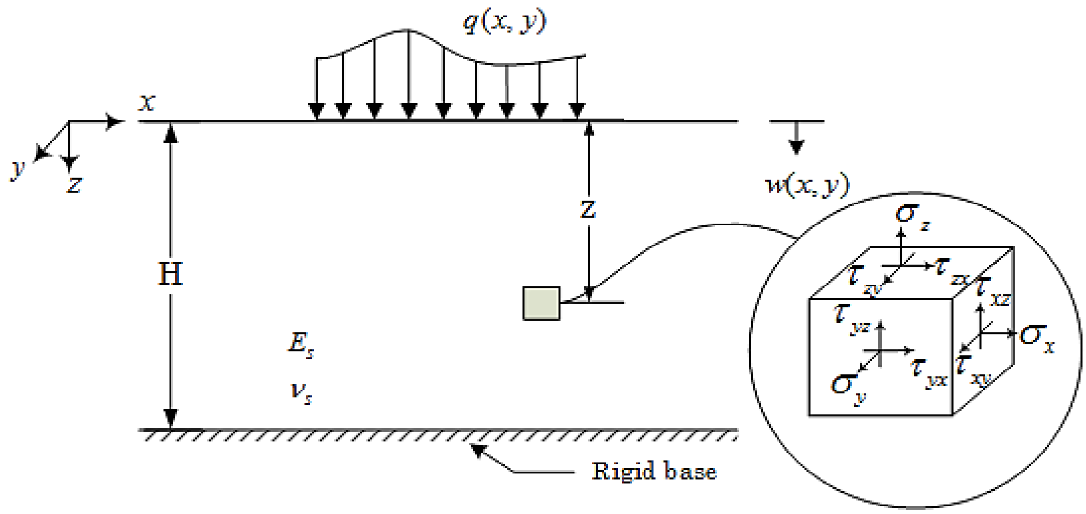

Figure 2.5: Worku Elastic Continuum Subgrade Model

According to this model, the depthwise variation of all components of the stress tensor in the subgrade is fully regarded. Lateral normal stresses are expressed in terms of vertical normal stress. Applying the Necessary boundary conditions and stress-strain, strain-displacement relationships, Worku came up with the following differential equation for his model

$$p(x,y)-\frac{G_s}{E_s K_I}\left(L_{gI}-\frac{K_{gI}L_g}{K_g}\right)\nabla^2 p(x,y)=\frac{E_s}{K_g}w_0(x,y)-\frac{G_s L_{gI}}{K_g K_I}\nabla^2 w_0(x,y) \qquad (2.11)$$

Where

$$K_g=\int_0^H g(z)dz;\;\; K_I=\int_0^H I_z(z)dz;\;\; K_{gI}=\int_0^H g(z)\tilde{I}_z(z)dz;$$

$$L_g=\int_0^H\left[\int g(z)dz-\left(\int g(z)dz\right)_{Z=H}\right]dz;$$

$$L_{gI}=\int_0^H\left[\int g(z)\tilde{I}_z(z)dz-\left(\int g(z)\tilde{I}_z(z)dz\right)_{Z=H}\right]dz;$$

$$g(z)=1-v_s\left[g_x(z)-g_y(z)\right];\; g_x(z)=\frac{\sigma_x(z)}{\sigma_y(z)};\;\; g_y(z)=\frac{\sigma_y(z)}{\sigma_z(z)}; \qquad (2.12)$$

$$\tilde{I}_z(z)=\left[\int I_z(z)dz\right]_{z=0}-\int I_z(z)dz$$

$$I_z(z)=\frac{\tau_{xz}(x,y,z)}{\bar{\tau}_{xz}(x,y)}=\frac{\tau_{yz}(x,y,z)}{\bar{\tau}_{yz}(x,y)}$$

Equation (2.11) is the mathematical model for the generalized case of an elastic subgrade, the elastic and shear moduli of which may vary with depth, and in which no simplifying assumption has been made with respect to stress, strains, or displacements. This formulation shows that the maximum order of the governing differential equation of the non-homogeneous, isotropic elastic subgrade is two and not more.

The equation has the same order and form to that of Kerr's mechanical model Equation (2.6). For this reason, it is referred to as the Kerr-type generalized continuum model. Based on this generalized model, Worku noted that a number of model variants can be obtained by introducing different simplifying assumption on the lateral deformations, the vertical shear stress, and the depth-wise variation of the functions $g_x(z), g_y(z)$ and $I_z(z)$. He also showed that the above presented simplified continuum models and others are subsets of his generalized model.

2.2.2.2. Synthesis of Mechanical and Continuum Models

The approaches and origins of the mechanical model and simplified continuum models are different. However, there is similarity in their governing differential equations. This similarity can be utilized to synthesize corresponding models of the two categories so that the mechanical model parameters can be quantified in terms of the continuum parameters. Thus, Synthesis of the two approaches has the benefit of using the strengths of both models (Worku, 2013).

Equating the corresponding terms in Equation (2.5) and Equation (2.11) and based on the observation of stress variation with depth, Worku (2010) employed an exponentially decaying function for the ratios of horizontal-to-vertical normal stresses, $g_x(z), g_y(z)$ and a bilinear variation of the vertical shear stresses $I_z(z)$ and obtained expressions for Kerr's model parameters.

The fact that the thickness, H, of the continuum appears in the denominator of the spring coefficients makes the surface deflection sensitive to this quantity. This becomes particularly clear when thinking of a plate of a given width is placed on top of an elastic layer of increasing values of the thickness. For this reason, an approach was employed, which H is removed from the expressions through the introduction of a dimensionless parameter, $\chi = H / B$, where B is the foundation width (Worku, 2013). This parameter is then used to calibrate or adjust the model parameters with the help of the FE based software together with other analytical considerations. The calibrated parameters took the following form

$$k_{Ku} = \frac{E_s}{\left(0.46 - 0.18\nu_s\right)\chi B}$$

$$k_{Kl} = \frac{E_s}{\left(0.54 - 0.26\nu_s\right)\chi B} \tag{2.13}$$

$$G_K = \frac{0.33 - 0.15\nu_s}{0.14 - 0.11\nu_s} G_s \chi B$$

2.2.2.3. The new Kerr-Equivalent Pasternak model

For practical applications, the two-parameter Pasternak model is easier, more convenient, and more commonly used than the three-parameter Kerr model. Recognizing the advantage Worku (2014) established Kerr-equivalent Pasternak parameters by seeking equivalence of performance to the calibrated Kerr model parameters stated in Equation (2.13). By setting identical shear interaction for the models, introducing the evaluated definite integrals defined in Equation (2.12) and based on additional observations from different plots Worku came up with the following calibrated Kerr-equivalent Pasternak model parameters

$$k_p = \frac{\left(0.4\nu_s + 0.67\right)E_s}{\chi B}$$

$$G_p = \left(1.36\nu_s + 2.28\right)G_s B\chi \tag{2.14}$$

This Kerr-equivalent Pasternak model yields the same results as the calibrated rigorous Kerr model. Because of its convenience for incorporation into structural analysis software and for direct use in the analysis of plates and beams, the Pasternak model with the above parameters is recommended for practical use. This thesis attempts to calibrate the Kerr- equivalent Pasternak-type model for Rectangular plates under basic practical loading cases.

2.3. The plate model

A plate is a thin and flat structural element with dimensions that are large compared to its thickness. The plate, being originally flat, develops shear forces, bending and twisting moments to resist transverse loads. Because the loads are generally carried in both directions and because the twisting rigidity in isotropic plates is quite significant, a plate is considerably stiffer than a beam of comparable span and thickness. Plates may be classified into two groups: thin and thick plates. A plate is said to be thin if its thickness to length and width ratio, h_p / B, remains less than 1/10, otherwise, the plate is said to be thick (Ansel, 2010; Ventsel and Krauthammer, 2001).

Mathematically exact stress analysis of a thin plate subjected to loads acting normal to its surface requires the solution of the differential equations of three-dimensional elasticity Though, in reality, such a member is a three-dimensional body, analysis using the three-dimensional theory of elasticity is not essential if the thickness is small compared to the in-plane dimensions (Szilard, 2004).

By assuming reasonably realistic variations through the thickness, of displacements, strains, and stresses, the problem can be reduced to one of two-dimensional analysis. Such a two-dimensional theory, most commonly employed for practical analysis, is the Classical Plate Theory (CPT), also referred to as the Kirchhoff's classical theory of thin plates. The theory leads to simplification of the plate problem without unacceptable loss of accuracy (Ansel, 2010).

Classical Plate Theory is formulated in terms of transverse deflections, $w(x, y)$, for which the governing differential equation is of the fourth order, requiring only two boundary conditions to be satisfied at each edge. The simplifications used in the derivation of the plate equation are based on the following basic assumptions (Ansel, 2010; Reddy, 2007; Szilard, 2004; Timoshenko and Woinowsky-Krieger, 1959; Ventsel and Krauthammer, 2001):

1. The plate material is linear elastic and follows Hooke's law.
2. The plate material is homogeneous and isotropic. Its elastic deformation is characterized by Young's modulus E_p and Poisson's ratio ν_p.

3. The plate is initially flat.
4. The x–y plane coincides with the middle plane of the plate in the undeformed geometry.
5. The middle surface of the plate remains unstrained during bending.
6. The transverse deflections, $w(x,y)$, is small in comparison to the thickness of the plate: i.e. $w(x,y) \ll h_p$.
7. The constant thickness of the plate, h_p, is small compared to its other dimensions; that is, the smallest lateral dimension of the plate is at least 10 times larger than its thickness.
8. The transverse deflections, $w(x,y)$, are small so that the curvature is approximated by the second derivative of the deflection with respect to coordinates in the plane of the plate
9. Slopes of the defected middle surface are small compared to unity.
10. Sections taken normal to the middle surface before deformation remain plane and normal to the deflected middle surface. Consequently, shear deformations are neglected. This assumption represents an extension of Bernoulli's hypothesis for beams to plates.
11. The normal stress σ_z in the direction transverse to the plate surface can be neglected.

With the help of these assumptions, the originally three-dimensional stress problems of elasticity are reduced to two-dimensional problems of plates. Many of these assumptions are familiar since they have their equivalent counterparts in elementary beam theory (Ansel, 2010).

2.3.1. Basic equations

The abovementioned assumptions of thin plate theory make it possible to drive the basic equations for thin plates. The state of deformation can, therefore, be described in terms of the transverse displacement, w, alone. Making use of the simplifying assumptions introduced above, the following relationships between in-plane displacements and the transverse displacement, w, exist:

$$
\begin{aligned}
& w = w(x.y) \\
& u = u_0 - z\frac{\partial w}{\partial x} \\
& v = v_0 - z\frac{\partial w}{\partial y}
\end{aligned}
\tag{2.15}
$$

Where u_0 and v_0 are displacements in the x-direction and y-direction respectively, of a point lying in the middle plane of the plate whereas u and v are displacements of a point lying at a distance z from the reference plane.

Based on Assumption 6, it is clear that $u_0 = v_0 = 0$. Thus, Equations (2.15) have the following form

$$
w = w(x.y),\ u = -z\frac{\partial w}{\partial x} \text{ and } v = -z\frac{\partial w}{\partial x}
\tag{2.16}
$$

Hence, the strain-displacement relations can be found by differentiating Equations (2.16):

$$
\begin{aligned}
& \varepsilon_x = \frac{\partial u}{\partial x} = -z\frac{\partial^2 w}{\partial x^2} \\
& \varepsilon_y = \frac{\partial v}{\partial y} = -z\frac{\partial^2 w}{\partial y^2} \\
& \gamma_{xy} = \frac{\partial u}{\partial y} + \frac{\partial v}{\partial x} = -2z\frac{\partial^2 w}{\partial x \partial y}
\end{aligned}
\tag{2.17}
$$

The curvatures, the rate of change of the angular displacements, of the plate are defined as:

$$
k_x = -\frac{\partial^2 w}{\partial x^2},\ k_y = -\frac{\partial^2 w}{\partial y^2} \text{ and } k_{xy} = -2\frac{\partial^2 w}{\partial x \partial y}
\tag{2.18}
$$

Stress-strain relationships for the plate are taken to be the case of plane stress because the plate is thin and all the stress components with respect to the z-direction are assumed zero.

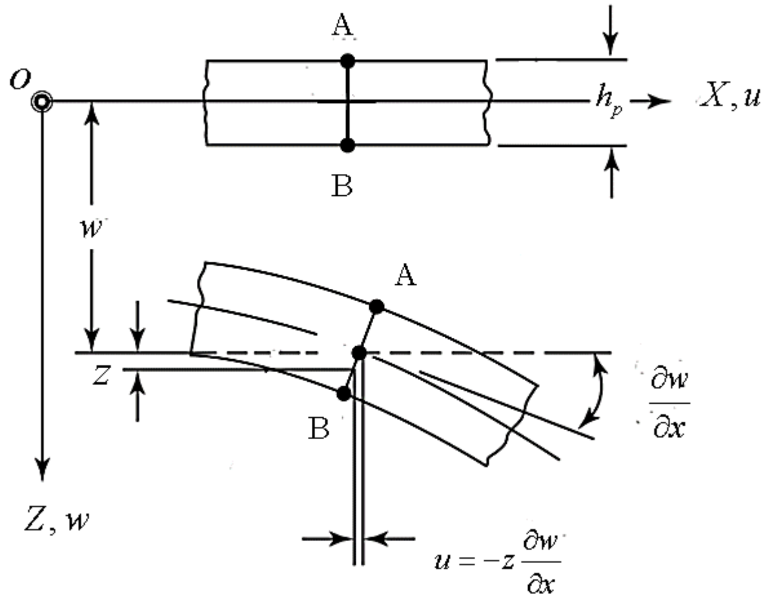

Figure 2.6: Part of the plate before and after the deflection after Ansel (2010)

Using the strain-displacement relations and assuming isotropic material, Hooke's Law can be written in terms of derivatives of displacement w:

Thus, for isotropic material

$$\sigma_x = -\frac{E_p z}{1-\nu_p^2}\left(\frac{\partial^2 w}{\partial x^2} + \nu_p \frac{\partial^2 w}{\partial y^2}\right)$$

$$\sigma_y = -\frac{E_p z}{1-\nu_p^2}\left(\frac{\partial^2 w}{\partial y^2} + \nu_p \frac{\partial^2 w}{\partial x^2}\right) \tag{2.19}$$

$$\tau_{xy} = -2Gz\frac{\partial^2 w}{\partial x \partial y}$$

Where: E_p = Modulus of Elasticity of the plate

G = Shear Modulus of the plate

ν_p = Poisson's Ratio

And G is related to E_p by $G = \dfrac{E_p}{2\left(1+\nu_p\right)}$

Internal stresses in plates produce bending moments and shear forces as illustrated in Figures (2.7a) and (2.7b). The bending moments M_x, M_y, and M_{xy} transverse shear forces Q_x and Q_y defined as

$$M_x = \int_{-h/2}^{h/2} \sigma_x z dz$$

$$M_y = \int_{-h/2}^{h/2} \sigma_y z dz$$

$$M_{xy} = \int_{-h/2}^{h/2} \tau_{xy} z dz \qquad (2.20)$$

$$Q_x = \int_{-h/2}^{h/2} \tau_{xz} dz$$

$$Q_y = \int_{-h/2}^{h/2} \tau_{yz} dz$$

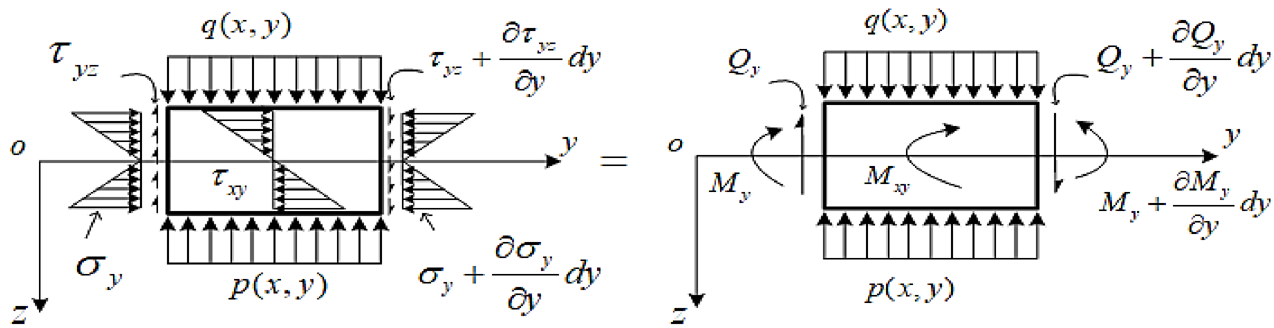

(a)

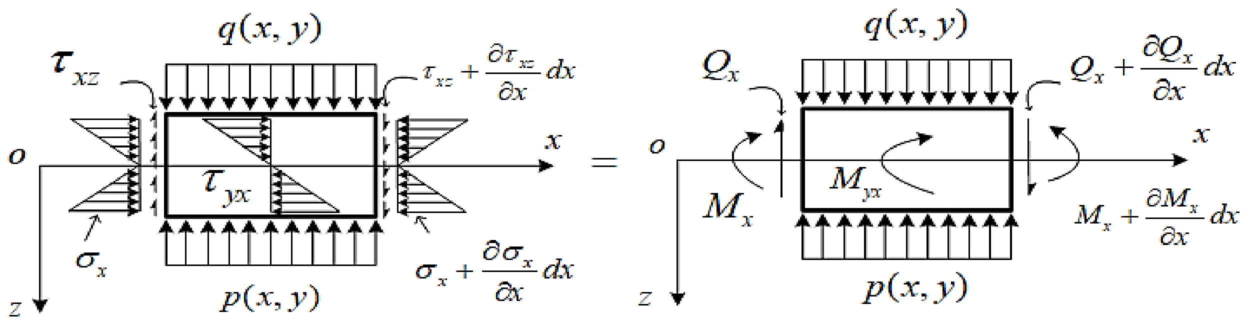

(b)

Figure 2.7: Stresses, flexural moments, and shearing forces on a plate element acting a) in the y-z plane, b) the x-z plane (Selvadurai, 1979: Timoshenko and Woinowsky-Krieger, 1959).

Substituting Equations (2.19) into Equations (2.20) and integrating over the plate thickness, the following formulas are derived for the stress resultants and couples in terms of the curvatures and the deflection (Timoshenko and Woinowsky-Krieger, 1959):

$$M_x = -D\left(\frac{\partial^2 w}{\partial x^2} + \nu_p \frac{\partial^2 w}{\partial y^2}\right) = D\left(k_x + \nu_p k_y\right)$$

$$M_y = -D\left(\frac{\partial^2 w}{\partial y^2} + \nu_p \frac{\partial^2 w}{\partial x^2}\right) = D\left(k_y + \nu_p k_x\right) \tag{2.21}$$

$$M_{xy} = M_{yx} = -D\left(1-\nu_p\right)\frac{\partial^2 w}{\partial x \partial y} = D\left(1-\nu_p\right)k_{xy}$$

Where, D is known as flexural rigidity of the plate and is given by,

$$D = \frac{E_p h_p^3}{12\left(1-\nu_p^2\right)} \tag{2.22}$$

2.3.2. Governing equation for deflection of plates in Cartesian coordinates

Consider the equilibrium of an infinitesimal element of the plate dx by dy subject to a vertical distributed load of intensity $q(x, y)$ and supporting external reaction $p(x, y)$ applied normal to the upper and lower surface of the plate, respectively, as shown in Figure (2.4). Since the stress resultants and stress couples are assumed to be applied to the middle plane of this element, the net applied load is transferred to the mid-plane. Considering the equilibrium of forces and moments acting on the element one obtains the following equations (Timoshenko and Woinowsky-Krieger, 1959; Szilard, 2004):

1. The force summation in the z-axis gives

$$\frac{\partial Q_x}{\partial x}dxdy + \frac{\partial Q_y}{\partial y}dxdy + \left(q-p\right)dxdy = 0$$

i.e. $$\frac{\partial Q_x}{\partial x} + \frac{\partial Q_y}{\partial y} = -\left(q-p\right) \tag{2.23}$$

2. Moment equilibrium about a line parallel to the y-axis and passing through the center of the element:

$$\frac{\partial M_x}{\partial x} + \frac{\partial M_{yx}}{\partial y} = -Q_x \tag{2.24}$$

3. Moment equilibrium about a line parallel to the x-axis and passing through the center of the element:

$$\frac{\partial M_y}{\partial y} + \frac{\partial M_{xy}}{\partial x} = -Q_y \tag{2.25}$$

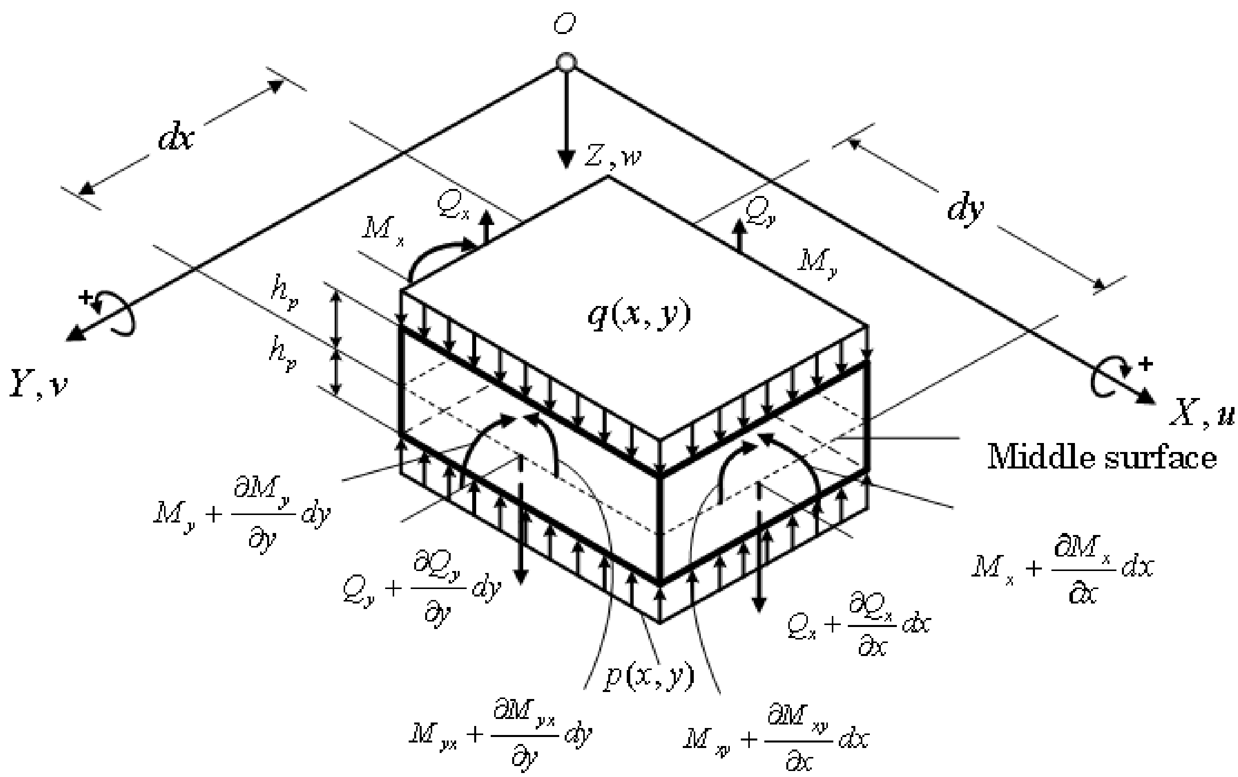

Figure 2.8: External and internal forces on the element of the plate after Szilard (2004).

Equations (2.23)-(2.25) are the equilibrium equations of CPT and have to be satisfied at every point of the plate. Eliminating Q_x and Q_y from (2.24) and (2.25), and setting $M_{xy} = M_{yx}$ yields the following moment equilibrium equation in terms of the applied loads:

$$\frac{\partial^2 M_x}{\partial x^2} + 2\frac{\partial^2 M_{xy}}{\partial x \partial y} + \frac{\partial^2 M_y}{\partial y^2} = -(q - p) \tag{2.26}$$

Finally, the introduction of the expressions for M_x, M_y and M_{xy} from Equations (2.21) into Equation (2.26) yields

$$\frac{\partial^4 w}{\partial x^4} + 2\frac{\partial^4 w}{\partial x^2 \partial y^2} + \frac{\partial^4 w}{\partial y^4} = \frac{(q-p)}{D} \tag{2.27}$$

This is the governing differential equation for the deflections of a thin plate bending analysis based on the classical plate theory (CPT). Mathematically, the differential Equation (2.27) can be classified as a linear partial differential equation of the fourth order having constant coefficients.

2.4. Computational Approach

One of the primary goals of this research is to develop a realistic, practical, and easily applicable procedure for the analysis of plates on an elastic foundation. The solution of this type of soil engineering problem, which involves equilibrium equations together with constitutive relations, compatibility considerations, and complex boundary conditions, would require such an effort that analytical approach is impractical.

An alternative approach is to use a numerical analysis technique that will provide approximate solutions as close to the exact solutions as required for practical engineering design problems. Numerical methods, such as the finite difference method, the finite strip method, the finite element method, and the boundary element method, have been applied to analyze soil–structure interaction problems.

Both the finite-element method and the method of finite differences were considered. Each method will generate and require solutions for a set of simultaneous equations; however, the use of the finite-element method will generate a coefficient matrix that is much larger than that generated by the use of the finite-difference method. This means that there are many more unknowns to be solved in the FE approach, which motivates the use of finite difference method to solve the problem of rectangular plates.

2.4.1. The finite difference method (FDM)

The analytical solutions of differential equations have been limited to homogeneous plates with simple geometry, load configuration, and boundary conditions. Solutions for finite plates are also mainly restricted to circular plates subjected to axisymmetric loadings (Wang 2005). For this case, it is not always possible to derive analytical solutions, and therefore approximate numerical approaches are more appropriate. The use of numerical approaches enables the engineer to expand the ability to solve design problems of practical significance (Ansel, 2010). Among the most important of the numerical approach is the method of finite differences. Finite difference methods are based on a mathematical discretization of the plate continuum which offers a means of deriving approximations to the derivatives, at selected points along the plate, in terms of the unknown deflections at these and adjacent points.

Although currently, the FEM has attained almost exclusive dominance in the numerical analysis of structures, the FDM could also be considered as a viable alternative in the analysis of plates on an elastic foundation.

The advantages of ordinary FDM are as follows:

- It is simple both from a mathematical and coding perspective
- It is entirely transparent in its operations.
- It is versatile.
- It has readily usable and reusable finite difference patterns (stencils).
- The size of the coefficient matrix is much smaller in comparison to that of the FEM Since only the deflection ordinates are the unknowns.
- Acceptable accuracy for all technical purposes can be achieved with relative ease.
- More importantly, the number of unknowns to achieve an acceptable degree of accuracy is much less than that required by an equivalent finite element solution.

The disadvantages of the FDM are as follows:

- It is not well suited without the use of electronic digital computers for the solution of very large plate systems involving hundreds or even thousands of equations.

- Beyond certain mesh widths, the convergence of the solution becomes slow.
- The resulting coefficient matrix is not symmetrical, causing some difficulties in the numerical solution of this system
- Using FDM is not recommended when higher than fourth-order derivatives are involved (E.g. when using Kerr subgrade model, which gives sixth-order differential equation).

2.4.1.1. Finite difference Expressions

When using an ordinary finite difference method, a grid needs to be defined where the differences are computed. The most simple and natural option is to use an equally spaced grid. Depending on which grid points are used to compute the finite difference we will get the three most used forms of finite differences (Jones, 1997):

1. Forward difference: the forward $(m+1)$ point of the function is used to compute the difference.

$$f'(x_m) \approx \frac{f\left(x_m + \Delta x\right) - f(x_m)}{\Delta x} \tag{2.28}$$

2. Backward difference: the backward $(m-1)$ point of the function is used to compute the difference.

$$f'(x_m) \approx \frac{f\left(x_m\right) - f(x_m - \Delta x)}{\Delta x} \tag{2.29}$$

3. Central difference: the central points of the function are used to compute the difference.

$$f'(x_m) \approx \frac{f\left(x_m + \Delta x\right) - f(x_m - \Delta x)}{2\Delta x} \tag{2.30}$$

The derivatives at any point can be approximated using Forward and Backward difference for a spacing of Δx, and it can be shown that these formulas give a first order approximation to $f'\left(x\right)$, meaning that the size of the error is roughly proportional to Δx. Whereas the central difference approximation gives a second order accurate approximation (the error is proportional to Δx^2) and hence is much smaller than the error in a first order approximation when Δx is small.

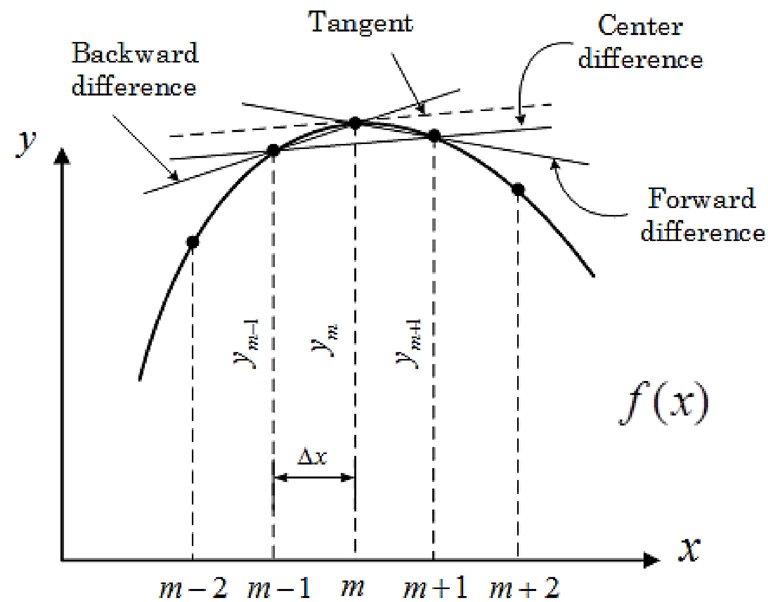

Figure 2.9: Approximating $f\,'(x)$ using backward, forward and central differences

Thus, the derivatives at any point can be approximated more accurately by the corresponding central differences (Selvadurai, 1979). Consequently, derivatives, which are based on central differences, are the only ones that will be considered here. These finite difference expressions are schematically represented in Table (2.1), including the first error terms (ε) obtained by using the Taylor series approach.

Table 2.1: Representation of Derivatives by Central Differences after Szilard (2004)

	Coefficients					First error term
	$m-2$	$m-1$	m	$m+1$	$m+2$	
$\left(\frac{dy}{dx}\right)_m = \frac{1}{2\Delta x}$		-1	0	+1		$-\frac{1}{6}(\Delta x)^2 \frac{d^3 y_m}{dx^3}$
$\left(\frac{d^2 y}{dx^2}\right)_m = \frac{1}{(\Delta x)^2}$		+1	-2	+1		$-\frac{1}{12}(\Delta x)^2 \frac{d^4 y_m}{dx^4}$
$\left(\frac{d^3 y}{dx^3}\right)_m = \frac{1}{2(\Delta x)^3}$	-1	+2	0	-2	+1	$-\frac{1}{4}(\Delta x)^2 \frac{d^5 y_m}{dx^5}$
$\left(\frac{d^4 y}{dx^4}\right)_m = \frac{1}{(\Delta x)^4}$	+1	-4	+6	-4	+1	$-\frac{1}{6}(\Delta x)^2 \frac{d^6 y_m}{dx^6}$

3. Analysis of a rectangular plate on an elastic foundation (PEF)

3.1. Mathematical formulation of PEF

The deflection, $w(x,y)$, of a rectangular plate, subjected to a transverse load $q(x,y)$ and continuously supported by an elastic foundation is given by Equation (2.27), which is rewritten as

$$D\left(\frac{\partial^4 w(x,y)}{\partial x^4}+2\frac{\partial^4 w(x,y)}{\partial x^2 \partial y^2}+\frac{\partial^4 w(x,y)}{\partial y^4}\right)=q(x,y)-p(x,y) \tag{3.1}$$

Where $p(x,y)$ = the contact pressure of the soil

D represents the bending or flexural rigidity of the plate and expressed as

$$D=\frac{E_p h_p^{\;3}}{12(1-v_p^2)} \tag{3.2}$$

Where E_p is the modulus of elasticity, h_p is the plate thickness and v_p is Poisson's ratio.

To solve the final form of the soil-structure interaction Equations (3.1), the soil reaction, $p(x,y)$ has to be combined in the equation, which is dependent on the plate and soil characteristics and the bond at the interface. Assuming frictionless contact, and complete bond at the interface between the plate and the soil $p(x,y)$ can be expressed in terms of the soil displacement at the surface according to the subgrade model employed.

To overcome the shortcomings of Winkler's model, two-parameter models, which permit interaction among the springs, were proposed. Among the two-parameter models, Pasternak's model introduces the second parameter, which is a pure-shear layer to connect the springs. When the contact pressure of the soil is represented by the Pasternak model, Equation (2.4) is applicable:

$$p(x,y)=k_p w(x,y)-G_p\nabla^2 w(x,y) \tag{3.3}$$

Combining Equation (3.1) with Equation (3.3) and rearranging, one obtains

$$D\nabla^4 w(x,y) - G_p \nabla^2 w(x,y) + k_p w(x,y) = q(x,y) \tag{3.4}$$

Since the two-parameter model is considered here, the Winkler case can be recovered when G_p is equal to zero.

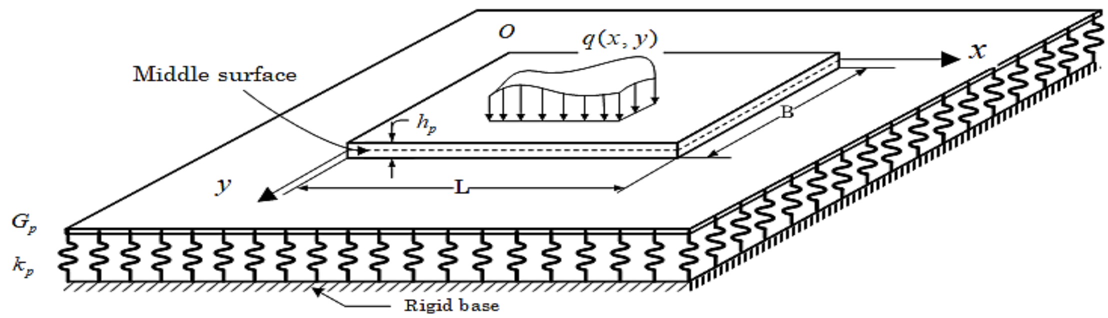

Figure 3.1: Plate on Pasternak's foundation

Outside the domain of the plate, the field equation that controls the surface displacement of the subgrade is given by

$$k_p w_F(x,y) - G_p \nabla^2 w_F(x,y) = 0 \tag{3.5}$$

Where $w_F(x,y)$ is the deflection of the foundation beyond plate edges.

3.1.1. Moments and Forces

The actions in the plate are expressed in terms of bending and twisting moments and transverse shear forces per unit length. The positive directions of these actions are displayed in Figure (3.2). In terms of the transverse deflection, $w(x,y)$, the bending moments per unit length at any point of the plate in Equations (2.21) is re-written as:

$$\begin{aligned} M_x &= -D\left(\frac{\partial^2 w}{\partial x^2} + \nu_p \frac{\partial^2 w}{\partial y^2}\right) \\ M_y &= -D\left(\frac{\partial^2 w}{\partial y^2} + \nu_p \frac{\partial^2 w}{\partial x^2}\right) \end{aligned} \tag{3.6}$$

and the twisting moment per unit length by:

$$M_{xy} = M_{yx} = -D(1-\nu_p)\frac{\partial^2 w}{\partial x \partial y} \tag{3.7}$$

Because of the existence of the shear layer in the subgrade, it is necessary to define the general shear force, which takes into account the effects of the shearing stresses in the subgrade as well as the shearing stresses in the plate. Straughan (1990) calculated the shearing forces per unit length as:

$$\begin{aligned} V_x &= Q_x + N_x = -\frac{\partial}{\partial x}(\nabla^2 w) + G_p\frac{\partial w}{\partial x} = -D\frac{\partial}{\partial x}\left(\frac{\partial^2 w}{\partial x^2}+\frac{\partial^2 w}{\partial y^2}\right) + G_p\frac{\partial w}{\partial x} \\ V_y &= Q_y + N_y = -\frac{\partial}{\partial y}(\nabla^2 w) + G_p\frac{\partial w}{\partial y} = -D\frac{\partial}{\partial y}\left(\frac{\partial^2 w}{\partial x^2}+\frac{\partial^2 w}{\partial y^2}\right) + G_p\frac{\partial w}{\partial y} \end{aligned} \tag{3.8}$$

Where Q_x and Q_y are transverse shear forces per unit length of the plate given by Equation (2.25) - (2.26) whereas N_x and N_y are shear forces per unit length of the soil medium.

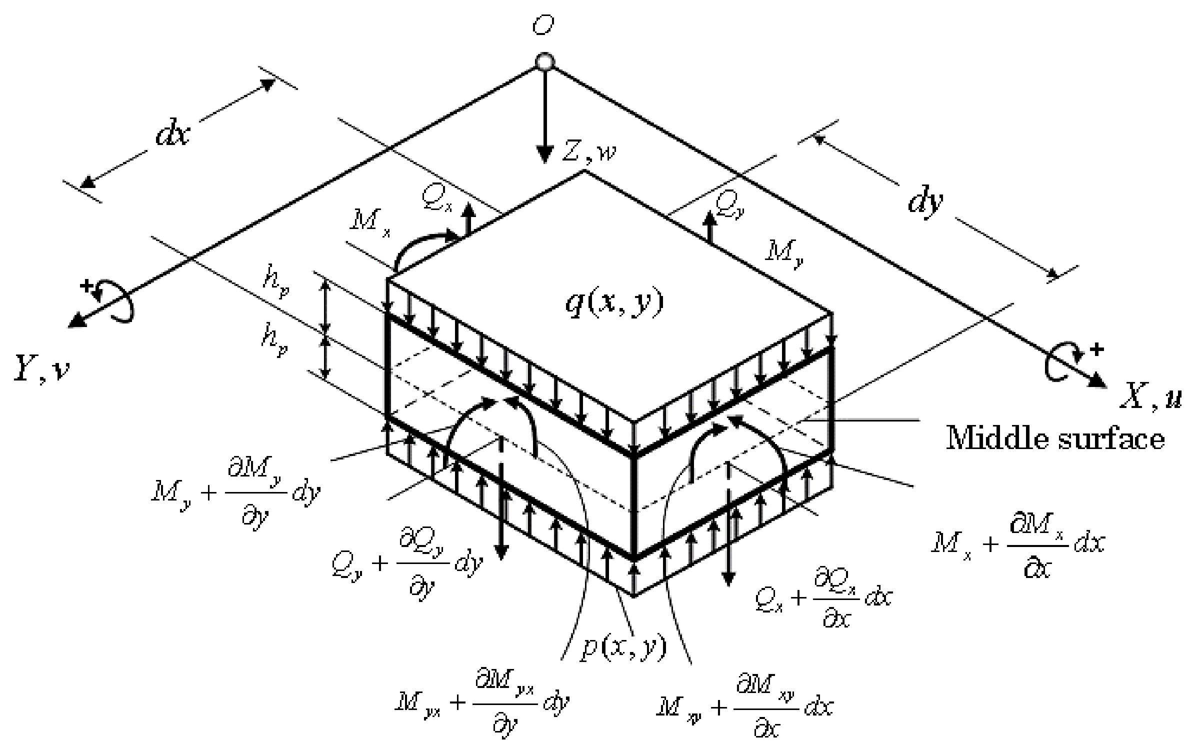

Figure 3.2: External and internal forces on the element of the plate after Szilard (2004).

Following Kirchhoff (Timoshenko and Krieger, 1959; Vlasov and Leontev, 1966), the shearing force at the edge of the plate consists of two terms, that is, transverse shear and the effect of the torsional moment. The vertical edge forces per unit length can be written as

$$R_x = V_x + \frac{\partial m_{yx}}{\partial y} = -D\left[\frac{\partial^3 w}{\partial x^3} + (2-v_p)\frac{\partial^3 w}{\partial x \partial y^2}\right] + G_p\frac{\partial w}{\partial x} \qquad \text{at } x = 0, L \tag{3.9a}$$

$$R_y = V_y + \frac{\partial m_{xy}}{\partial x} = -D\left[\frac{\partial^3 w}{\partial y^3} + (2-v_p)\frac{\partial^3 w}{\partial x^2 \partial y}\right] + G_p\frac{\partial w}{\partial y} \qquad \text{at } y = 0, B \tag{3.9b}$$

3.1.2. Boundary Conditions

The boundary conditions are the known conditions on the surfaces of the plate which must be prescribed in advance in order to obtain the solution of Equation (3.4) corresponding to the soil-structure problem. For a plate, the solution of Equation (3.4) requires that two boundary conditions be satisfied at each edge (each boundary). The most common boundary condition in foundations is the statical boundary, which is a free-edge boundary condition (Figure 3.3).

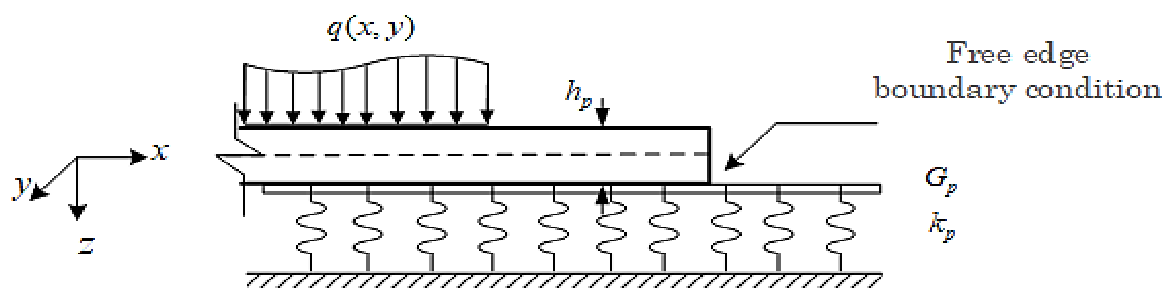

Figure 3.3: Free end boundary condition

When free end boundary conditions associated with rectangular plates resting on two parameter media are considered, it is necessary to consider the concentrated edge reactions that occur along the boundaries of the plate due to deformation of the soil medium beyond the plate edges. In addition to these edge reactions, concentrated reactions occur at the corners of the rectangular plate. The effect of corner reaction has been neglected in the study as Vlasov and Leont'ev (1966) observed the magnitude of these reactions is relatively small and their influence on the flexure of the plate is negligible. Furthermore, the absence of sharp plate corners and in the case of soil media the occurrence of plastic deformations will tend to minimize the magnitude of the corner reactions.

The boundary conditions for the free boundaries of the plate are derived from the following physical considerations (Barton, 1948; Kerr, 1964; Selvadurai, 1979; Katsikadelis and Kallivokas, 1988):

- The deflection is continuous across the domain
- The bending moment of the plate vanishes on the edge.
- The shear force in the plate is equal to the effective shear force in the shear layer of the subgrade.

Using rectangular coordinates the above conditions in terms of the deflections w of the plate and the deflection w_F of the foundation are expressed as

1. Free edge (x = constant)

At $(0, y)$ and (L, y);

$$\left.\begin{aligned} &[w]_x = [w_F]_x \\ &M_x = -D\left(\frac{\partial^2 w}{\partial x^2} + \nu_p \frac{\partial^2 w}{\partial y^2}\right)_x = 0 \\ &-D\left[\frac{\partial^3 w}{\partial x^3} + (2-\nu_p)\frac{\partial^3 w}{\partial x \partial y^2}\right]_x = G_p\left(\left[\frac{\partial w_F}{\partial x}\right] - \left[\frac{\partial w}{\partial x}\right]\right)_x \end{aligned}\right\} \tag{3.10}$$

2. Free edge (y = constant)

At $(x, 0)$ and (x, B);

$$\left.\begin{aligned} &[w]_y = [w_F]_y \\ &M_y = -D\left(\frac{\partial^2 w}{\partial y^2} + \nu_p \frac{\partial^2 w}{\partial x^2}\right)_y = 0 \\ &-D\left[\frac{\partial^3 w}{\partial y^3} + (2-\nu_p)\frac{\partial^3 w}{\partial x^2 \partial y}\right]_y = G_p\left(\left[\frac{\partial w_F}{\partial y}\right] - \left[\frac{\partial w}{\partial y}\right]\right)_y \end{aligned}\right\} \tag{3.11}$$

3. Free corner

At $(0,0)$, $(0,B)$, $(L,0)$, and (L,B);

$$\left.\begin{aligned}
&[w]_c = [w_F]_c \\
&M_x = M_y = 0, \left(\frac{\partial^2 w}{\partial x^2}\right)_c = \left(\frac{\partial^2 w}{\partial y^2}\right)_c = 0 \\
&R_x = -D\left[\frac{\partial^3 w}{\partial x^3} + (2-v_p)\frac{\partial^3 w}{\partial x \partial y^2}\right]_c = G_p\left(\left[\frac{\partial w_F}{\partial x}\right] - \left[\frac{\partial w}{\partial x}\right]\right)_c \\
&R_y = -D\left[\frac{\partial^3 w}{\partial y^3} + (2-v_p)\frac{\partial^3 w}{\partial x^2 \partial y}\right]_c = G_p\left(\left[\frac{\partial w_F}{\partial y}\right] - \left[\frac{\partial w}{\partial y}\right]\right)_c \\
&R_{xy} = -2D(1-v_p)\frac{\partial^2 w}{\partial x \partial y} = 0
\end{aligned}\right\} \tag{3.12}$$

In order to determine the concentrated edge reactions, the distribution of vertical displacements of the elastic foundation surface beyond the plate edges must be known. The displacements are obtained by solving Equation (3.5) re-written as

$$k_p w_F(x,y) - G_p \nabla^2 w_F(x,y) = 0 \tag{3.13}$$

For a rectangular plate with dimensions of B in the y-direction and L in the x-direction, Equation (3.13) can easily be solved using the method of separation of variables.

Dividing the domain outside of the plate into eight regions (Figure 3.4), the following equations account for the deformation of the soil medium beyond the plate boundary. The general solution is outlined in Appendix I

Region I and V

$$w_F(x,y) = w_L(y)e^{-\lambda(x-L)}, \text{ for } 0 \le y \le B \text{ and } 0 \le x < \infty \tag{3.14}$$

$$w_F(x,y) = w_L(y)e^{\lambda x}, \text{ for } 0 \le y \le B \text{ and } -\infty < x \le 0 \tag{3.15}$$

Region III and VII

$$w_F(x,y) = w_B(x)e^{-\lambda(y-B)}, \text{ for } 0 \le x \le L \text{ and } B \le y < \infty \tag{3.16}$$

$$w_F(x,y) = w_B(x)e^{\lambda x}, \text{ for } 0 \le x \le L \text{ and } -\infty < y \le 0 \tag{3.17}$$

Region II, IV, VI, and VIII

$$w_F(x,y) = w_c e^{-\lambda(y-B)} e^{-\lambda(x-L)}, \text{ for } L \geq x > \infty \text{ and } B \geq y > \infty \tag{3.18}$$

$$w_F(x,y) = w_c e^{-\lambda(x-L)} e^{\lambda y}, \text{ for } L \geq x > \infty \text{ and } 0 \leq y < -\infty \tag{3.19}$$

$$w_F(x,y) = w_c e^{\lambda x} e^{\lambda y}, \text{ for } 0 \leq x < -\infty \text{ and } 0 \leq y < -\infty \tag{3.20}$$

$$w_F(x,y) = w_c e^{\lambda x} e^{-\lambda(y-B)}, \text{ for } 0 \leq x < -\infty \text{ and } B \geq y > \infty \tag{3.21}$$

Where w_L is the vertical displacement of the plate at $x = 0$ and $x = L$

w_B is the vertical displacement of the plate at $y = 0$ and $y = B$

w_c is the vertical displacement of the plate at the corners and

$$\lambda = \sqrt{\frac{k_p}{G_p}}$$

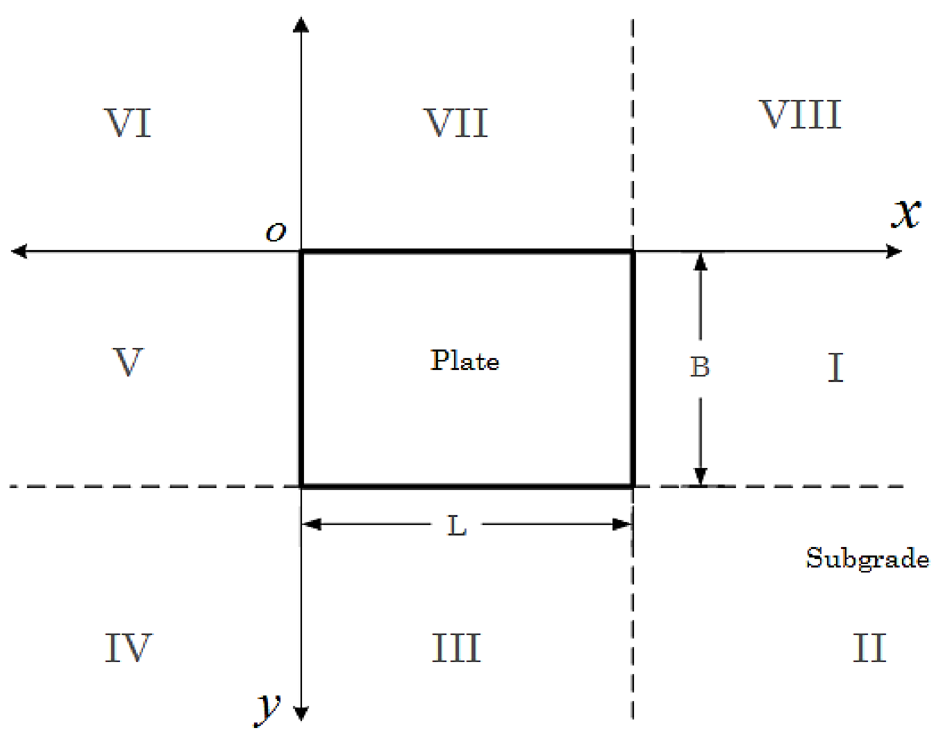

Figure 3.4: Rectangular plate-soil surface divided into regions

By using Equations (3.14) to (3.21), the boundary conditions of the plate Equations (3.10) to (3.12) can be rewritten as

1. Free edge (x = constant)

At $(0, y)$ and (L, y);

$$\left.\begin{aligned} &M_x = -D\left(\frac{\partial^2 w}{\partial x^2} + \nu_p \frac{\partial^2 w}{\partial y^2}\right)_x = 0 \\ &-D\left[\frac{\partial^3 w}{\partial x^3} + (2-\nu_p)\frac{\partial^3 w}{\partial x \partial y^2}\right]_x = G_p\left(\pm\sqrt{\frac{k_p}{G_p}}w - \left[\frac{\partial w}{\partial x}\right]\right)_x \end{aligned}\right\} \tag{3.22}$$

2. Free edge (y= constant)

At $(x, 0)$ and (x, B);

$$\left.\begin{aligned} &M_y = -D\left(\frac{\partial^2 w}{\partial y^2} + \nu_p \frac{\partial^2 w}{\partial x^2}\right)_y = 0 \\ &-D\left[\frac{\partial^3 w}{\partial y^3} + (2-\nu_p)\frac{\partial^3 w}{\partial x^2 \partial y}\right]_y = G_p\left(\pm\sqrt{\frac{k_p}{G_p}}w - \left[\frac{\partial w}{\partial y}\right]\right)_y \end{aligned}\right\} \tag{3.23}$$

3. Free corner

At $(0,0)$, $(0,B)$, $(L,0)$, and (L,B);

$$\left.\begin{aligned} &M_x = M_y = 0, \left(\frac{\partial^2 w}{\partial x^2}\right)_c = \left(\frac{\partial^2 w}{\partial y^2}\right)_c = 0 \\ &R_x = -D\left[\frac{\partial^3 w}{\partial x^3} + (2-\nu_p)\frac{\partial^3 w}{\partial x \partial y^2}\right]_c = G_p\left(\pm\sqrt{\frac{k_p}{G_p}}w - \left[\frac{\partial w}{\partial x}\right]\right)_c \\ &R_y = -D\left[\frac{\partial^3 w}{\partial y^3} + (2-\nu_p)\frac{\partial^3 w}{\partial x^2 \partial y}\right]_c = G_p\left(\pm\sqrt{\frac{k_p}{G_p}}w - \left[\frac{\partial w}{\partial y}\right]\right)_c \\ &R_{xy} = -2D(1-\nu_p)\frac{\partial^2 w}{\partial x \partial y} = 0 \end{aligned}\right\} \tag{3.24}$$

3.2. Solutions of the partial differential equations (PDE)

The finite difference method is used to discretize the governing differential equation as indicated in Chapter 2. It is an approximate method, which allows the conversion of a set of differential equations into a set of linear algebraic equations that may be solved simultaneously by applying matrix methods. This section provides detailed numerical procedure on solving the governing equation.

3.2.1. Discretization

To assist the discretization of the governing equations, the following scheme is used at the point (m,n). For the rectangular network shown in Figure (3.5), the approximate values of the derivatives in terms of central finite differences of the values of the deflections at the pivotal points are shown below (Barton, 1948; Selvadurai, 1979; Szilard, 2004).

Let $\alpha = \dfrac{\Delta x}{\Delta y}$ and $\Delta x = \alpha \Delta y = \iota$

$$\left(\frac{\partial w}{\partial x}\right)_{m,n} = \frac{1}{2\iota}\left(w_{m+1,n} - w_{m-1,n}\right) \tag{3.25}$$

$$\left(\frac{\partial^2 w}{\partial x^2}\right)_{m,n} = \frac{1}{\iota^2}\left(w_{m-1,n} - 2w_{m,n} + w_{m+1,n}\right) \tag{3.26}$$

$$\left(\frac{\partial^3 w}{\partial x^3}\right)_{m,n} = \frac{1}{2\iota^3}\left(-w_{m-2,n} + 2w_{m-1,n} - 2w_{m+1,n} + w_{m+2,n}\right) \tag{3.27}$$

$$\left(\frac{\partial^4 w}{\partial x^4}\right)_{m,n} = \frac{1}{\iota^4}\left(w_{m-2,n} - 4w_{m-1,n} + 6w_{m,n} - 4w_{m+1,n} + w_{m+2,n}\right) \tag{3.28}$$

$$\left(\frac{\partial w}{\partial y}\right)_{m,n} = \frac{\alpha}{2\iota}\left(w_{m,n+1} - w_{m,n-1}\right) \tag{3.29}$$

$$\left(\frac{\partial^2 w}{\partial y^2}\right)_{m,n} = \frac{\alpha^2}{\iota^2}\left(w_{m,n-1} - 2w_{m,n} + w_{m,n+1}\right) \tag{3.30}$$

$$\left(\frac{\partial^3 w}{\partial y^3}\right)_{m,n} = \frac{\alpha^3}{2\iota^3}\left(-w_{m,n-2} + 2w_{m,n-1} - 2w_{m,n+1} + w_{m,n+2}\right) \tag{3.31}$$

$$\left(\frac{\partial^4 w}{\partial y^4}\right)_{m,n} = \frac{\alpha^4}{\iota^4}\left(w_{m,n-2} - 4w_{m,n-1} + 6w_{m,n} - 4w_{m,n+1} + w_{m,n+2}\right) \tag{3.32}$$

The mixed derivatives are also represented by

$$\left(\frac{\partial^2 w}{\partial x \partial y}\right)_{m,n} = \frac{\alpha}{4\iota^2}\left(w_{m-1,n-1} + w_{m+1,n-1} + w_{m-1,n+1} + w_{m+1,n+1}\right) \tag{3.33}$$

$$\left(\frac{\partial^3 w}{\partial x \partial y^2}\right)_{m,n} = \frac{\alpha^2}{2\iota^3}\left(\begin{array}{l} 4w_{m,n} - 2\left(w_{m-1,n} + w_{m+1,n} + w_{m,n-1} + w_{m,n+1}\right) + \\ w_{m-1,n-1} + w_{m+1,n-1} + w_{m-1,n+1} + w_{m+1,n+1} \end{array}\right) \tag{3.34a}$$

$$\left(\frac{\partial^3 w}{\partial x \partial y^2}\right)_{m,n} = \frac{\alpha^2}{2\iota^3}\left(\begin{array}{l} 4w_{m,n} - 2\left(w_{m-1,n} + w_{m+1,n} + w_{m,n-1} + w_{m,n+1}\right) + \\ w_{m-1,n-1} + w_{m+1,n-1} + w_{m-1,n+1} + w_{m+1,n+1} \end{array}\right) \tag{3.34b}$$

$$\left(\frac{\partial^4 w}{\partial x^2 \partial y^2}\right)_{m,n} = \frac{\alpha^2}{\iota^4}\left(\begin{array}{l} 4w_{m,n} - 2\left(w_{m-1,n} + w_{m+1,n} + w_{m,n-1} + w_{m,n+1}\right) + \\ w_{m-1,n-1} + w_{m+1,n-1} + w_{m-1,n+1} + w_{m+1,n+1} \end{array}\right) \tag{3.35}$$

The subscripts in the finite difference equations indicate the position in the stencil.

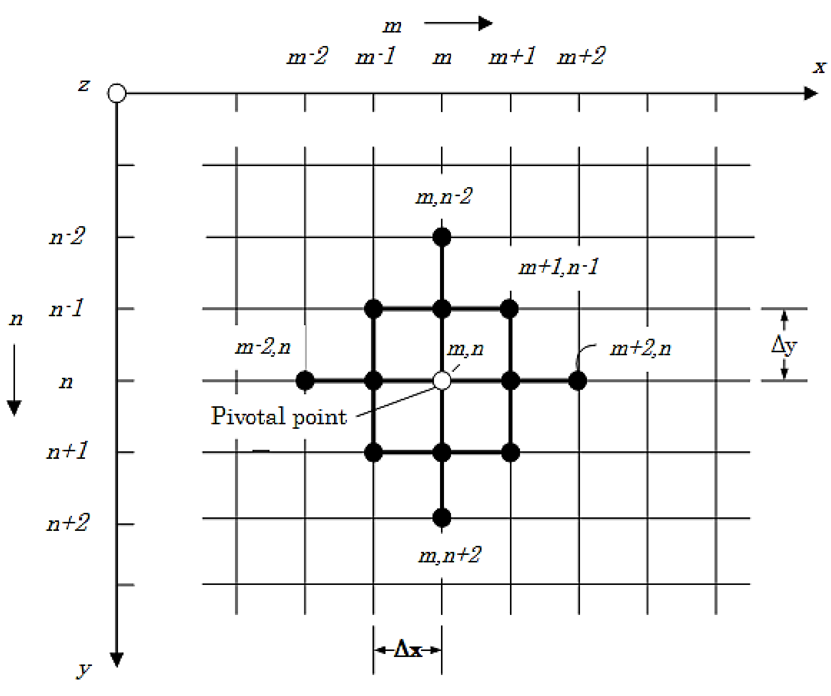

Figure 3.5: Rectangular mesh after Szilard (2004)

The discretized form of the fourth order governing differential equation of the plate Equation (3.4) can be written as.

$$\begin{pmatrix} \left(6+8\alpha^2+6\alpha^4+2(1+\alpha^2)\hat{G}_p+\hat{k}_p\right)w_{m,n}+\alpha^4\left(w_{m,n-2}+w_{m,n+2}\right)- \\ \left(4(1+\alpha^2)+\hat{G}_p\right)\left(\alpha^2\left(w_{m,n-1}+w_{m,n+1}\right)+w_{m-1,n}+w_{m+1,n}\right)+ \\ 2\alpha^2\left(w_{m-1,n-1}+w_{m+1,n-1}+w_{m-1,n+1}+w_{m+1,n+1}\right)+w_{m-2,n}+w_{m+2,n} \end{pmatrix}=\left(\frac{q(x,y)\iota^4}{D}\right)_{m,n} \tag{3.36}$$

The schematic diagram of the stencil used to solve the governing equation is shown in Figure (3.6).

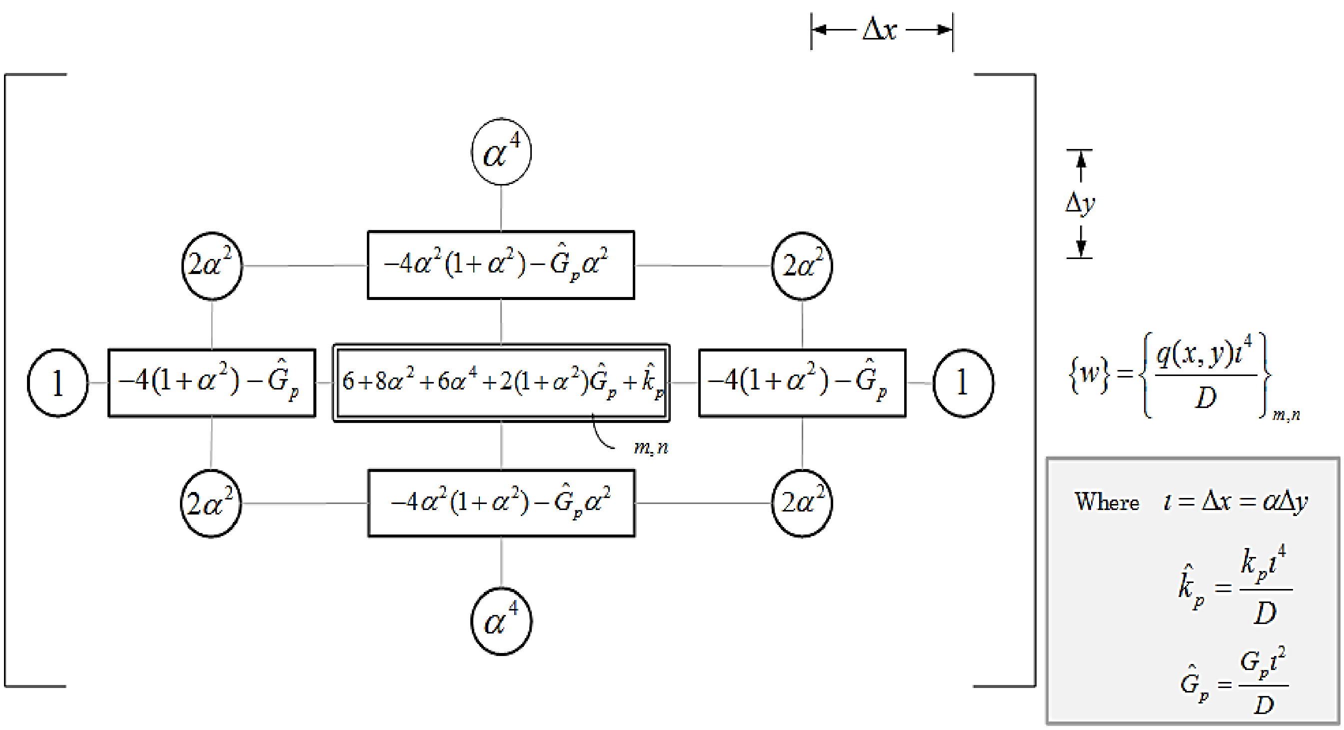

Figure 3.6: stencil for interior mesh point

3.2.2. Boundary Conditions

The solution of the governing plate Equation (3.4) by the finite difference method also requires proper finite difference representation of the boundary conditions. Consequently, the expressions of the various boundary conditions in Equations (3.22) to (3.24) can be replaced by the finite difference expressions.

In terms of the finite difference equation, the boundary conditions may be expressed as

1. Free edge (x = constant)

At $(0, y)$ and (L, y);

$$\left.\begin{array}{l} -2(1+\nu_p\alpha^2)w_{m,n} + \nu_p\alpha^2(w_{m,n-1}+w_{m,n+1}) + w_{m-1,n} + w_{m+1,n} = 0 \\ \begin{bmatrix} \left(2+4\alpha^2-2\nu_p\alpha^2\right)(w_{m-1,n}-w_{m+1,n}) + \\ (2-\nu_p)\alpha^2\begin{pmatrix} -w_{m-1,n-1} - w_{m-1,n+1} \\ +w_{m+1,n-1} + w_{m+1,n+1}\end{pmatrix} - \\ w_{m-2,n} + w_{m+2,n}\end{bmatrix} = -\dfrac{G_p\iota^2}{D}\begin{pmatrix} \left(2(1+\nu_p\alpha^2) + 2\iota\sqrt{\dfrac{k_p}{G_p}}\right)w_{m,n} - \\ \nu_p\alpha^2\left(w_{m,n-1}+w_{m,n+1}\right) - 2w_{m\pm1,n}\end{pmatrix}\end{array}\right\} \quad (3.37)$$

2. Free edge (y = constant)

At $(x, 0)$ and (x, B);

$$\left.\begin{array}{l} -2(\nu_p+\alpha^2)w_{m,n} + \alpha^2(w_{m,n-1}+w_{m,n+1}) + \nu_p(w_{m-1,n} + w_{m+1,n}) = 0 \\ \begin{bmatrix} \left(4+2\alpha^2-2\nu_p\right)(w_{m,n-1}-w_{m,n+1}) + \\ \left(2-\nu_p\right)\begin{pmatrix} -w_{m-1,n-1} - w_{m+1,n-1} \\ +w_{m-1,n+1} + w_{m+1,n+1}\end{pmatrix} + \\ \alpha^2(-w_{m,n-2} + w_{m,n+2})\end{bmatrix} = -\dfrac{G_p\iota^2}{D\alpha^2}\begin{pmatrix} \left(2(\nu_p+\alpha^2) + 2\iota\alpha\sqrt{\dfrac{k_p}{G_p}}\right)w_{m,n} - \\ \nu_p\left(w_{m-1,n}+w_{m+1,n}\right) - 2\alpha^2 w_{m,n\pm1}\end{pmatrix}\end{array}\right\} \quad (3.38)$$

3. Free corner

At $(0,0)$, $(0,B)$, $(L,0)$, and (L,B);

$$\left.\begin{array}{l} w_{m-1,n} - 2w_{m,n} + w_{m+1,n} = 0 \\ w_{m,n-1} - 2w_{m,n} + w_{m,n+1} = 0 \\ \begin{bmatrix} \left(2+4\alpha^2-2\nu_p\alpha^2\right)(w_{m-1,n}-w_{m+1,n}) + \\ (2-\nu_p)\alpha^2\begin{pmatrix} -w_{m-1,n-1} - w_{m-1,n+1} \\ +w_{m+1,n-1} + w_{m+1,n+1}\end{pmatrix} - \\ w_{m-2,n} + w_{m+2,n}\end{bmatrix} = -\dfrac{G_p\iota^2}{D}\left(\left(1+\iota\sqrt{\dfrac{k_p}{G_p}}\right)w_{m,n} - w_{m\pm1,n}\right) \\ \begin{bmatrix} \left(4+2\alpha^2-2\nu_p\right)(w_{m,n-1}-w_{m,n+1}) + \\ \left(2-\nu_p\right)\begin{pmatrix} -w_{m-1,n-1} - w_{m+1,n-1} \\ +w_{m-1,n+1} + w_{m+1,n+1}\end{pmatrix} + \\ \alpha^2(-w_{m,n-2} + w_{m,n+2})\end{bmatrix} = -\dfrac{G_p\iota^2}{D\alpha}\left(\left(\alpha+\iota\sqrt{\dfrac{k_p}{G_p}}\right)w_{m,n} - \alpha w_{m,n\pm1}\right) \\ w_{m-1,n-1} - w_{m+1,n-1} - w_{m-1,n+1} + w_{m+1,n+1} = 0 \end{array}\right\} \quad (3.39)$$

The finite-difference representation of the fourth-order governing equation as shown in Figure (3.6) is valid for all points within the plate domain, including the plate edge nodes. However, the application of this equation at the boundary and specific nodes will result in nodes that are off the plate. Thus by utilizing the known boundary conditions, the following different types of points must be treated specifically, as shown in Figure (3.7) (Barton, 1948; Qin and Jahn, 2015).

- Points on free edge;
- Points adjacent to the free edge;
- Points on the free corner;
- Points inside free-free corner;
- Points adjacent to free corner on free edge;
- Points on the inner domain.

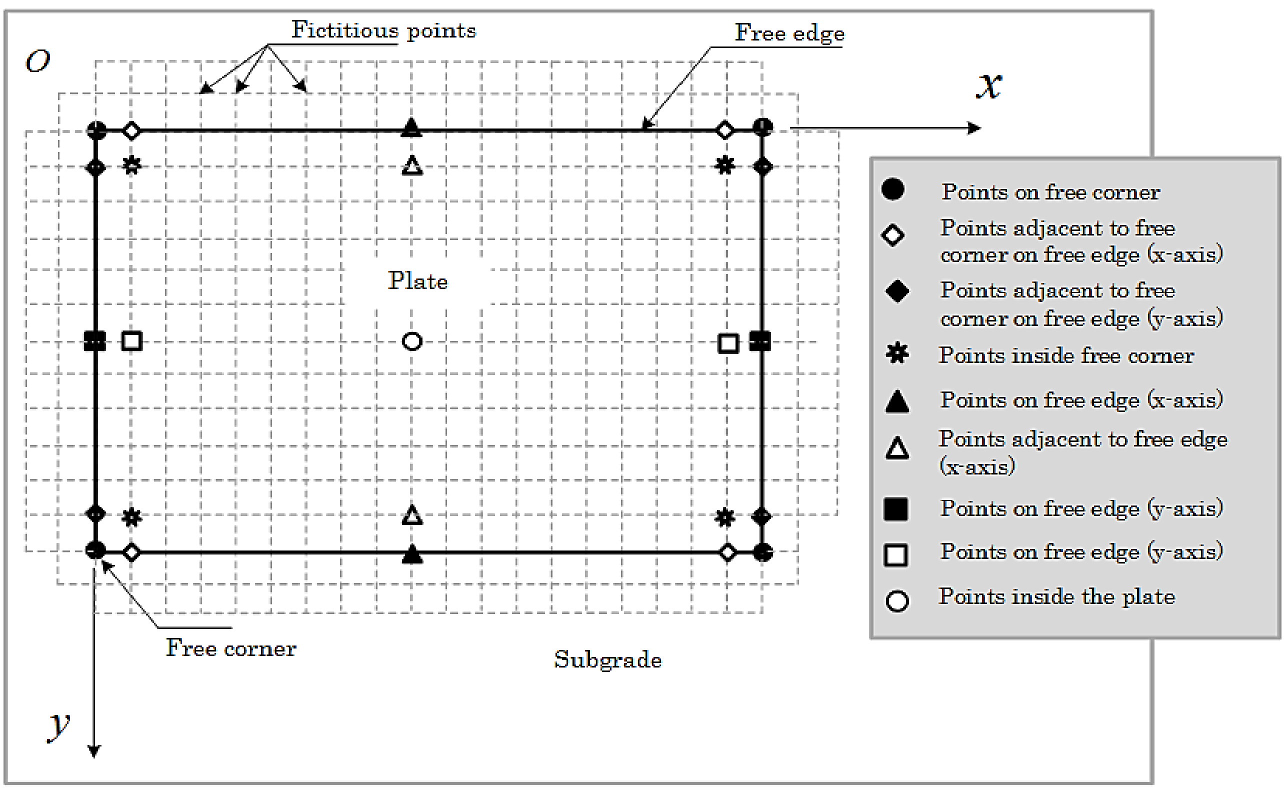

Figure 3.7: Schematic diagram of boundary and different specific points.

Take for example the pivotal point (m,n) is at the free edge along $y = 0$. Four fictitious points outside of the plate must be introduced (Figure 3.8). Deflections, $w_{m,n-1}$, $w_{m,n-2}$, $w_{m-1,n-1}$, and $w_{m+1,n-1}$, of fictitious points can be evaluated in terms of deflections of the mesh points located on the plate.

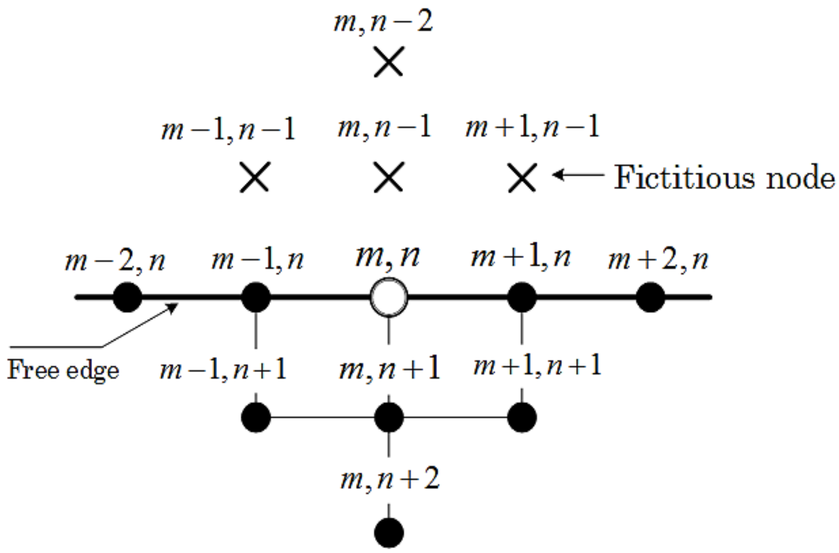

Figure 3.8: Pivotal point on the free edge after Szilard (2004)

Since four points are to be eliminated, five conditions are specified along the free edges.

General equation:

$$\begin{pmatrix} \left(6+8\alpha^2+6\alpha^4+2(1+\alpha^2)\hat{G}_p+\hat{k}_p\right)w_{m,n}+\alpha^4\left(w_{m,n-2}+w_{m,n+2}\right)- \\ \left(4(1+\alpha^2)+\hat{G}_p\right)\left(\alpha^2\left(w_{m,n-1}+w_{m,n+1}\right)+w_{m-1,n}+w_{m+1,n}\right)+ \\ 2\alpha^2\left(w_{m-1,n-1}+w_{m+1,n-1}+w_{m-1,n+1}+w_{m+1,n+1}\right)+w_{m-2,n}+w_{m+2,n} \end{pmatrix}=\left(\frac{q(x,y)\iota^4}{D}\right)_{m,n} \qquad (3.40)$$

Moment at m,n:

$$-2(\nu_p+\alpha^2)w_{m,n}+\alpha^2(w_{m,n-1}+w_{m,n+1})+\nu_p(w_{m-1,n}+w_{m+1,n})=0 \qquad (3.41)$$

Moment at $m-1,n$:

$$-2(\nu_p+\alpha^2)w_{m-1,n}+\alpha^2(w_{m-1,n-1}+w_{m-1,n+1})+\nu_p(w_{m-2,n}+w_{m,n})=0 \qquad (3.42)$$

Moment at $m+1,n$:

$$-2(\nu_p+\alpha^2)w_{m+1,n}+\alpha^2(w_{m+1,n-1}+w_{m+1,n+1})+\nu_p(w_{m,n}+w_{m+2,n})=0 \tag{3.43}$$

Shear at m,n:

$$\begin{bmatrix} \left(4+2\alpha^2-2\nu_p\right)(w_{m,n-1}-w_{m,n+1})+ \\ \left(2-\nu_p\right)\begin{pmatrix} -w_{m-1,n-1}-w_{m+1,n-1} \\ +w_{m-1,n+1}+w_{m+1,n+1} \end{pmatrix}+ \\ \alpha^2(-w_{m,n-2}+w_{m,n+2}) \end{bmatrix} = -\frac{G_p\iota^2}{D\alpha^2}\begin{pmatrix} \left(2(\nu_p+\alpha^2)+2\iota\alpha\sqrt{\dfrac{k_p}{G_p}}\right)w_{m,n}- \\ \nu_p\left(w_{m-1,n}+w_{m+1,n}\right)-2\alpha^2 w_{m,n+1} \end{pmatrix} \tag{3.44}$$

Eliminating $w_{m,n-1}$, $w_{m,n-2}$, $w_{m-1,n-1}$, and $w_{m+1,n-1}$ from these equations gives

$$\begin{pmatrix} c11\left(w_{m,n}\right)+c12\left(w_{m-1,n}+w_{m+1,n}\right)+c13\left(w_{m-2,n}+w_{m+2,n}\right)+ \\ c21\left(w_{m,n+1}\right)+c22\left(w_{m-1,n+1}+w_{m+1,n+1}\right)+2\alpha^4 w_{m,n+2} \end{pmatrix} = \left(\frac{q(x,y)\lambda^4}{D}\right)_{m,n} \tag{3.45}$$

Where

$$c11=6+8\alpha^2+2\alpha^4-8\nu_p\alpha^2-6\nu_p^2+2(1+\alpha^2+\iota\sqrt{\frac{k_p}{G_p}})\hat{G}_p+\hat{k}_p$$

$$c12=-4(1+\alpha^2)+4\nu_p\alpha^2+4\nu_p^2-\hat{G}_p$$

$$c13=1-\nu_p^2$$

$$c21=-4\alpha^2\left(2+\alpha^2-\nu_p\right)-2\alpha^2\hat{G}_p$$

$$c22=2\alpha^2\left(2-\nu_p\right)$$

$$\hat{k}_p=\frac{k_p\iota^4}{D}$$

$$\hat{G}_p=\frac{G_p\iota^2}{D}$$

$$\alpha=\frac{\Delta x}{\Delta y}$$

$$\iota=\Delta x=\alpha\Delta y$$

Other boundary and specific points have been determined in a similar manner and results are outlined in Appendix B.

3.2.3. Load Representation

In the derivation of the relevant finite difference equations for plate flexure, it is convenient to replace the applied loads by equivalent systems of nodal point loads. Generally, the external loading, $q(x, y)$, is distributed in such a way that an average pressure intensity, with units of stress, can be assigned to each node in the grid system. For uniformly distributed load the equivalent nodal point load can be represented by

$$\{q\}_{m,n} = (q_o)_{m,n} \tag{3.46}$$

In addition to this type of loading the type of external loads that may be applied over a localized area or at a point should also be considered. When such a concentrated load acts at a nodal point, the weighted representation of load at the pivotal point becomes

$$\{q\}_{m,n} = \left(\frac{P}{(\Delta x)(\Delta y)}\right)_{m,n} = \left(\frac{P\alpha}{\iota^2}\right)_{m,n} \tag{3.47}$$

Where $\Delta x = \alpha \Delta y = \iota$ and $\alpha = \dfrac{\Delta x}{\Delta y}$.

3.2.4. Development of the Coefficient Matrix

By representing the governing differential equation of the plate and the equations defining the prescribed boundary conditions of a given problem by finite difference expressions, the continuum of the plate has been replaced with a pattern of discrete points. Consequently, the original problem of solving the plate equation has been transformed into the solution of a set of simultaneous algebraic equations in the form

$$[C]\{w\} = \{q\} \tag{3.48}$$

Where $[C]$ symbolizes the resulting coefficient matrix, $\{w\}$ is the vector of the nodal displacements and $\{q\}$ represents the applied equivalent-loads vector.

3.2.5. Moments, Shears and Reactions

After the simultaneous equations have been solved for the deflections, the moments, shears, and reactions of the soil can be easily determined at each node in the grid system of the plate. The discretization form of M_x, M_y and M_{xy} in terms of finite differences at the point (m,n) is given by

$$(M_x)_{m,n} = -\frac{D}{\iota^2}\left[-2(1+v_p\alpha^2)w_{m,n} + v_p\alpha^2(w_{m,n-1}+w_{m,n+1}) + w_{m-1,n} + w_{m+1,n}\right]$$

$$(M_y)_{m,n} = -\frac{D}{\iota^2}\left[-2(v_p+\alpha^2)w_{m,n} + \alpha^2(w_{m,n-1}+w_{m,n+1}) + v_p(w_{m-1,n} + w_{m+1,n})\right] \tag{3.49}$$

$$(M_{xy})_{m,n} = -\frac{D(1-v_p)\alpha}{4\iota^2}\left(w_{m-1,n-1} - w_{m+1,n-1} - w_{m-1,n+1} + w_{m+1,n+1}\right)$$

The discretized form of the shears also given by

$$\left(V_x\right)_{m,n} = -\frac{D}{2\iota^3}\begin{bmatrix}\left(2(1+\alpha^2)+\hat{G}_p\right)(w_{m-1,n}-w_{m+1,n}) - \alpha^2(w_{m-1,n-1}+w_{m-1,n+1}) + \\ \alpha^2(w_{m+1,n-1}+w_{m+1,n+1}) - w_{m-2,n} + w_{m+2,n}\end{bmatrix}$$

$$\left(V_y\right)_{m,n} = -\frac{D\alpha}{2\iota^3}\begin{bmatrix}\left(2(1+\alpha^2)+\hat{G}_p\right)\left(w_{m,n-1}-w_{m,n+1}\right) + \alpha^2(-w_{m,n-2}+w_{m,n+2}) - \\ w_{m-1,n-1} - w_{m+1,n-1} + w_{m-1,n+1} + w_{m+1,n+1}\end{bmatrix} \tag{3.50}$$

In the case that the moment, shear, or reaction expression is in terms of deflections off the plate, then the expressions must be modified by the application of the boundary conditions so that the points external to the plate are eliminated. This procedure is similar to that used before so that only the results will be indicated. Appendix C gives the expressions for moments, shears and soil reactions for specific points on or near various edges.

3.2.6. Convergence criteria of FDM

In planning the analysis of a plate by means of the ordinary FDM, the convergence characteristics of this numerical procedure must be considered. This can be done by determining the optimum mesh size of the FDM so that adequately accurate result is attained. Generally, the mesh size (Δx or Δy) represents the fineness of the mesh for finite difference discretization.

It affects the two kinds of errors, that is, truncation error and the round off error. The truncation error decreases with decreasing mesh size, while the round off error generally increases (Selvadurai, 1979).

When using very small subdivisions, the convergence becomes quite slow. In addition, the number of equations to be solved increases exponentially. Furthermore, an extremely fine mesh and the resulting large number of simultaneous equations may create round-off errors in their solution that adversely affect its accuracy (Szilard, 2004).

For this study convergence criteria has been studied for a $4m \times 4m \times 0.4m$ concrete plate resting on a strong soil with Elastic modulus of 80000 MPa and a Poisson's ratio of 0.25. The plate is centrally loaded with a concentrated load of 200 kN. In order to see the convergence characteristics the maximum deflection against the number of nodes has been plotted. The study starts with a 5×5 nodes (see window in Figure (3.9)) and then the number of nodes is increased until the maximum deflection values become more or less constant. As Figure (3.9) indicates, the ordinary FDM converges relatively fast toward the exact solution of a given plate problem, provided that the finite difference mesh is not too fine.

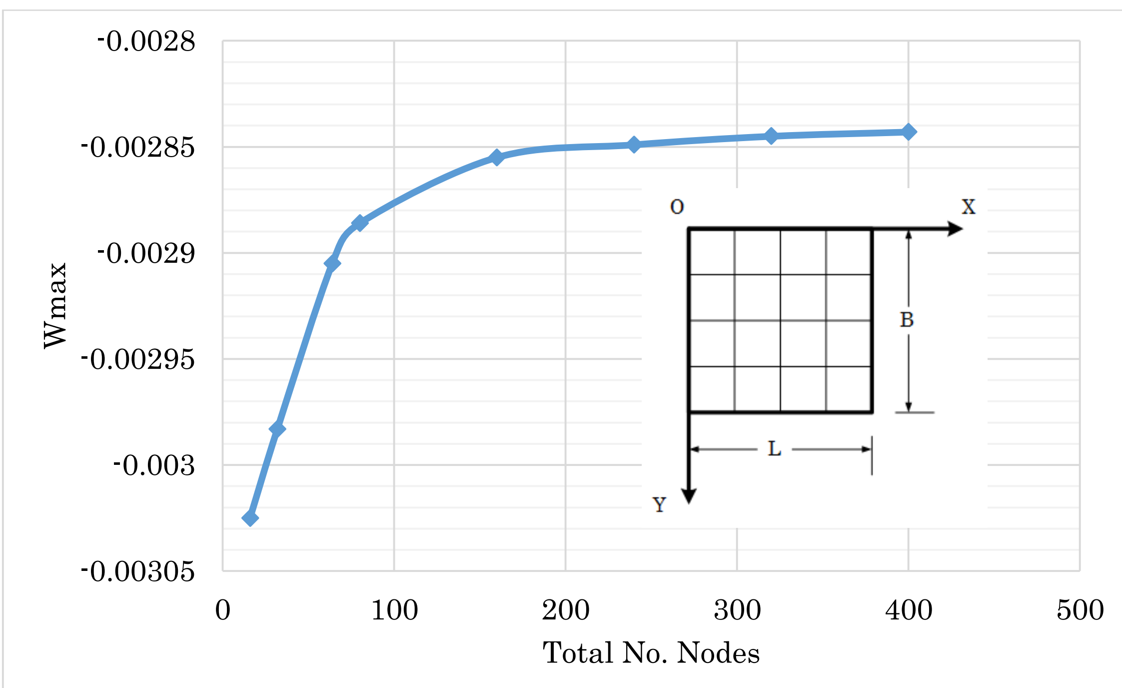

Figure 3.9: Convergence of ordinary FDM

3.3. Programming

MATLAB® program is written for the computation of the deflections and internal actions of the plate and provided in Appendix F. The program enables to analyze rectangular plate on elastic foundation subjected to concentrated load, uniformly distributed load, a concentrated moment, and different combinations of loadings. The program contains logical steps when implementing the finite difference method. The flow chart, which expresses the procedure of the computer program, is shown in Figure (3.10).

A typical finite difference program consists of the following sections

1. Pre-processing section

2. Processing section

3. Post-processing section

In the preprocessing section, the data and structures that define the particular problem statement are defined. These include the finite difference discretization, soil and plate properties, and loading condition. Table (3.1) shows lists of all necessary input parameters for the particular problem.

Table 3.1: Lists of input parameters for the MATLAB® program

The finite difference discretization	Soil properties	Plate properties		Loading
Number of nodes	Modulus of elasticity of the soil (E_s)	Modulus of elasticity of the plate (E_p)	Length of the plate (L)	Load magnitude
	Poisson's ratio of the soil (ν_s)	Poisson's ratio of the plate (ν_p)	Width of the plate (B)	Load location and span of the loaded region
	Thickness of the stratum(H)		Thickness of the plate (h_p)	

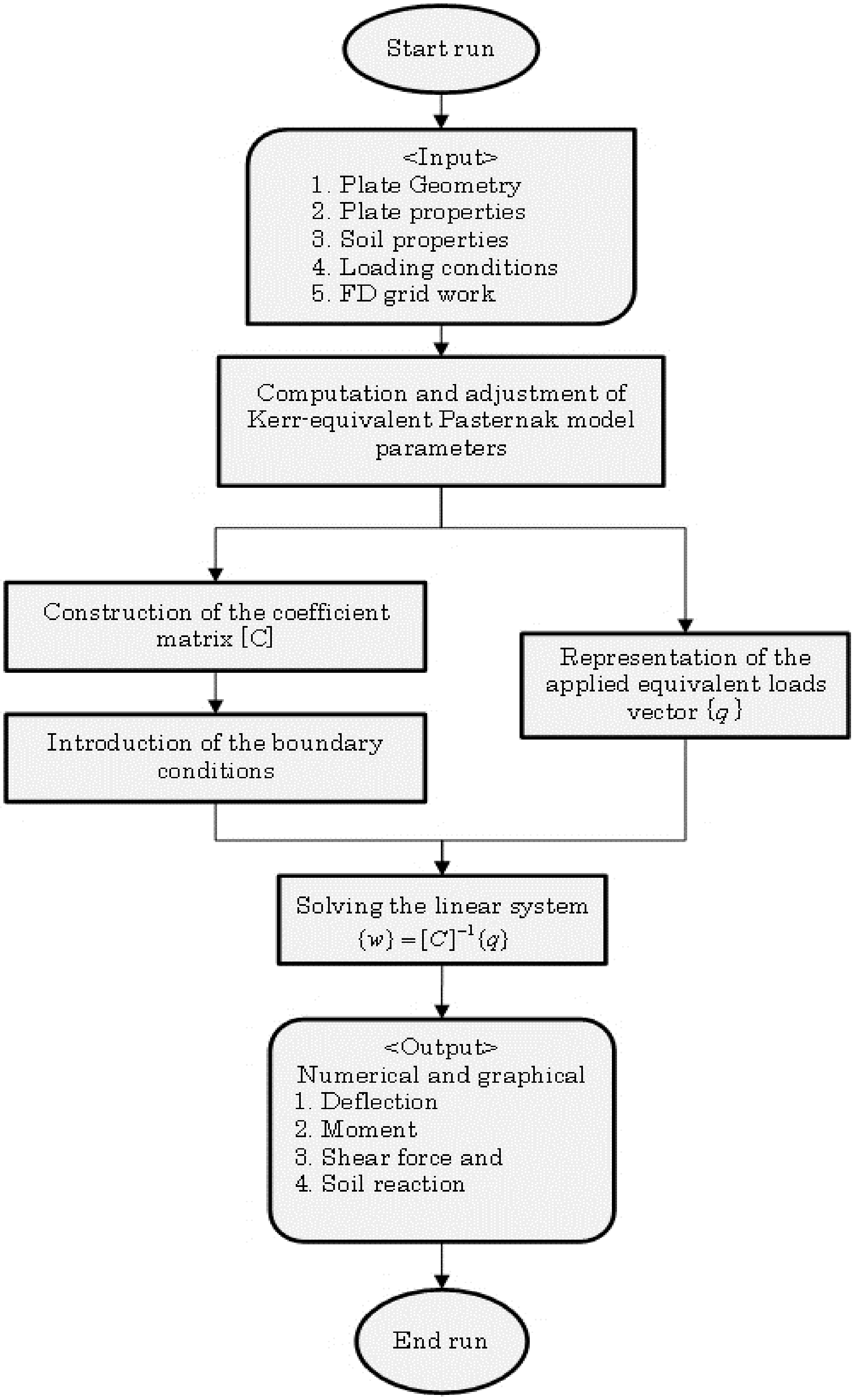

Figure 3.10: Flow chart of the general program.

The processing section includes the following steps

1. Definition of the coordinates (x_m, y_n) of any mesh point,
2. Construction of the linear system,
3. Introduction of the boundary conditions,
4. Solving the linear system,

The post-processing section is where the results from the processing section are analyzed. Here deflections and internal actions may be calculated and data can be visualized. The post-processing section comprises the following output results

- Deflection
- Moment
- Shear force and
- Soil reaction

4. Model Adjustment, Analysis, and Illustrations

4.1. General

In this chapter, a numerical study and adjustment of the selected model are conducted using the different solutions obtained for the rectangular plate on Pasternak-type subgrade model under several practical loading conditions. The solutions for different loadings supported by Pasternak's foundation are expressed in terms of the coefficients of the elastic spring, k_p and the shear layer, G_p. As these coefficients are dependent on the plate and soil parameters, various solutions of the deflection with the loading types are obtained. As mentioned before, the subgrade reaction is not a fundamental soil property. It rather varies with the foundation type, foundation dimension, and type of loading. The effects of these factors can be incorporated by introducing a different form of relative rigidity factor for the soil-plate system. One of such a definition is used by Kerr (1985) and Selvadurai (1979) and given by

$$\bar{\lambda} = \sqrt[4]{\frac{k_p}{D}} \tag{4.1}$$

Where k_p and D are as defined before.

However, this relative rigidity involves the spring coefficient that depends on the adjustment factor which is yet to be determined. Thus the following dimensionless stiffness factor or relative rigidity of the soil-plate system has been used as suggested by Gorbunov-Possadov and Serebrjanyi (1961) is found more convenient for this work:

$$K_r = \frac{\pi L^2 B E_s}{8D(1-v_s^2)} \tag{4.2}$$

Where L and B are the length and width of the plate, respectively.

The soil properties taken for analysis and illustration purpose are shown in Table (4.1).In the case of plate material properties, the most widely used material for the foundation is concrete which has an elastic modulus of about 30 GPa and Poisson's ratio of 0.2.

Table 4.1: Soil Properties (Bowles, 1997; Briaud, 2013, and Das and Sobhan, 2013)

Soil type	Es (kPa)	v_s
Weak soil (loose sand and soft clay)	10000-30000	0.35-0.5
Medium strength soil (Medium dense sand and Medium stiff clay)	30000-80000	0.25-0.4
Strong soil (Dense sand and Hard clay)	80000-150000	0.2-0.4

4.2. Adjustment of Kerr equivalent Pasternak-type model

All continuum models including the generalized continuum models developed by Worku are sensitive to the thickness of the stratum. Thus as the thickness of the soil layer increases, it may give excessive deformation. Therefore, it is important to adjust this model by using different methods. The adjustment can be done with the use of FE-based software, existing theoretical results, or laboratory model testing. For this study, adjustment of the model has been accomplished using the FE-based software since it is feasible and handy.

Among the FE-based softwares, Plaxis 3D has been selected for the study. It is a finite element program for geotechnical applications in which the soil behavior is simulated using different models. The program code has been developed with great care. Although a lot of testing and validation has been performed, it cannot be guaranteed that the Plaxis code is free of some numerical and modeling errors in general. Moreover, the accuracy depends highly on the expertise of the user regarding the modeling of the problem, the understanding of the soil models and their limitations, the selection of model parameters, and the ability to judge the reliability of the computational results (Brinkgreve, Engin, and Swolfs, 2013).

There are 2D and 3D versions of Plaxis, where the 2D package is intended for the two-dimensional analysis of deformation and stability in geotechnical engineering. Plaxis 3D Foundation is a three-dimensional Plaxis program, developed for the analysis of foundations including raft and pile structures. 3D version of Plaxis has been used for the modeling of Plates on an elastic foundation.

In order to adjust the model the first thing to do is to obtain the optimum mesh quality and size of the Finite element modeling so that a sufficiently accurate result is achieved. This is because all the output of the Plaxis 3D is affected by the mesh size. As the mesh size becomes finer, the quality of the mesh improves and results that are more accurate will be obtained but it will take a longer time to get the results. Hence, it is necessary to find the optimum mesh size to balance between the computation time and accuracy. This is obtained by plotting the average quality of the mesh and the maximum deflection against the mesh size.

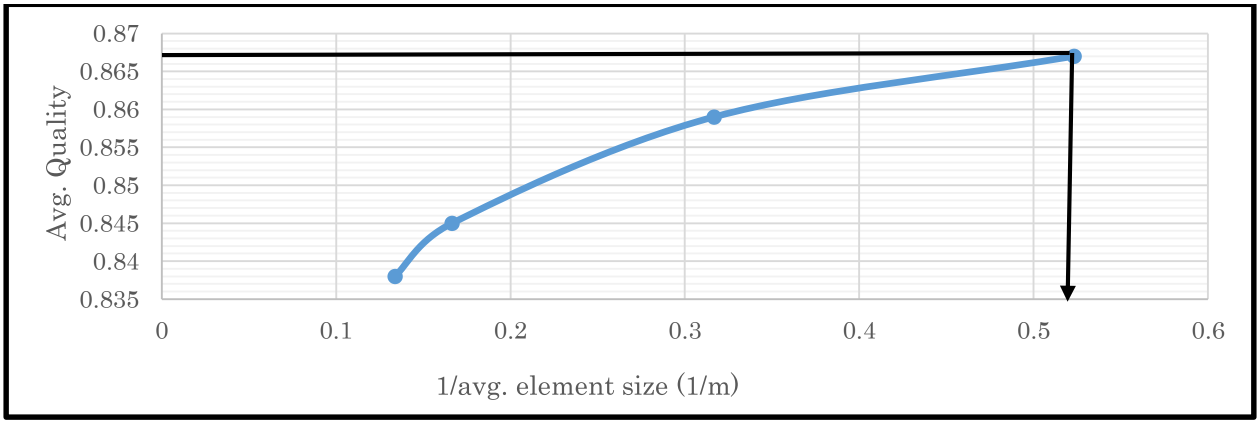

Figure 4.1: Quality of the mesh

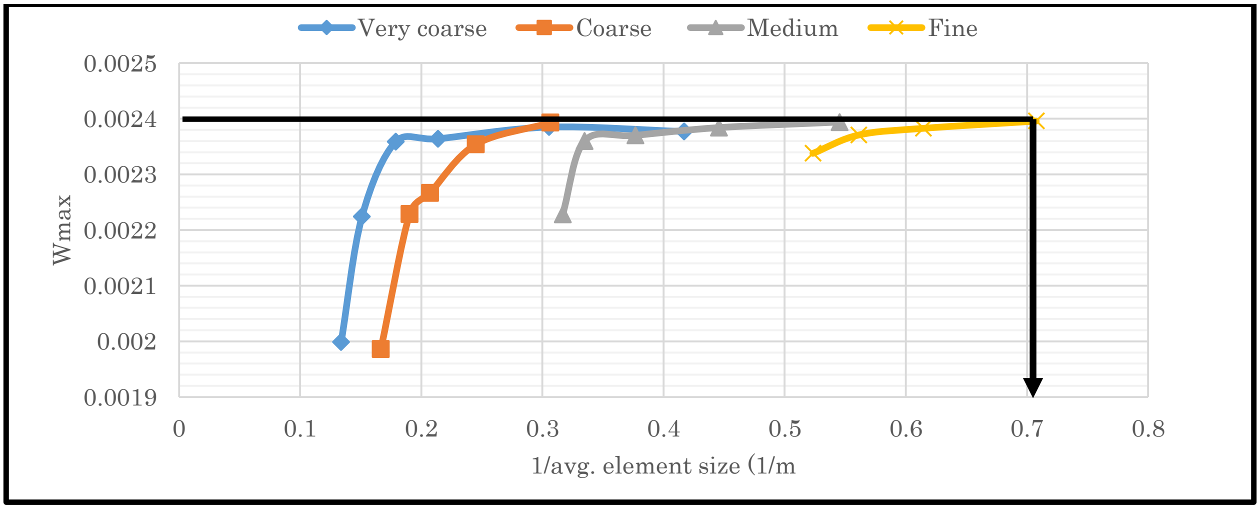

Figure 4.2: Effects of mesh size and local refinement on the deflection

As it is shown in Figures (4.2), the average mesh size is determined by drawing a horizontal tangent line where the maximum deflection becomes almost constant. It can be seen that the average element size which results in a more or less constant deflection is about

1.43 m. The graph also shows that within a global mesh size, local mesh refinement improves the accuracy of results.

The next step is the adjustment of the Kerr-equivalent Pasternak-type continuum model of Worku. This is achieved after a large number of analysis involving different types of soils is conducted, with the various relative thickness of the stratum. Subsequently, the maximum deflection (w_{max}), is plotted against the adjustment factor χ, for rectangular plates subjected to different loading cases (Figure 4.3). The analysis using Worku's analytical subgrade model is conducted with the help of the MATLAB® program based on the finite difference method presented in Chapter 3 and developed for this purpose.

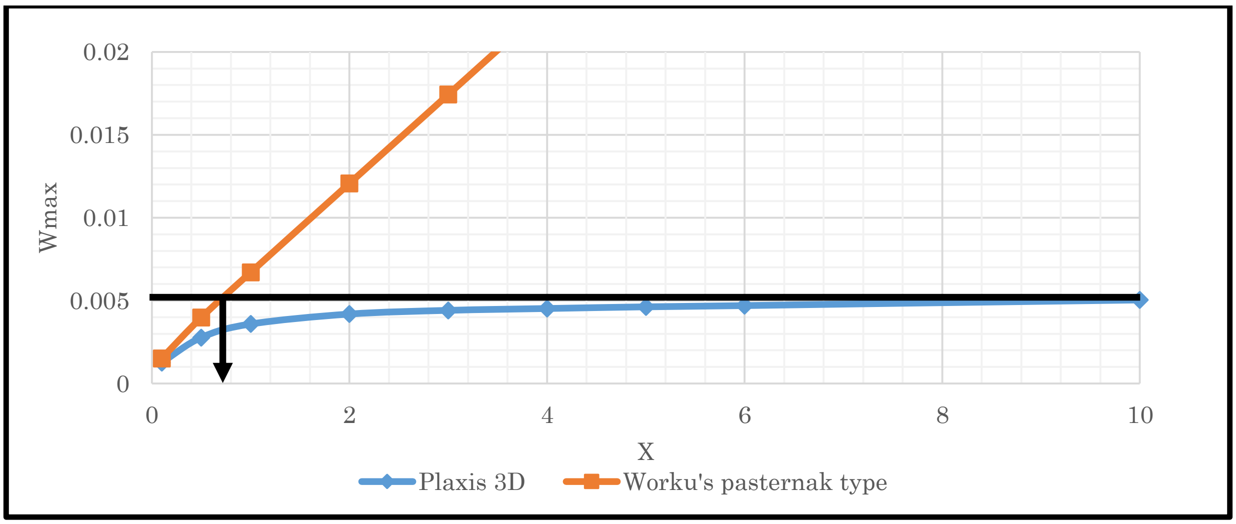

Figure 4.3: Determination of χ

This whole process is repeated for a sufficient range of relative rigidity values desired to cover any possible practical range for the different practical loading conditions. Finally, the best fitting trend is established for the model between adjustment factor, χ and the relative rigidity of the plate - soil system, K_r, for the ranges of values observed from Figure (4.3). These plots are presented in Figures (4.4) to (4.6). Thus the model adjustment factors in the analysis rectangular plates based on different L/B ratios are shown for concentrated loading in the Figure (4.4), for distributed loading in Figure (4.5), and for combined loading in Figure (4.6).

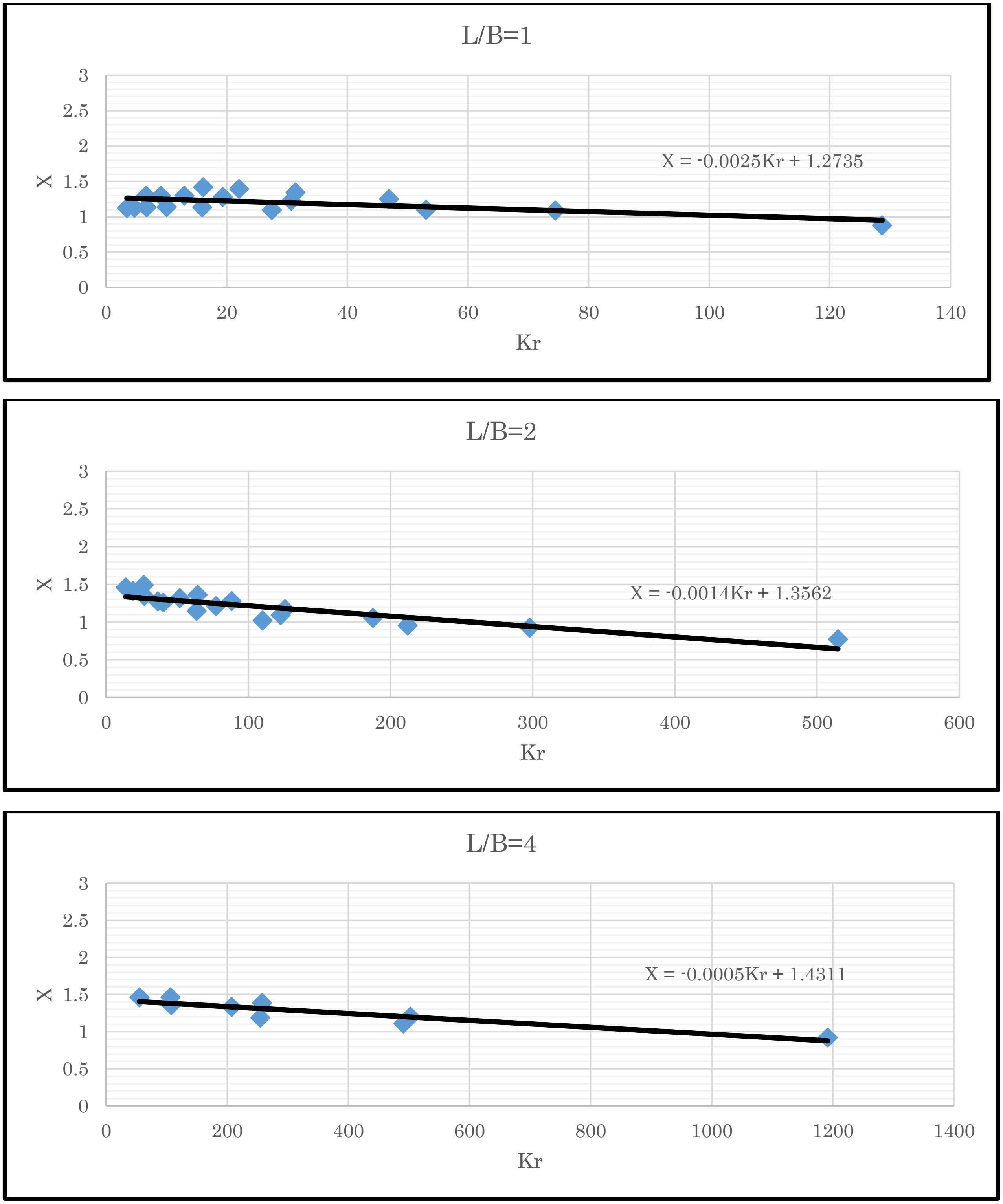

Figure 4.4: Adjustment factor for Pasternak's subgrade model for a centrally concentrated loading on rectangular plates with different L/B ratio.

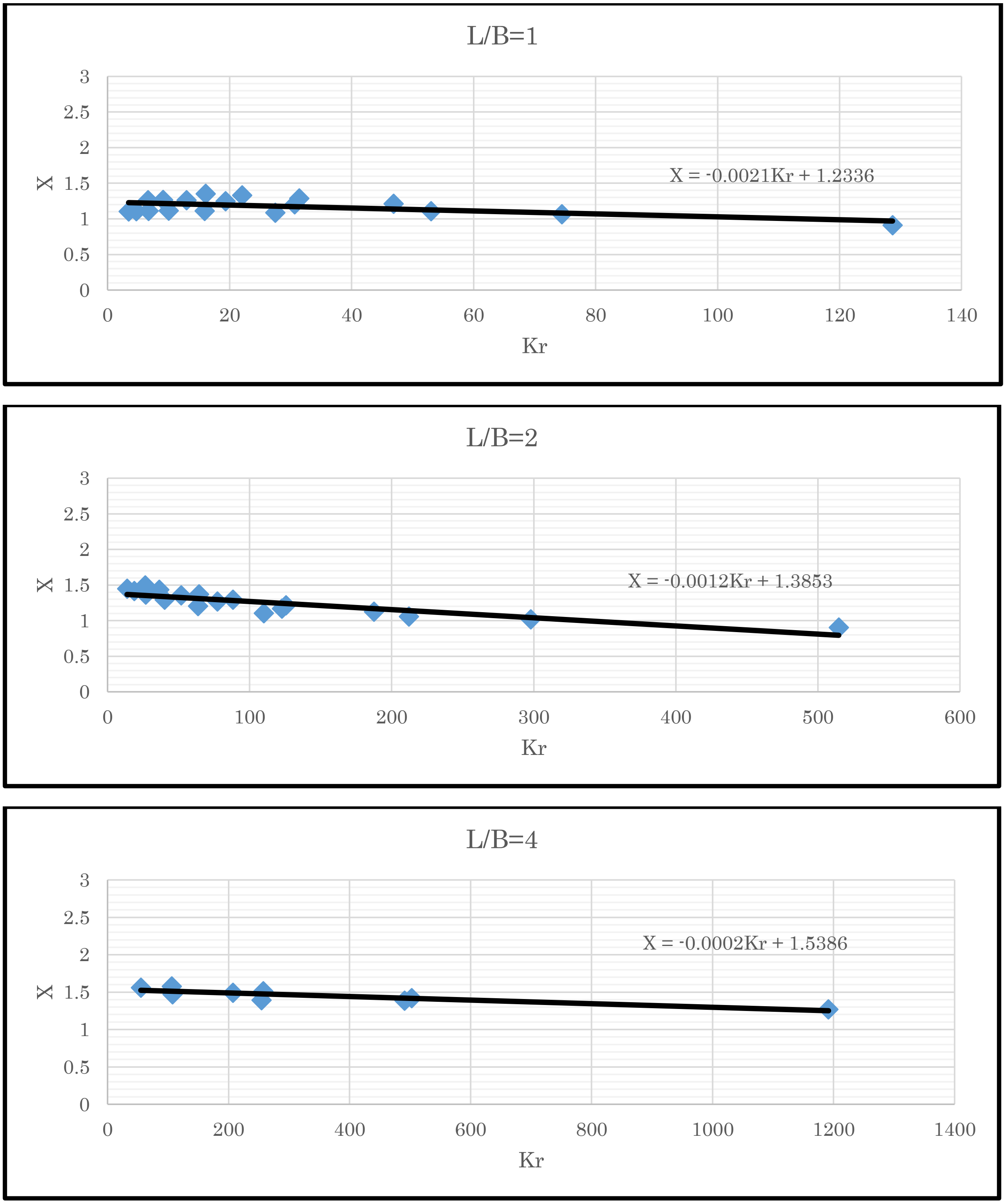

Figure 4.5: Adjustment factor for Pasternak's subgrade model for a distributed loading on rectangular plates with different L/B ratio.

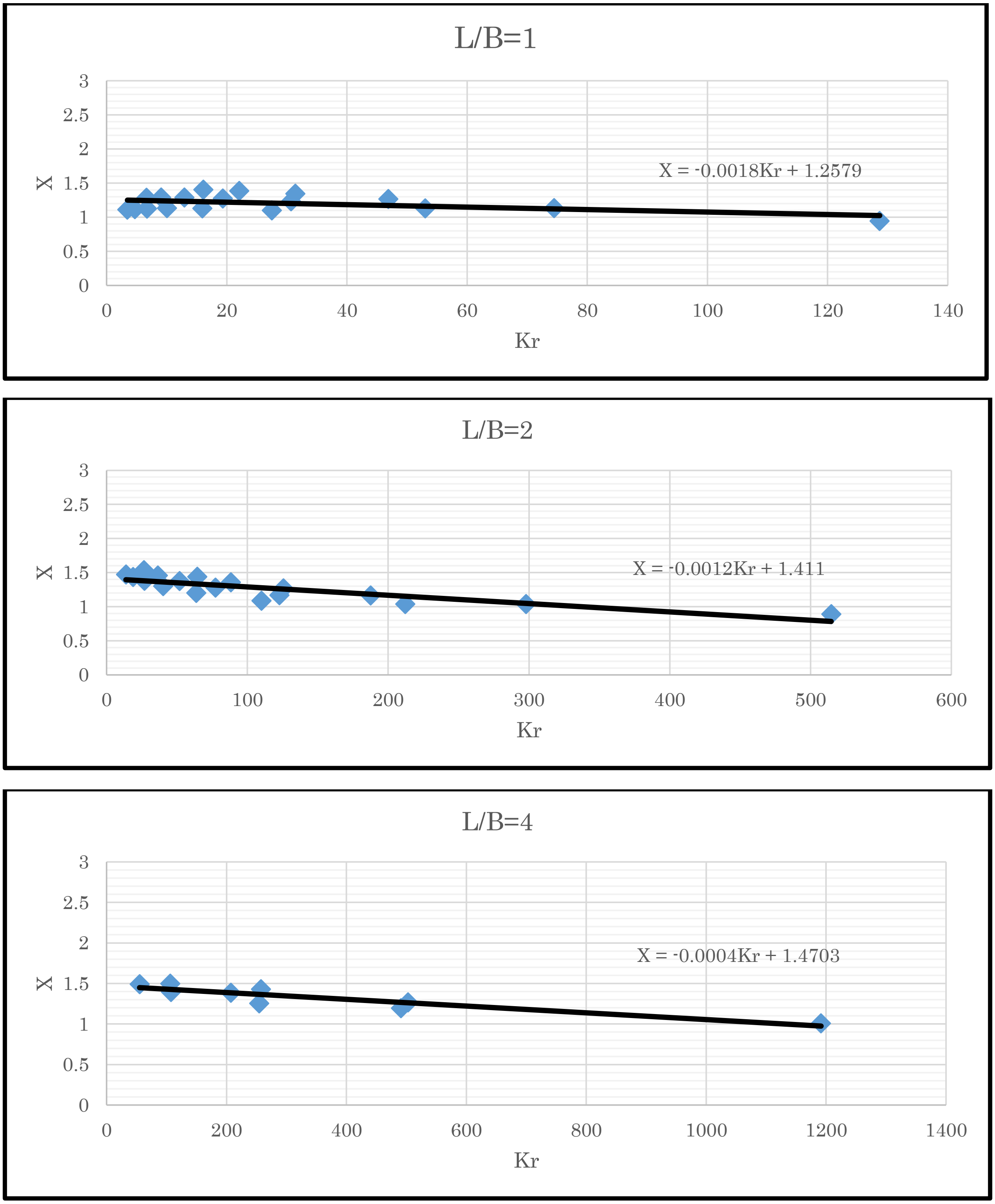

Figure 4.6: Adjustment factor for Pasternak's subgrade model for a combined loading on rectangular plates with different L/B ratio.

As shown in the above plots of the adjustment factor, χ, versus the soil-plate relative rigidity factor, K_r, it can be seen clearly that almost all points lie on a narrow band, and the plots show a consistent trend for different types of loading. Thus the trend of the fitted curves shows that the adjustment factor, χ, is not sensitive to soil and plate parameters and the magnitude of the load.

Furthermore, the influence of the load location on the adjustment factor has been studied which is not included here. As the load location moves away from the center the adjustment factor, χ, decreases steadily toward the edges and is about halved at the edge of the plate.

Subsequently, continuum models generally are sensitive to the thickness of the stratum for an actual stratum with $H > \chi B$, the adjustment factors shown in Figures (4.4) to (4.6) are to be employed; whereas in the case of $H < \chi B$, the actual soil stratum thickness is used.

Thus Worku's Kerr-equivalent Pasternak type model parameters together with the adjustment factors given for the subgrade model in Figures (4.4) to (4.6), may be expressed as (Worku 2014);

$$
\begin{aligned}
k_p &= \frac{\left(0.4\nu_s + 0.67\right) E_s}{\chi B} \\
G_p &= \left(1.36\nu_s + 2.28\right) G_s B \chi
\end{aligned}
\tag{4.2}
$$

4.3. Numerical Comparison

Numerical computations for a rectangular plate subjected to a concentrated lateral load, a uniformly distributed load, and combined loads are carried out for different types of soil. Subsequently, the results obtained from the Kerr-equivalent Pasternak-type subgrade model and the FE-based Plaxis 3D model are compared. The input parameters are given below.

Input Parameters:

A) Plate Properties (Concrete)
- Elastic modulus of the plate (Ep) =30 GPa
- Poisson's ratio(v_p) = 0.2

B) Plate geometry based on L/B ratio
  I. L/B=1
    - Length of the plate (L) = 5 m
    - Width of the plate (B) = 5 m
  II. L/B=2
    - Length of the plate (L) = 10 m
    - Width of the plate (B) = 5 m

C) The thickness of the plate (h_p) = 0.5 m

D) Soil data
- Medium strength soil
  - Elastic modulus of the soil (Es) = 40 MPa
  - Poisson's ratio (v_s) = 0.3
- Stratum thickens H=60 m for all types of soil

E) Loading Conditions
- Vertical Concentrated force at the center
  - P=2000 kN
- Uniformly distributed load
  - q=50 kN/m^2, centrally Loaded over L/2 m × B/2m area
- Combined load
  - P=2000 kN, and q=50 kN/m^2

F) The adjustment factor (χ) generated from the fitted curves (Figure (4.4)-(4.6)) based on L/B ratio

- L/B=1
  - Vertical Concentrated force: $\chi = 1.15$
  - Uniformly distributed load: $\chi = 1.26$
  - Combined load: $\chi = 1.29$
- L/B=2
  - Vertical Concentrated force: $\chi = 1.43$
  - Uniformly distributed load: $\chi = 1.49$
  - Combined load: $\chi = 1.51$

Finite Element (Plaxis 3D) Inputs

- Soil and plate material model
  - Linear elastic model
- Mesh type
  - Fine
- Element
  - 6-node triangular element for the plate and
  - 10-node tetrahedral element for the soil

Subgrade Model:

- Two parameter subgrade model
  - Worku's Kerr equivalent Pasternak-type model

Plaxis 3D and FDM analysis results of deflection, moments, and shear forces are evaluated and presented graphically for the plate and soil parameters given above. Shaded plots of deflection ($w(x,y)$), the moment about the y-axis (M_x), shear force in the x-axis (V_x), and torsional moment (M_{xy}) are presented. Furthermore, sectional plots of deflection ($w(x,y)$), the moment about the y-axis (M_x), and shear force in the x-axis (V_x) are also presented for comparison purpose. The deflection and all the internal actions can be found in Appendix D.

4.3.1. Numerical analysis of Rectangular plate with L/B=1

i. Concentrated load

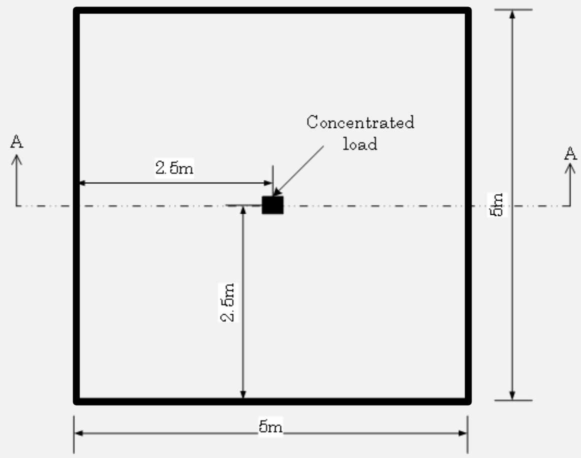

Worku's Pasternak type model (FDM) **Plaxis 3D**

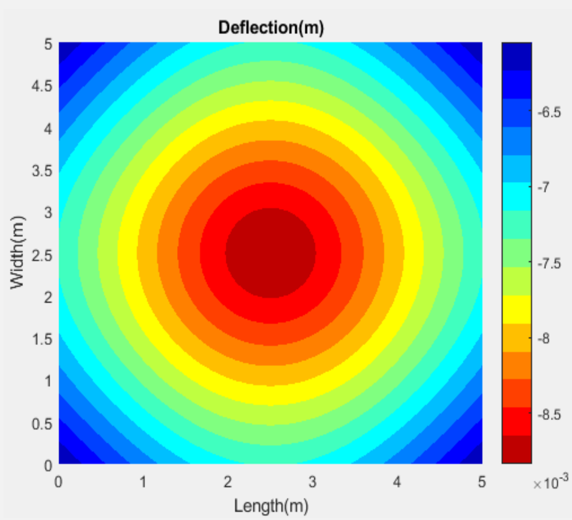

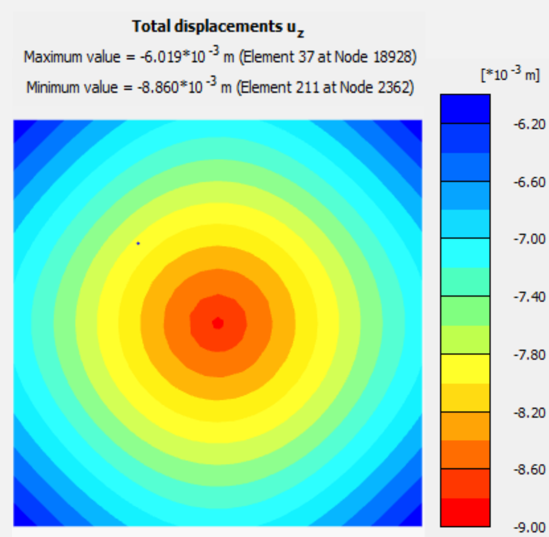

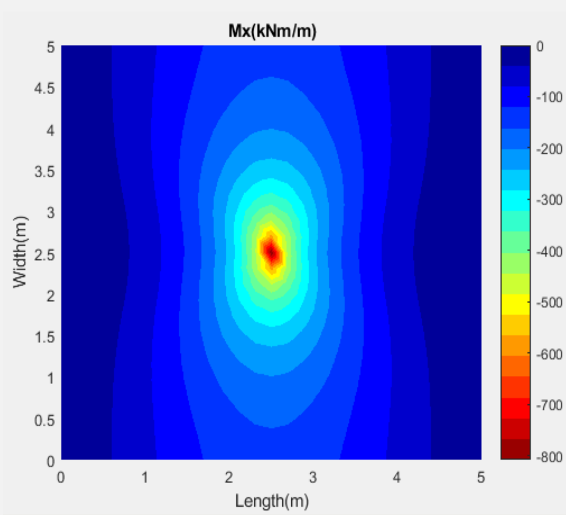

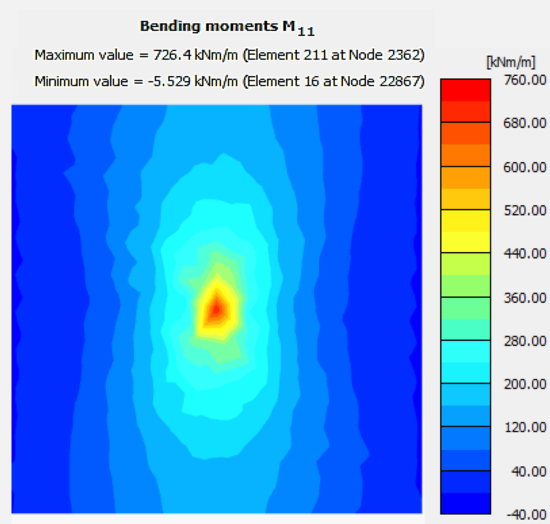

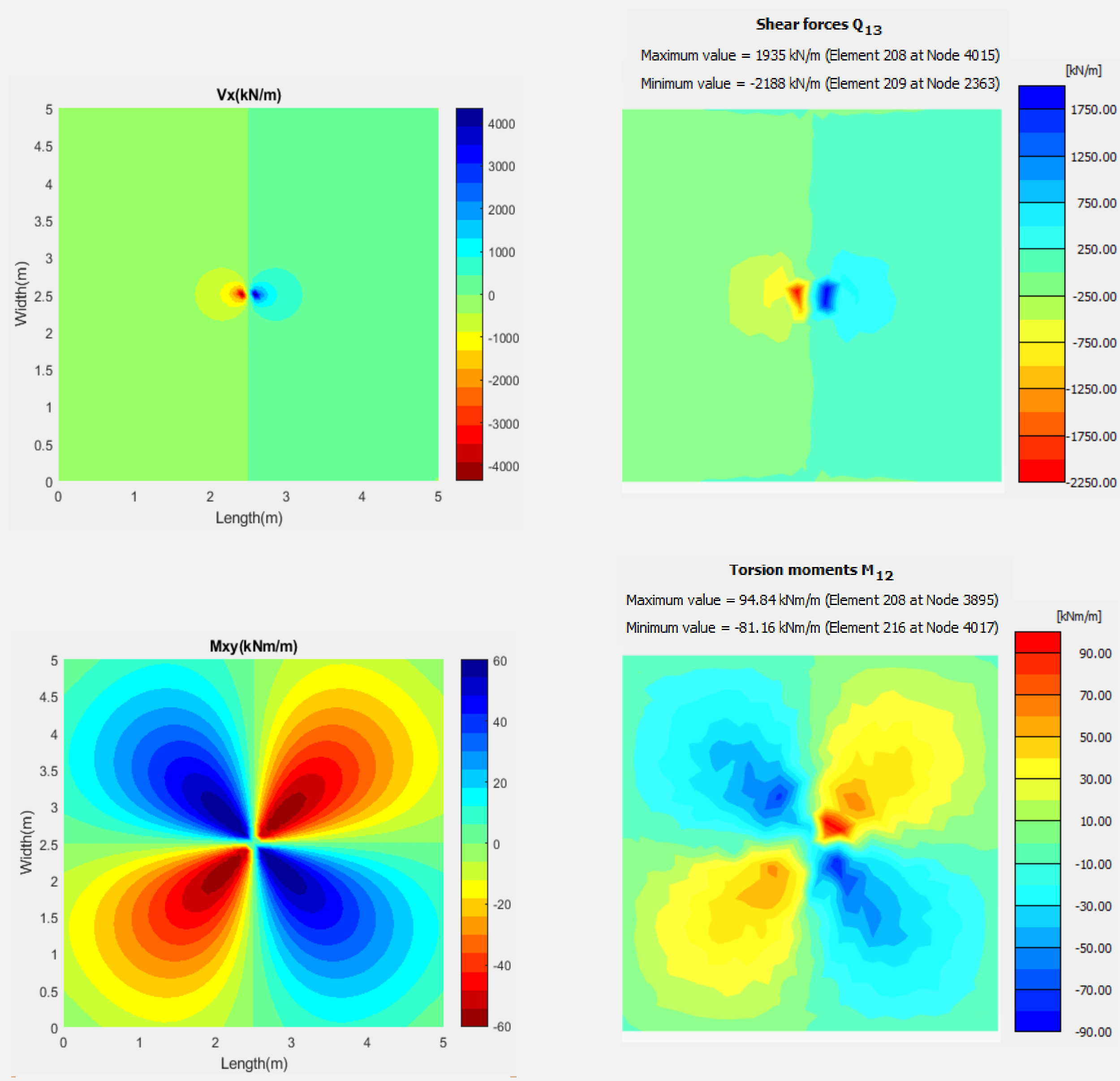

a) b)

Figure 4.7: Deflection and internal action of Rectangular plate (L/B=1) resting on Medium strength soil subjected to a vertical concentrated load based on; a) Worku's Pasternak type model (FDM) b) Plaxis 3D

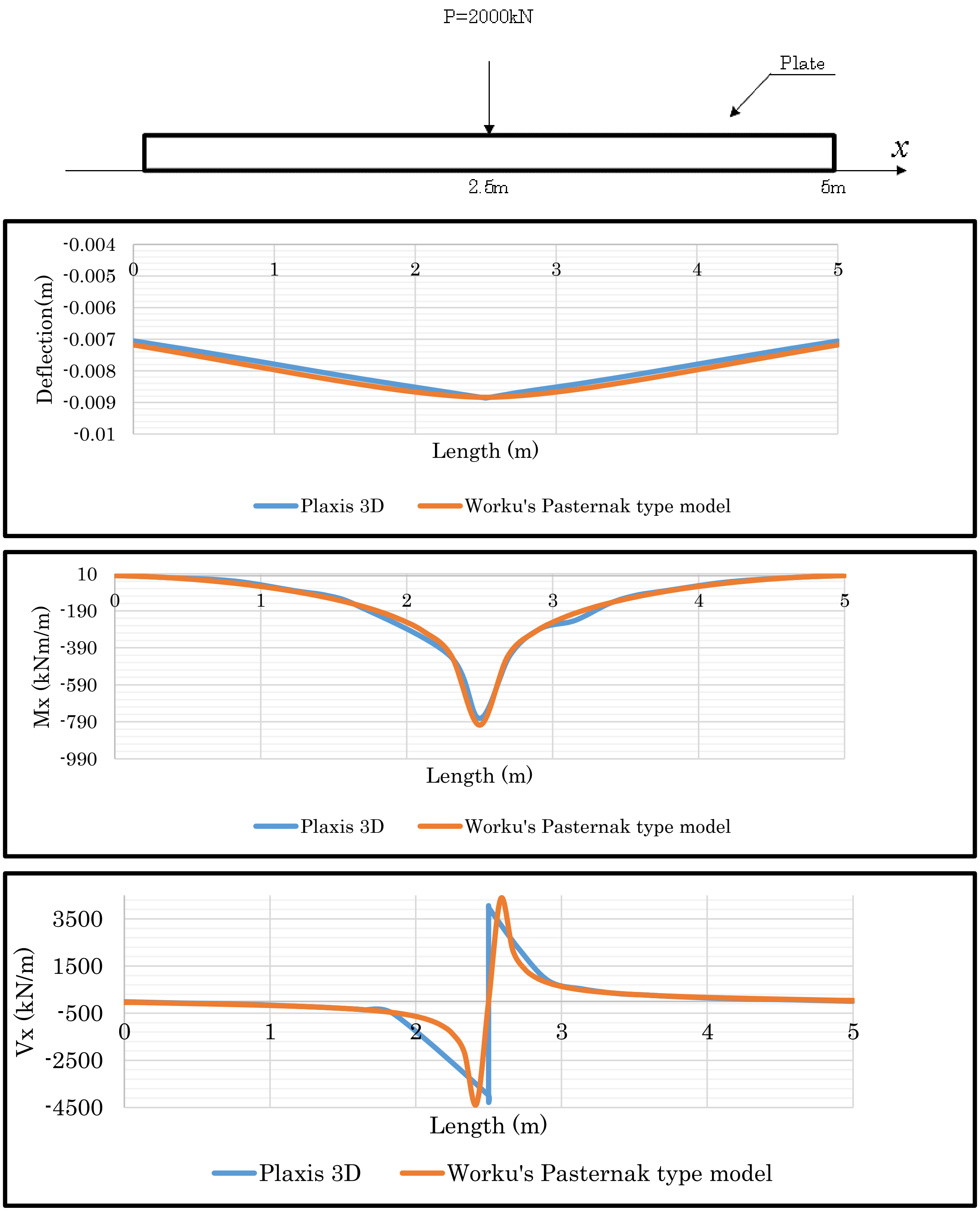

Figure 4.8: Section A-A view of the plate resting on medium soil subjected to a vertical concentrated load

Significant observations from the plotted results include

- The deflection obtained by using Worku's adjusted model is in a very good agreement with the Plaxis 3D model.
- Shear forces show a slight deviation. This can be attributed to mesh dependency of the FEM and FDM.
- Maximum moments shows little deviation which is minor.

ii. Uniformly distributed

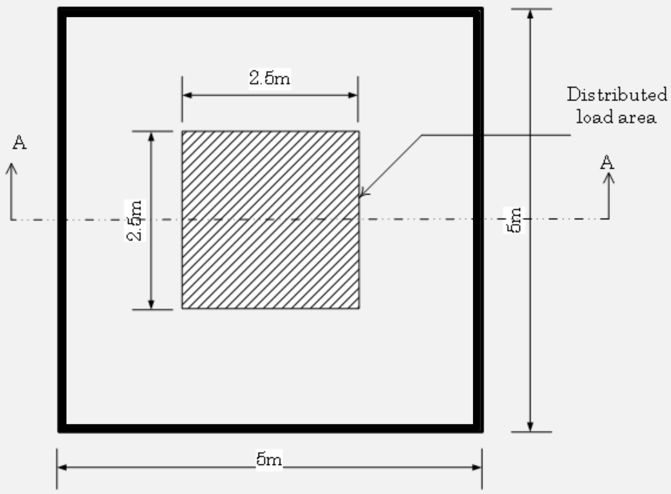

Worku's Pasternak type model (FDM) **Plaxis 3D**

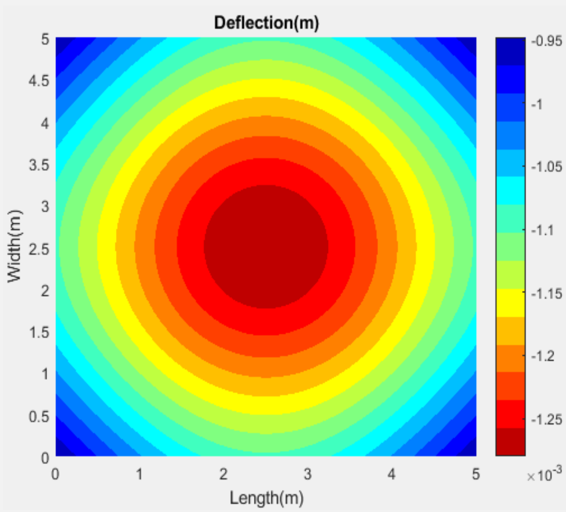

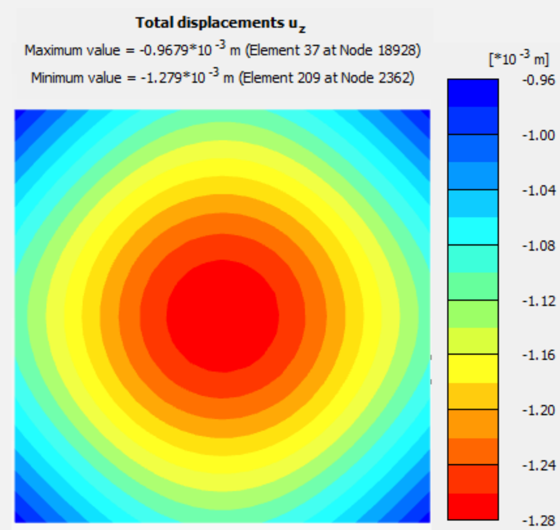

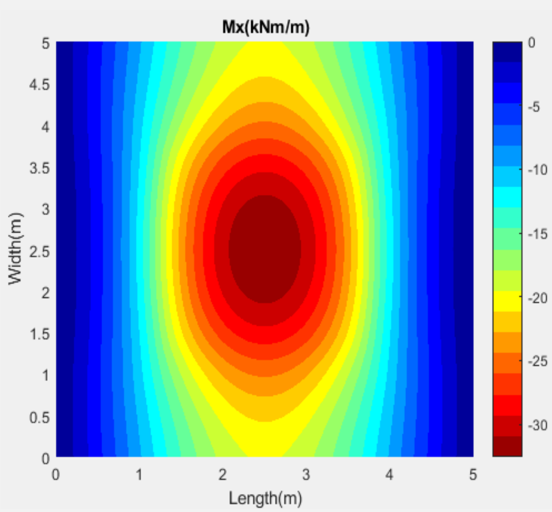

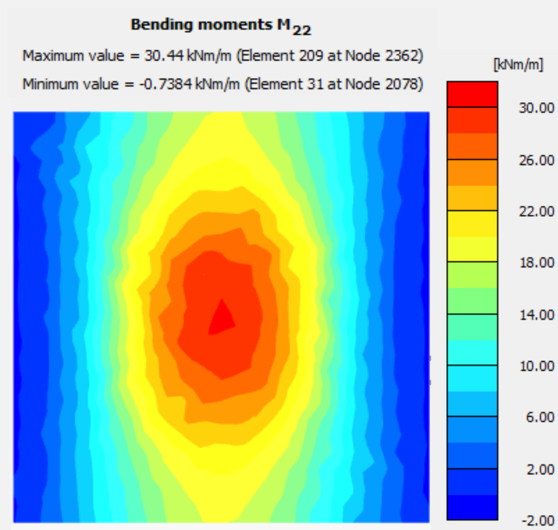

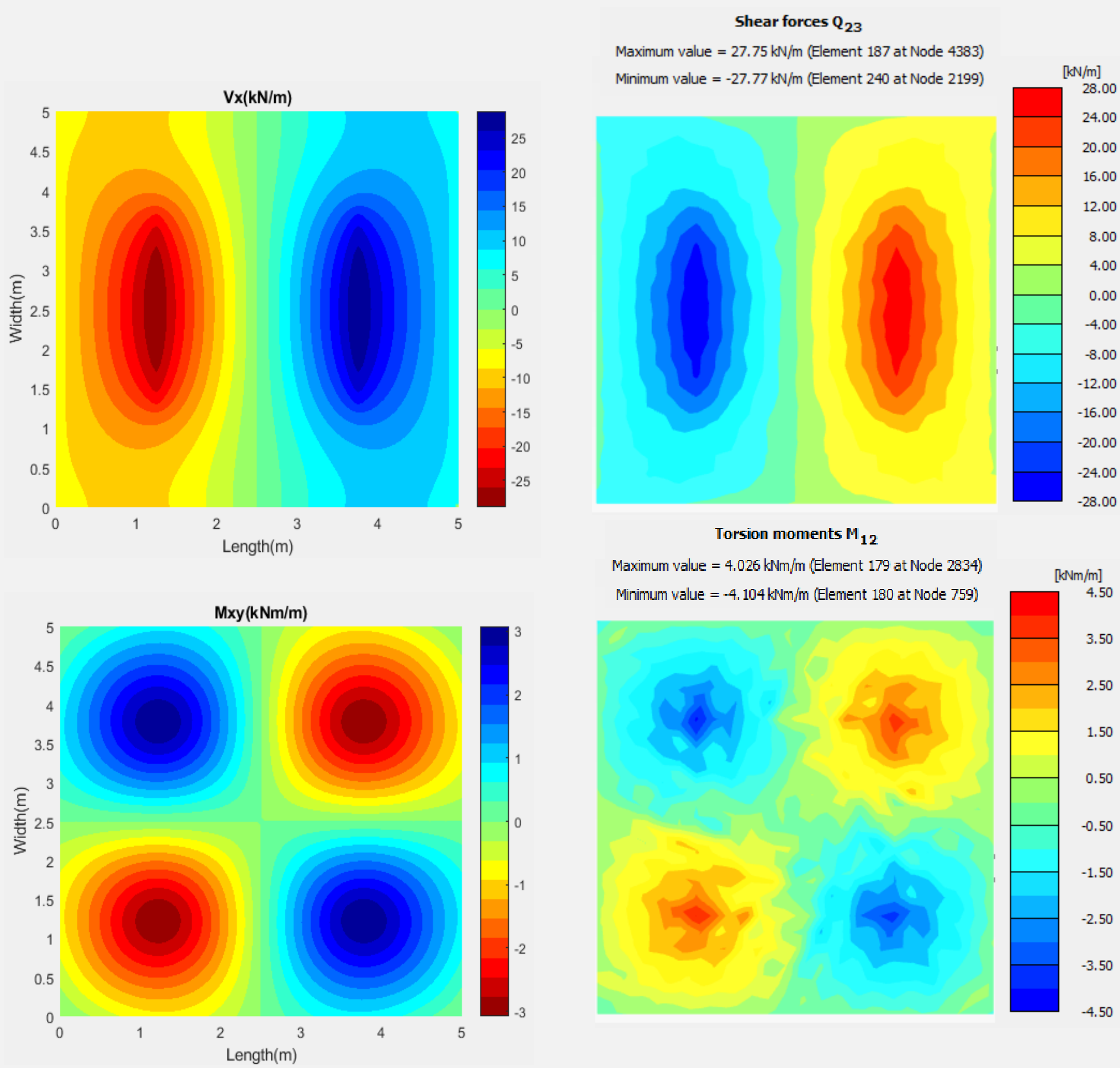

a) b)

Figure 4.9: Deflection and internal action of Rectangular plate (L/B=1) resting on Medium strength soil subjected to a uniformly distributed load based on a) Worku's Pasternak type model (FDM), b) Plaxis 3D

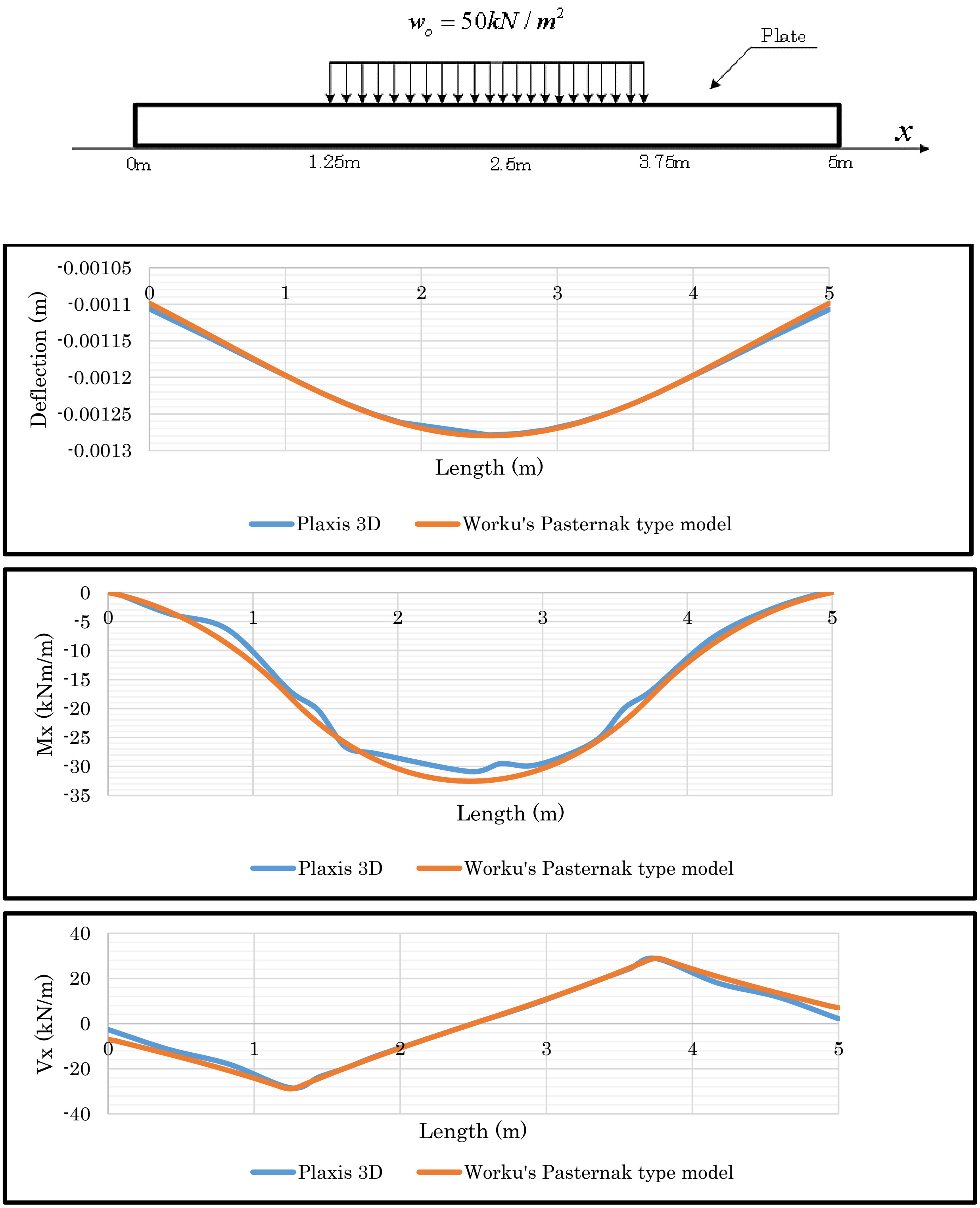

Figure 4.10: Section A-A view of the plate resting on medium soil subjected to uniformly distributed load

Significant observations from the plotted results include

- The deflection obtained by Worku's adjusted model is in a very good agreement with the Plaxis 3D model.
- The shear forces are also in good agreement with the FE results.
- The maximum moment shows a slight deviation, which is minor.

iii. Combined load

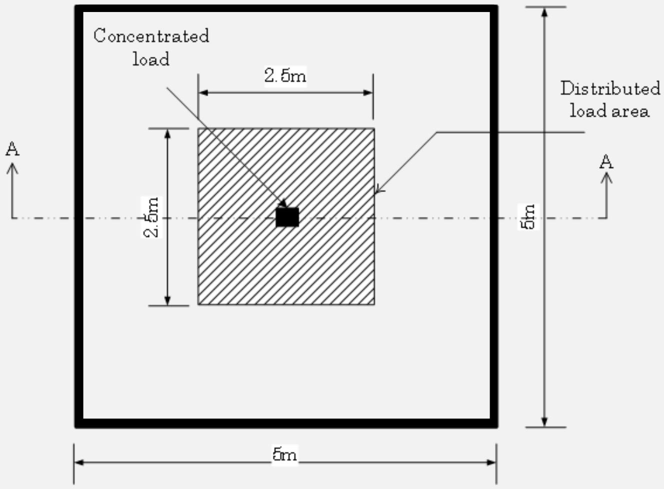

Worku's Pasternak type model (FDM) **Plaxis 3D**

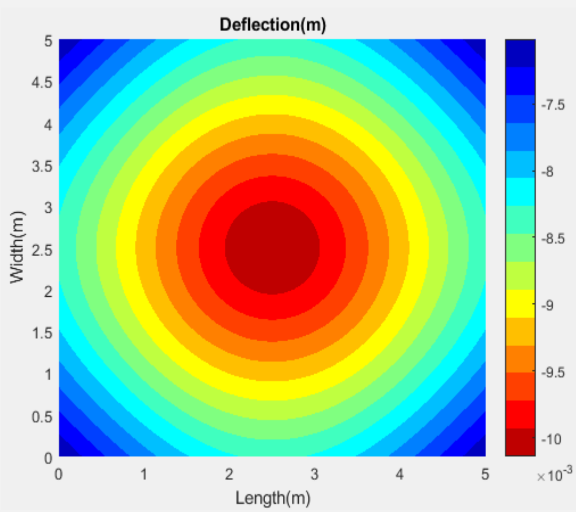

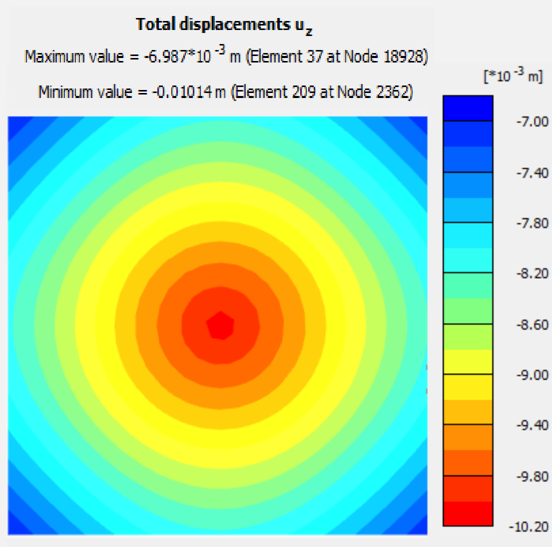

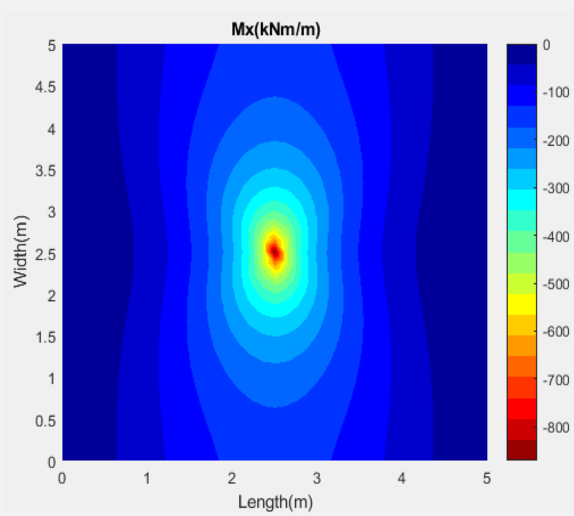

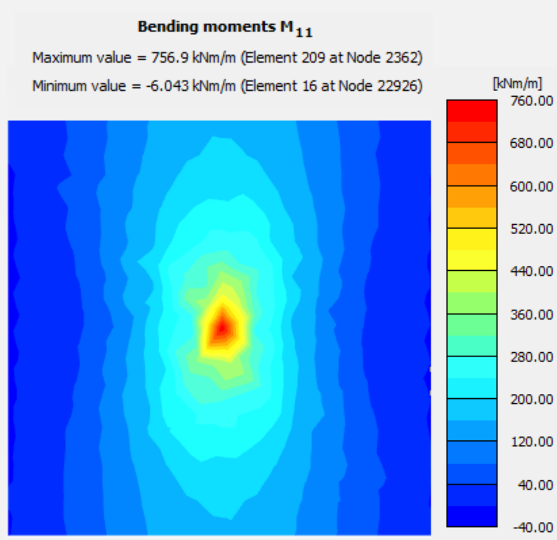

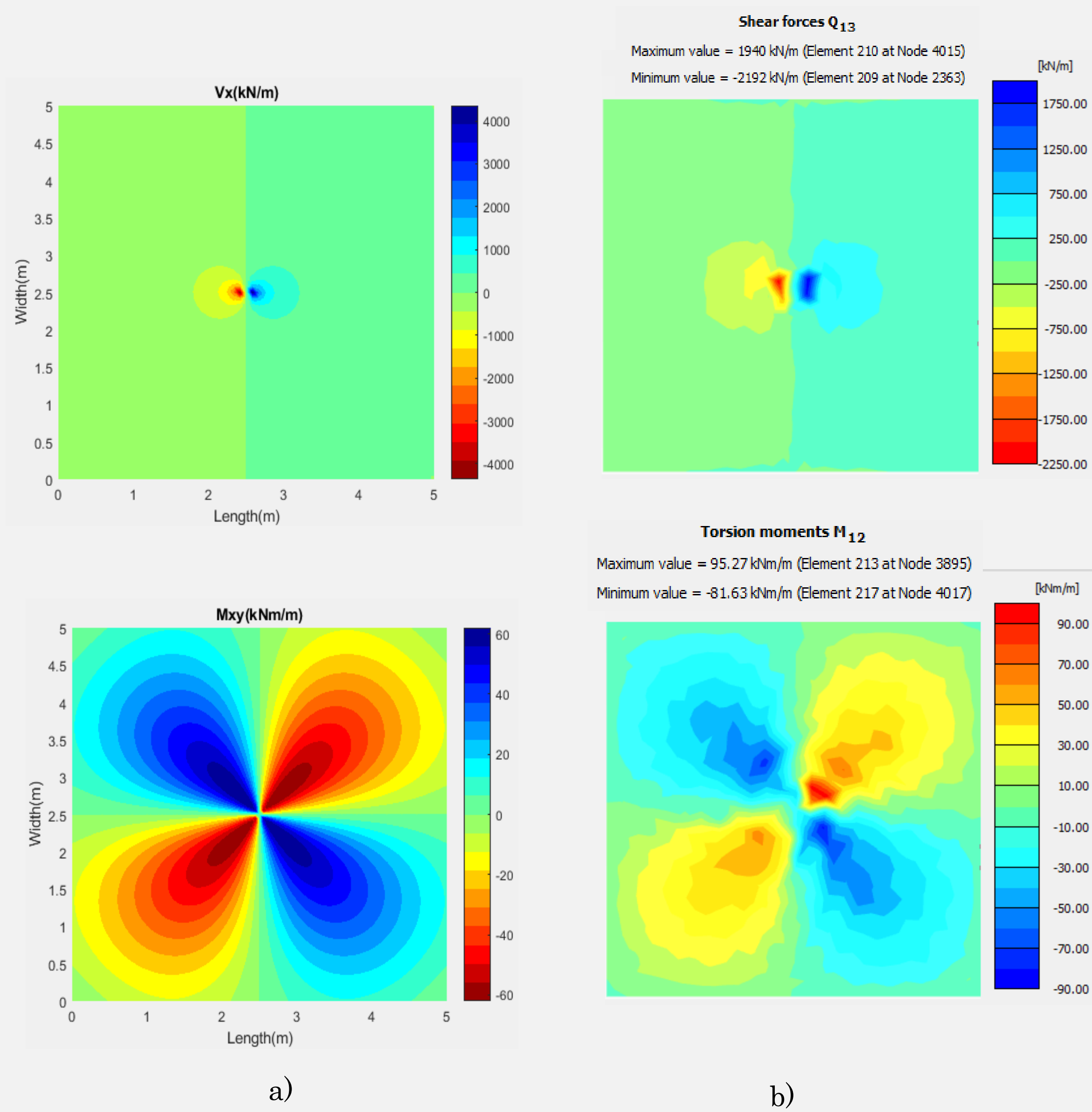

Figure 4.11: Deflection and internal action of Rectangular plate (L/B=1) resting on Medium strength soil subjected to a combined load based on a) Worku's Pasternak type model (FDM), b) Plaxis 3D

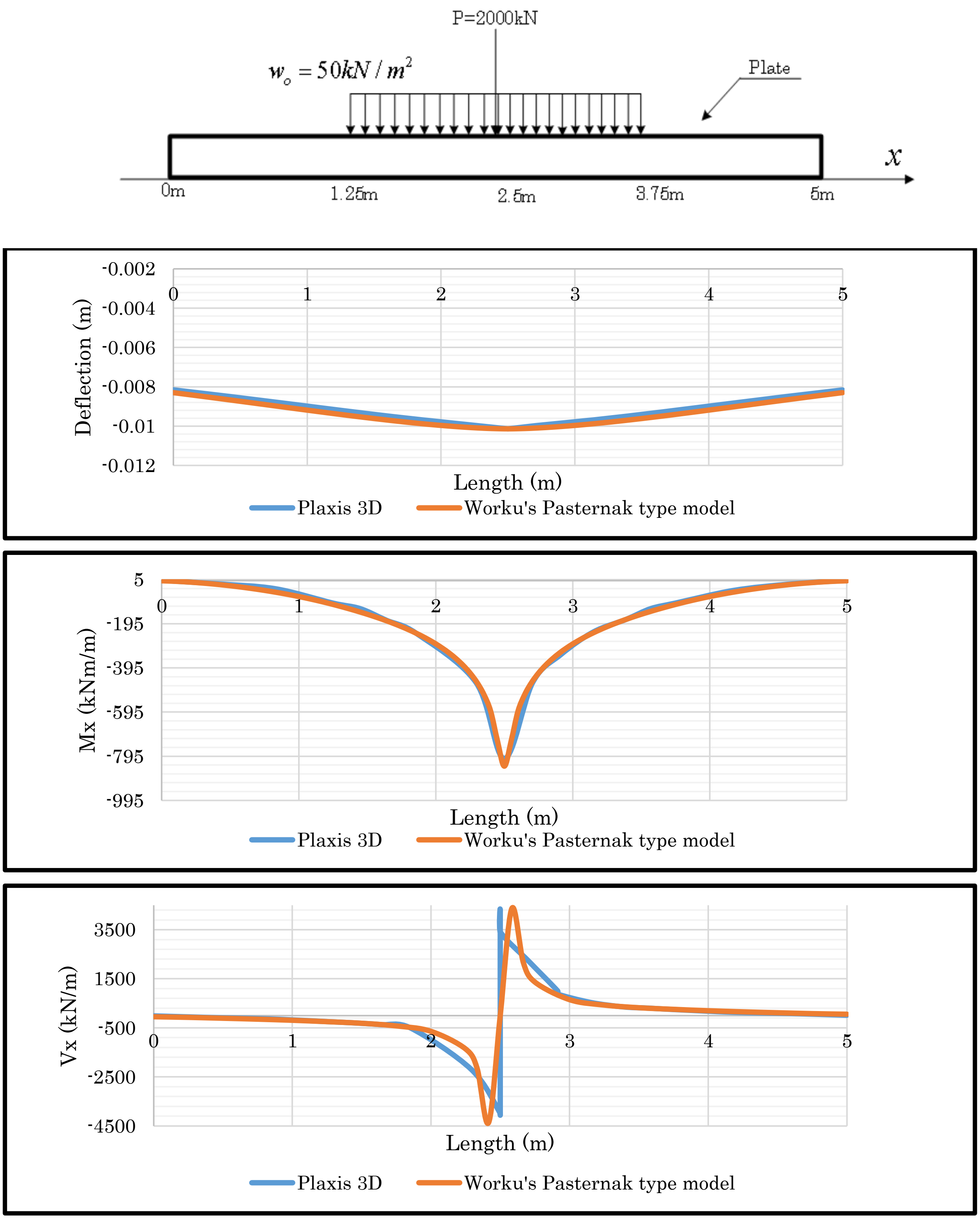

Figure 4.12: Section A-A view of the plate resting on medium soil subjected to the combined load

Significant observations from the plotted results include

- The deflection obtained by Worku's adjusted model is in a very good agreement with the Plaxis 3D model.
- The shear forces show variation in the mid-span of the plate. This problem is related to the effect of mesh size on the finite difference analysis.
- The maximum moment also in good agreement with the FE results.

4.3.2. Numerical analysis of Rectangular plate with L/B=2

i. Concentrated

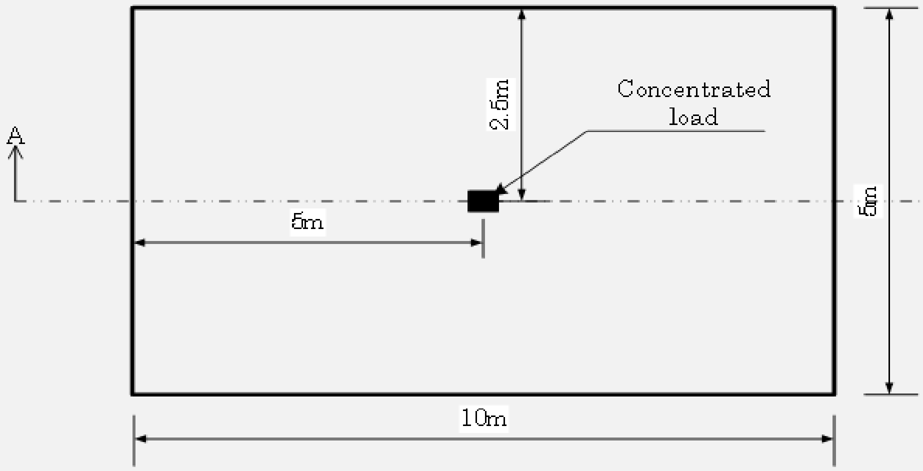

Figure 4.13: Rectangular plate with L/B=2

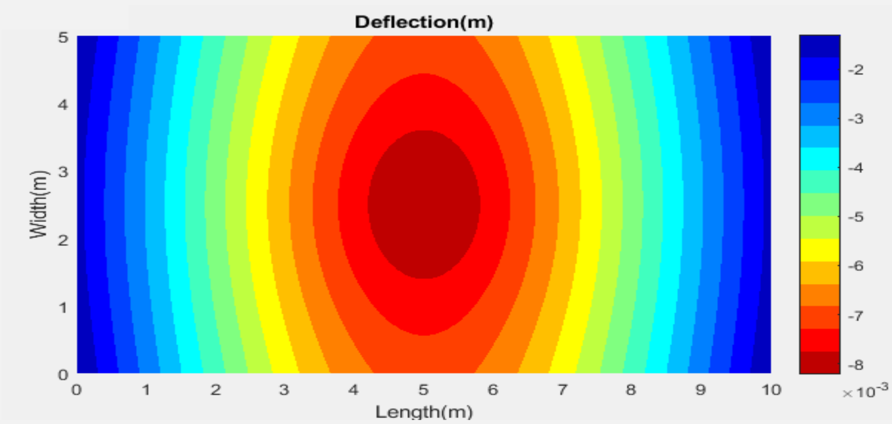

Worku's Pasternak type model (FDM)

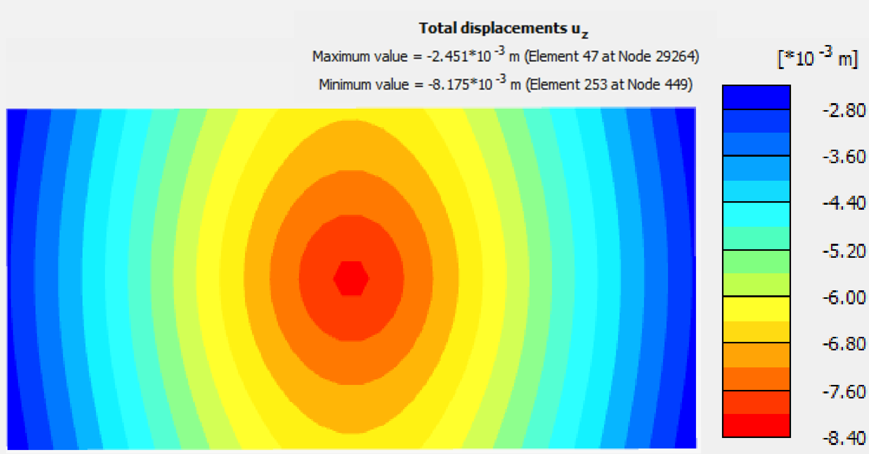

Plaxis 3D

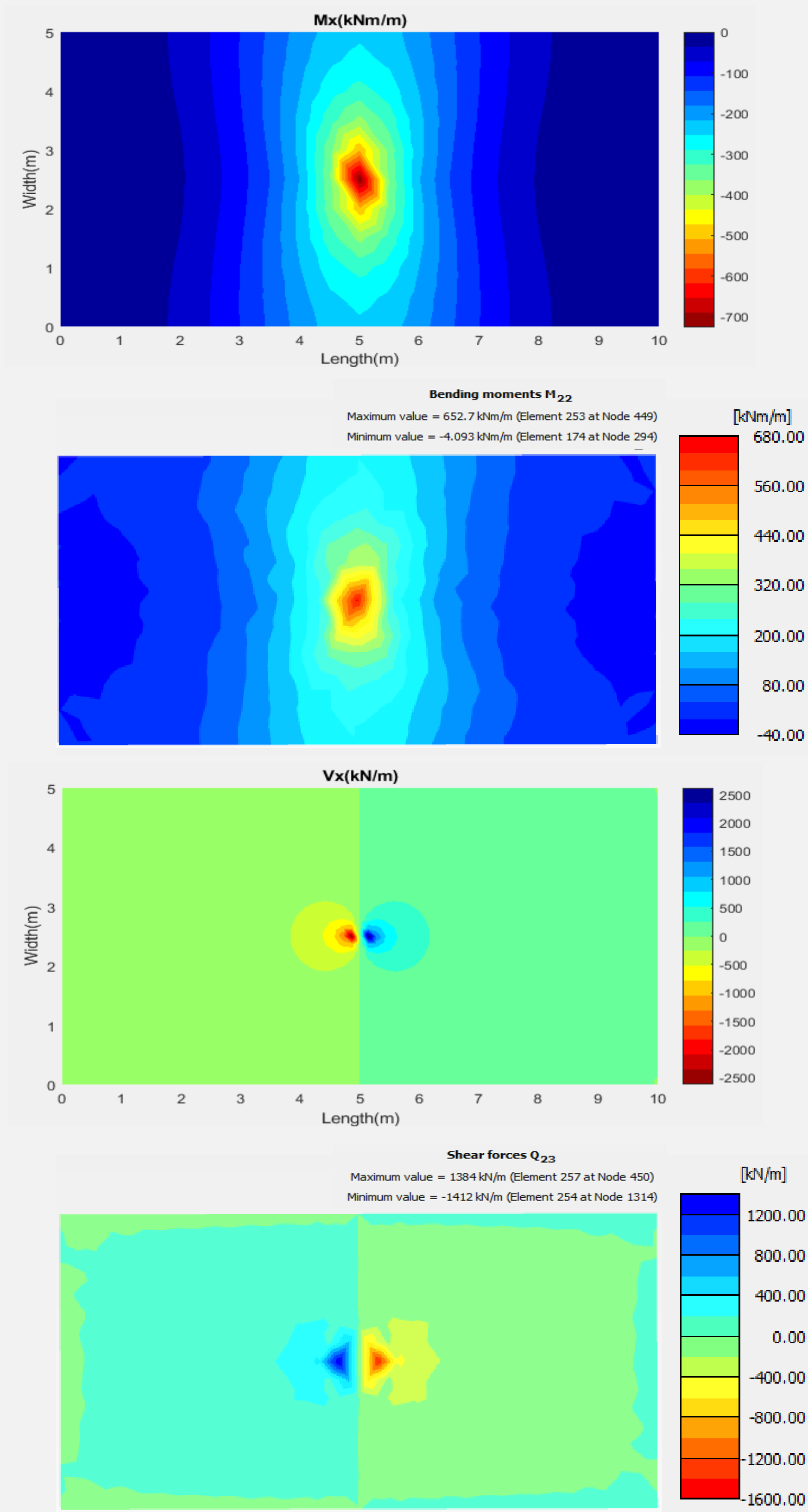

Worku's Pasternak type model (FDM)

Plaxis 3D

Worku's Pasternak type model (FDM)

Plaxis 3D

Figure 4.14: Deflection and internal action of Rectangular plate (L/B=2) resting on Medium strength soil subjected to a concentrated load

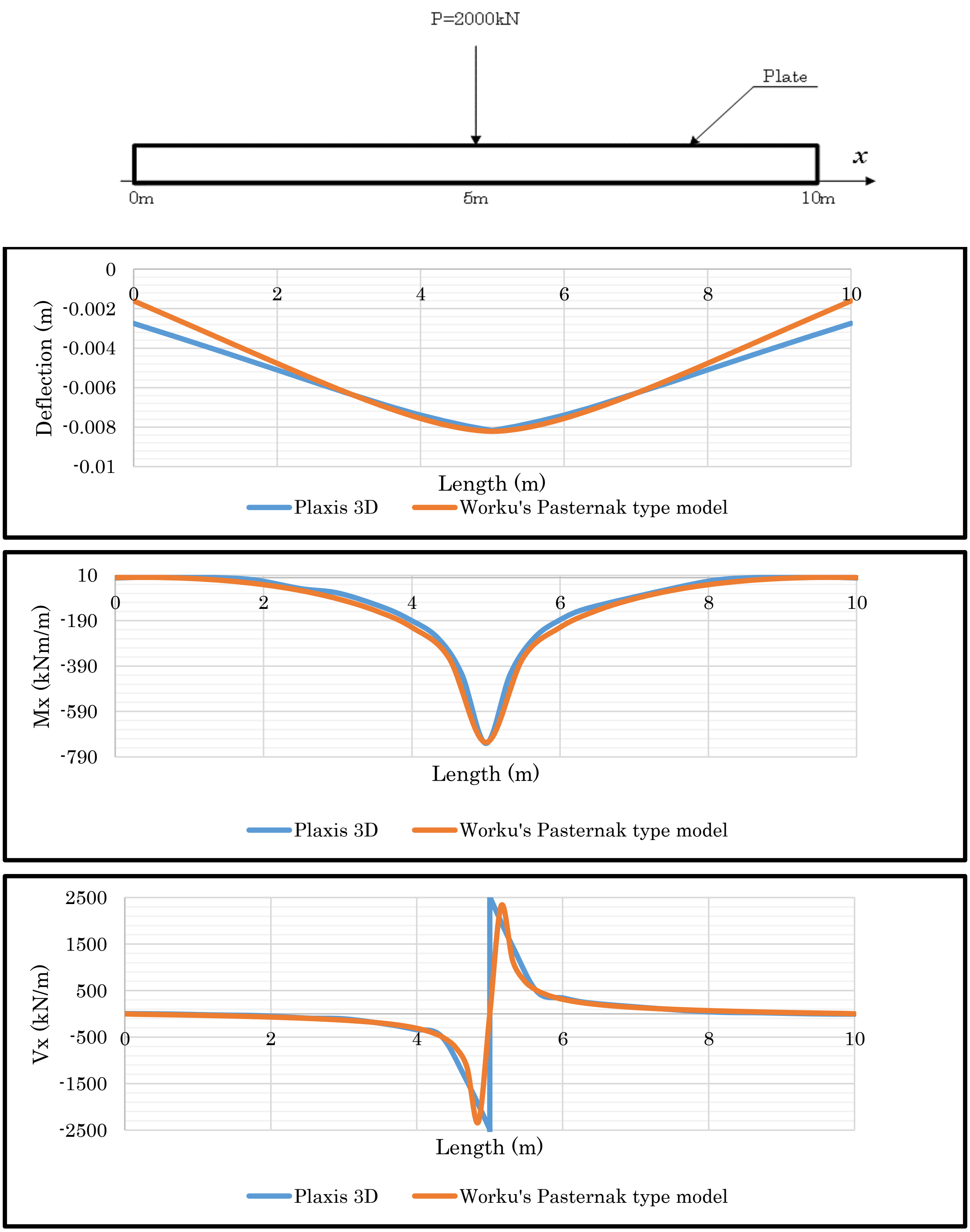

Figure 4.15: Section B-B view of the plate resting on medium soil subjected to a vertical concentrated load

Significant observations from plotted results;

- The deflection obtained by the calibrated model of Worku is in a very good agreement with the Plaxis 3D model. However, there is a deviation of deflection when moving away from the mid-span.
- The shear forces show some variation in the mid-span of the plate. This problem is related to the effect of mesh size on the finite difference analysis.
- Maximum moments are in a very good agreement with the FE results.

ii. Uniformly distributed

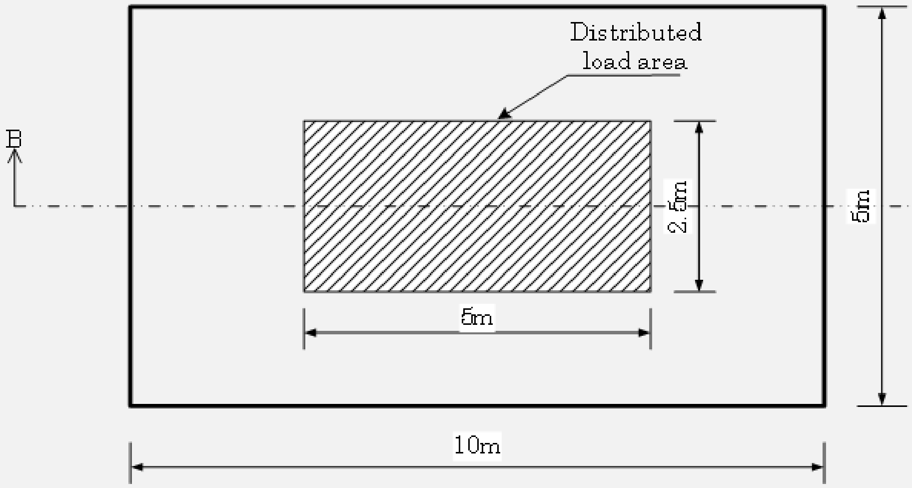

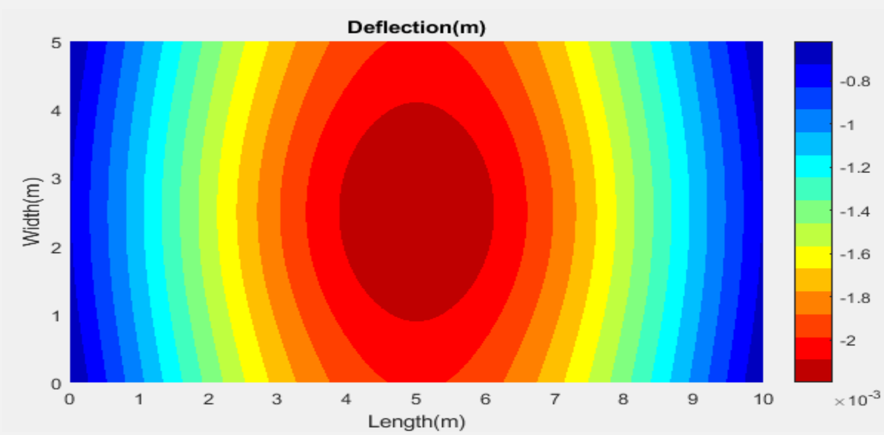

Worku's Pasternak type model (FDM)

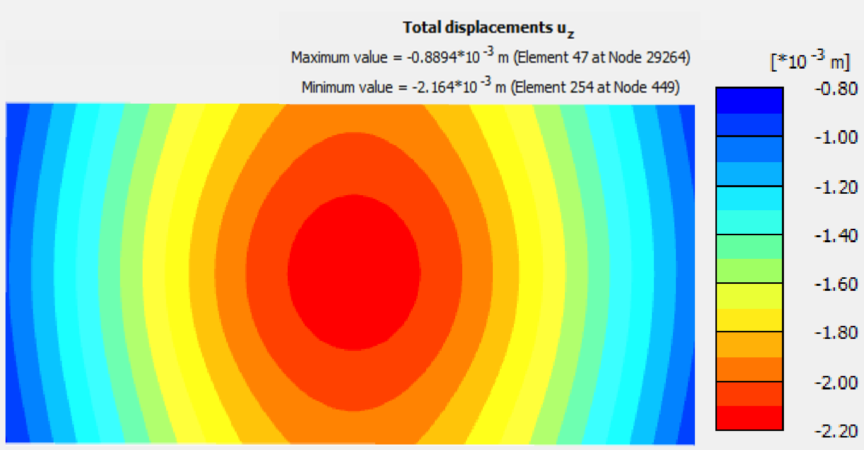

Plaxis 3D

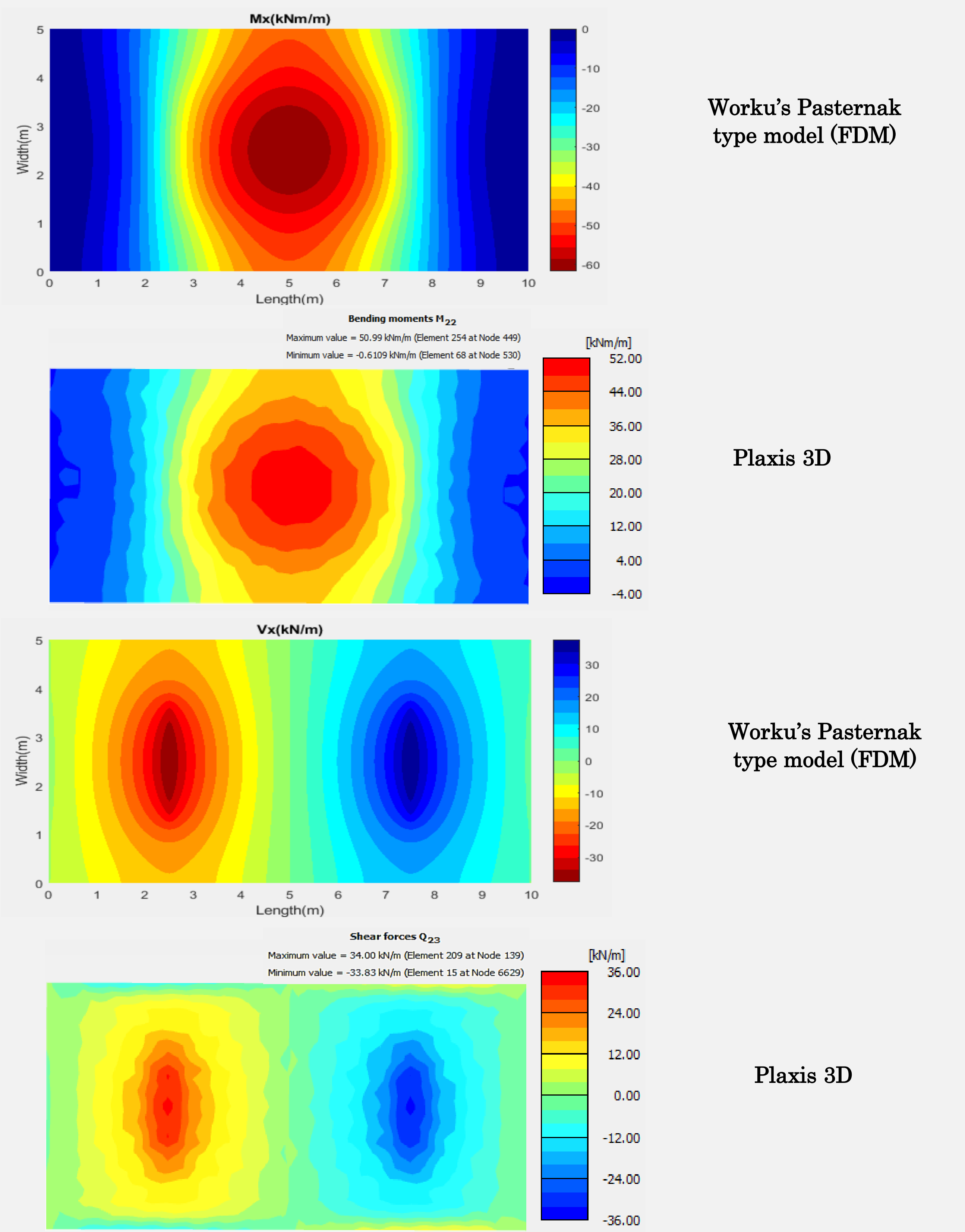

Figure 4.16: Deflection and internal action of Rectangular plate (L/B=2) resting on Medium strength soil subjected to uniformly distributed load

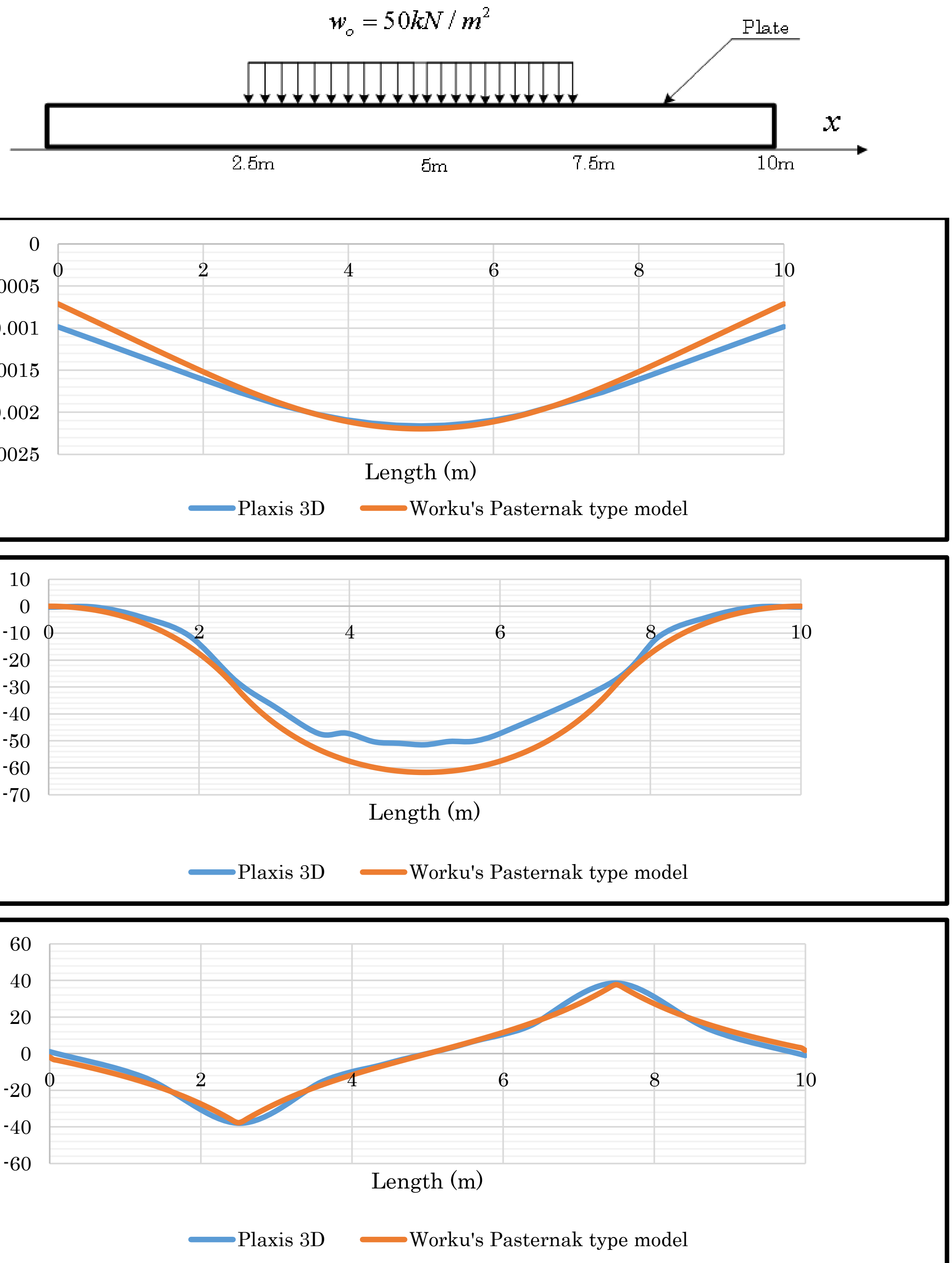

Figure 4.17: Section B-B view of the plate resting on medium soil subjected to uniformly distributed load

Significant observations from the plotted results include

- The deflection obtained by the adjusted model of Worku is in a very good agreement with the Plaxis 3D model.
- The shear forces are also in good agreement with the FE results.
- The maximum moment shows little deviation.

iii. Combined load

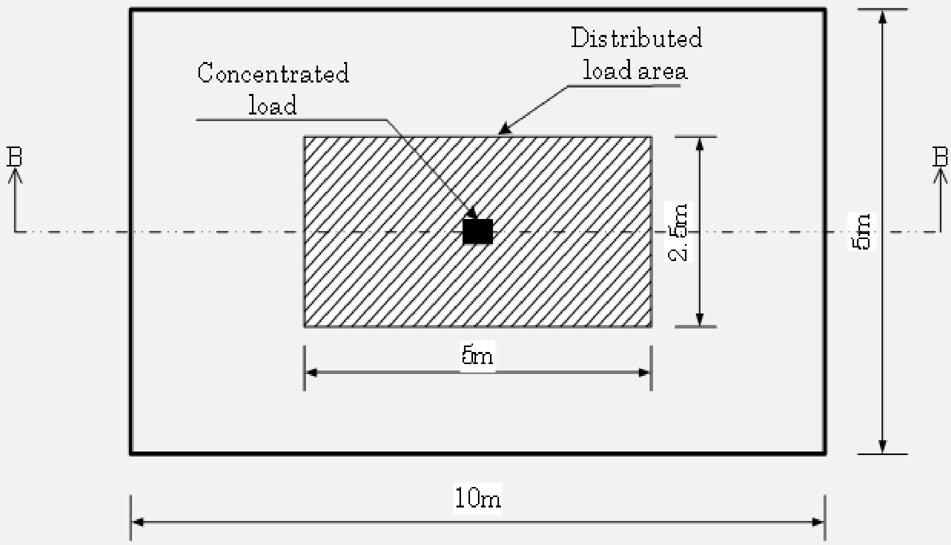

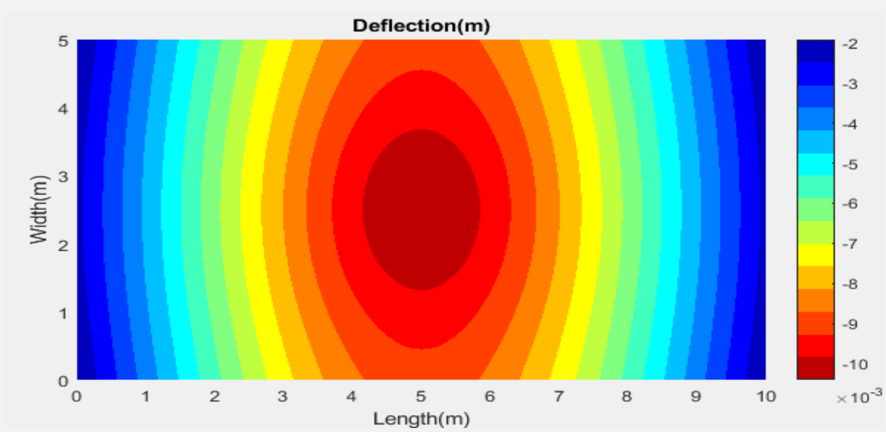

Worku's Pasternak type model (FDM)

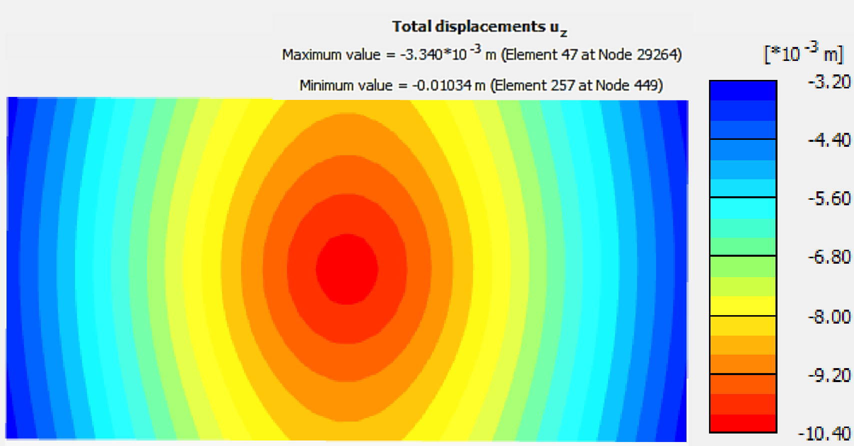

Plaxis 3D

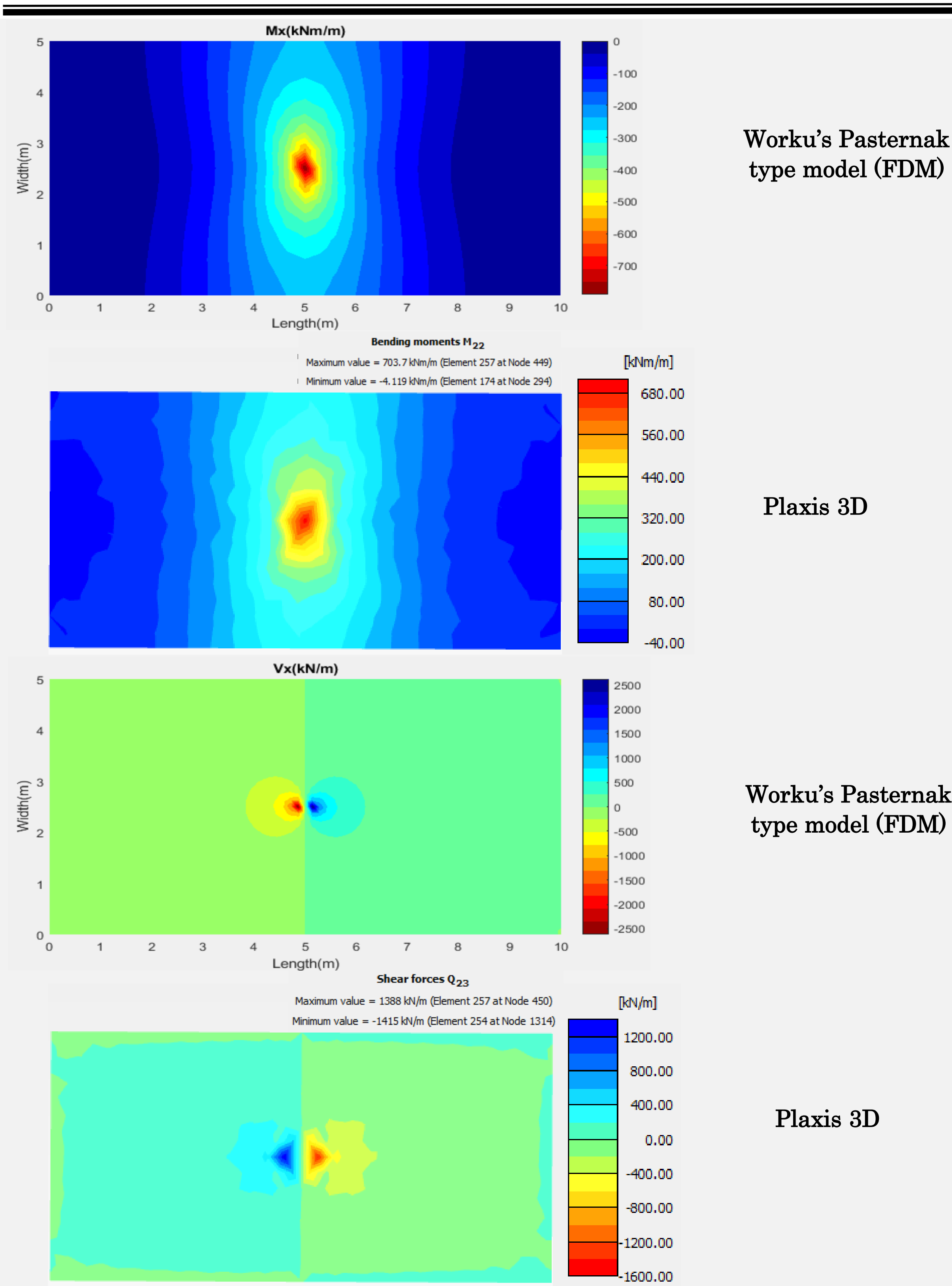

Figure 4.18: Deflection and internal action of Rectangular plate (L/B=2) resting on Medium strength soil subjected to the combined load

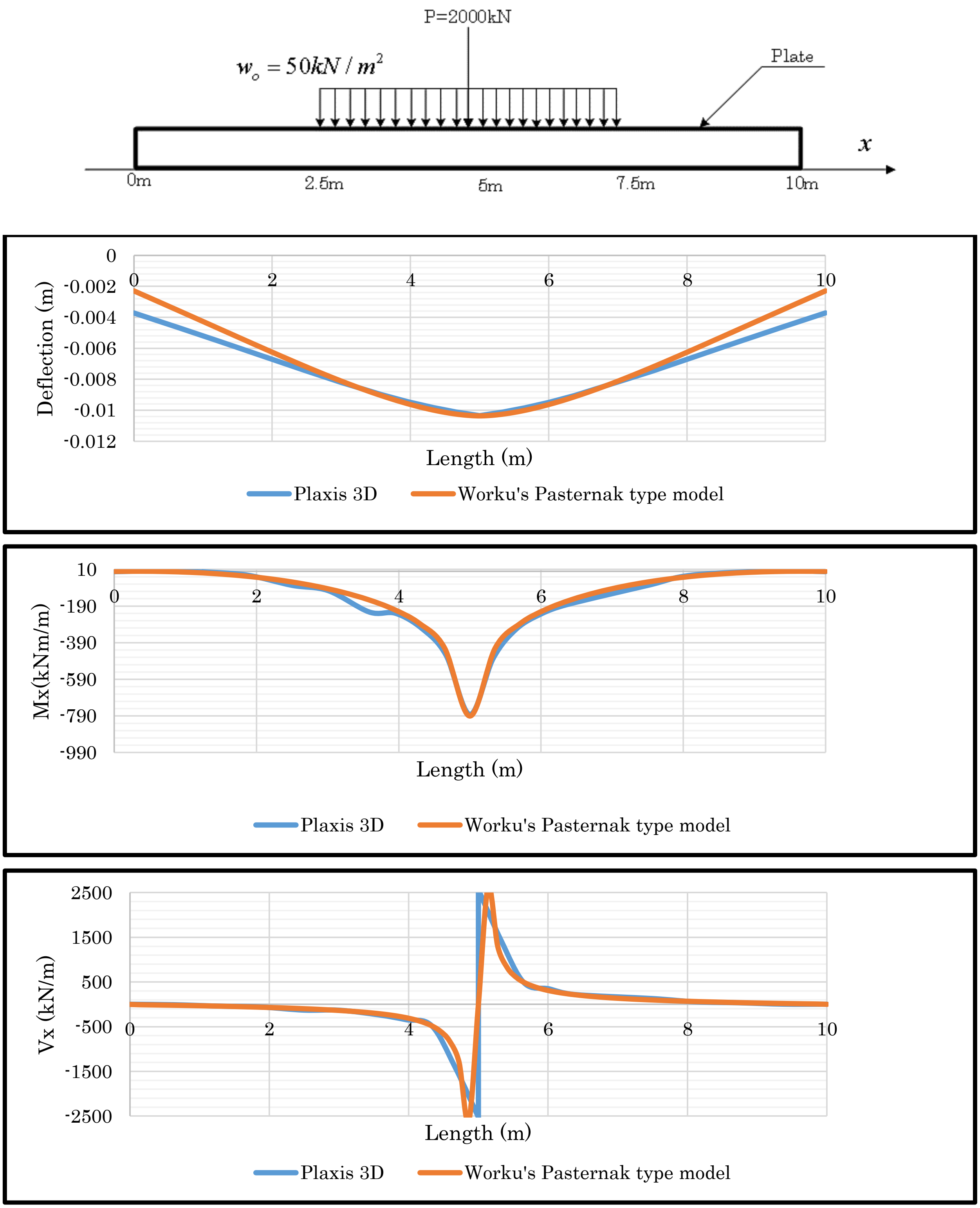

Figure 4.19: Section B-B view of the plate resting on medium soil subjected to the combined load

Significant observations from the plotted results include

- The deflection obtained by the adjusted model of Worku is in a very good agreement with the Plaxis 3D model. However, there is a deviation of deflection when moving away from the mid-span in the case of stronger soils.
- The shear forces show some variation in the mid-span of the plate. This problem is related to the effect of mesh size on the finite difference analysis.
- Maximum moments are generally in a very good agreement with the FE results.

The maximum deflection obtained using Worku's Kerr-equivalent Pasternak-type model is in a very good agreement with the FE based Plaxis 3D model. However, there is a minor deviation of deflection when moving away from the mid-span particularly in the case of stronger soils. This can be attributed to the inherent shear interaction existing between particles of the strong soils.

In the case of bending moments, Worku's model shows a slight deviation with the FE results, thus the results are relatively conservative. As far as the shear force is concerned, in the cases of the distributed load, the shear forces are practically the same with FE outputs. Moreover, the adjusted model gives a non-zero shear at the edge of the plate, which is visible in weak soils. This is due to the shear continuity. Whereas in the case of a concentrated vertical load, the shear force results show little deviation with the Plaxis 3D outputs. This problem is related to the effect of mesh size on the finite difference analysis where in particular the load condition is concentrated (point) load. This true for all numerical methods since external point loads generally affect the shear forces.

In general, the Kerr-Equivalent Pasternak model gives results in very good agreement with Finite Element based Plaxis 3D output for the different practical loading cases. Thus, this model can be proposed as an efficient means to analyze a rectangular plate on an elastic foundation.

5. Conclusions and Recommendations

5.1. General

The main goal of this study has been centered around the application of a recent generalized continuum model developed by Worku (2014) for the analysis of rectangular plates on elastic foundation. The finite difference method and analytical solutions are utilized to represent the differential equations. MATLAB® code is developed to compute displacements and the internal actions for selected practical loading conditions. Then Worku's generalized continuum model has been adjusted to obtain the final forms of the formulas for the model parameters. The results obtained after the adjustment are compared with FE-based Plaxis 3D results. Based on the results obtained, the following conclusions are drawn and recommendations are suggested.

5.2. Conclusions

The following major conclusions may be drawn:

1. A mathematical model is developed for determining displacements, bending moments, and shear forces in plates supported by an elastic foundation.
2. A special relative rigidity of the soil-plate system K_r has been introduced and used to include the effects of soil property, the foundation type, and foundation dimension, which generally affect subgrade reaction.
3. From the fitted curves, it can be shown that the adjustment factor χ is not sensitive to soil and plate parameters and the magnitude of the load.
4. In the case of unsymmetrical loading, the adjustment factor χ decreases steadily as the load moves away from the center toward the edges and is about halved at the edge of the plate.
5. In almost all cases, the adjusted Kerr-equivalent Pasternak type model gives consistently close results with the Plaxis 3D outputs. Nevertheless, there is a minor deviation of deflection when moving away from the mid-span particularly in the case of stronger soils.

6. Generally, the model slightly overestimates the bending moment. Hence, the results are on the safe side.
7. As far as the shear force is concerned, in the case of the distributed load, the shear forces are compatible with FE outputs. Whereas in the case of a concentrated vertical load, the shear force results show little deviation with the Plaxis 3D outputs. This problem is related to the effect of mesh size on the finite difference analysis where in particular the load condition is concentrated (point) load.

In general, the Kerr-equivalent Pasternak model well represents the real physical problem because it directly accounts for shear coupling. In all cases using the recommended adjustment factors provided in Figures (4.4) to (4.6), the model gives compatible results with the FE based results. Therefore, by using this model and the associated MATLAB® program, a practical analysis of rectangular plates on an elastic foundation can be easily performed and parametric studies conducted.

5.3. Recommendation

As the scope of this work is limited to rectangular thin plates subjected to selected loading conditions, the following actions could possibly strengthen, enhance, and expand the application of this research for future work.

1. A homogeneous soil is considered for this research. Thus, further study needs to be conducted on non-homogenous soil strata.
2. Symmetrical loading types are considered to analyze rectangular plate on an elastic foundation. For future works, other different cases of loading are recommended.
3. This research can be expanded by developing a technique to facilitate the use of other constitutive models such as von Mises, Drucker-Prager, and Mohr-Coulomb.
4. Large-scale experiments should be conducted to verify the computational results.

REFERENCES

Allen DN. & Seven RT. (1960). The stresses in foundation rafts-I. *Proceedings of the Institution of Civil Engineers,* 15: 35–48.

Ansel C. (2010). *Stresses in beams, plates, and shells*, Taylor and Francis, Third Edition.

Avramidis, I.E., and Morfidis, K. (2006). Bending of Beams on Three-Parameter Elastic Foundation. *Int. J. of Solids and Structures*, Elsevier, 43: 357-375

Barton M.V. (1948). *Finite difference equation for the analysis of thin rectangular plates with combinations of fixed and free edges*. Technical report, The University of Texas.

Bowles, J. (1996). *Principles of foundation engineering*, McGraw Hill, New York.

Brinkgreve, R. B. J., Engin, E., and Swolfs, W.M. (2013). *Manual of Plaxis 3D 2013 Foundation Software*, Delft University of Technology and Plaxis bv, Delft, Netherlands.

Chakravorty A.K. (1975). Finite difference solution for circular plates on elastic foundations. *International Journal For Numerical Methods in Engineering*, 9:73–84.

Colasanti, R. J., and Horvath, J. S. (2010). Practical subgrade model for improved soil-structure interaction analysis: Software implementation. *Pract. Period. Struct. Des. Constr.*, 15(4), 278–286.

Das, B. M., and Sobhan K. (2013). *Principles of Geotechnical Engineering*, McGraw Hill, New York.

Fai, M.K. (1988). Elastic Solution for Rectangular and Circular Plates on Non-Homogeneous Soil Foundation, University of Hong Kong.

Gorbunov-Possadov, M.and Serebrjanyi, R.V. (1961). Design of structures on elastic foundations. *Proceedings of the 5th International Conference on Soil Mechanics and Foundation Engineering*, Vol. I, pp.643-648.

Horvath, J.S. (2002). Basic SSI Concepts and Applications Overview. *Research Report No. CGT-2002-2*, Manhattan College, School of Engineering, New York.

Huang, M.H. and Thambiratnam, D.P. (2001). Analysis of Plate on Elastic Supports and Elastic Foundation by Finite Strip Method. *Journal of Computers and Structures*.

Jones, G. (1997). *Analysis of Beams on Elastic Foundations using Finite Difference Theory*, Thomas Telford, London, UK.

Katsikadelis, J.T. and Kallivokas, L.F. (1988). Plates on bi-parametric elastic foundation by BDIE method. *Journal of Mechanical Engineering*, 114 (5), pp. 847-875.

Kerr, A. D. and W. J. Rhines (1967). A further Study of Elastic Foundation Models. Report No. S-67-1, New York University, School of Engineering and Science, Bronx, N.Y., U.S.A.

Kerr, A.D. (1964). Elastic and Viscoelastic Foundation Models. *Journal of Applied Mechanics,* ASME, 25 (80); 491-498

Kerr, A.D. (1985). On the determination of foundation model parameters. *J. Geotech. Eng.*, 111(11), 1334–1340.

Kneifati M.C. (1985). Analysis of plate on Kerr Foundation Model. *Journal of Engineering Mechanics*, Vol.111, No. 11.

Nogami, T. and O'Neill, M.W. (1985). Beam on Generalized Two-Parameter Foundation. *Journal of Engineering Mechanics*, ASCE, 111 (5): 664-679

Poulos, H. (2018). Rational Assessment of Modulus of Subgrade Reaction. *Journal of the* SEAGS & AGSSEA, Vol. 49, No. 1, pp.453-460.

Poulos, H. G. (2002). Calculation of stress and settlement in soil masses. *Geotechnical engineering handbook.Vol.1: Fundamentals*, U.Smoltczyk, ed., Ernst & Sohn, Berlin, 259–312.

Poulos, H. G. and E. H. Davis. (1974). *Elastic solutions for soil and rock mechanics*. JohnWiley & Sons, Inc., New York, N.Y., U.S.A.

Qin K., Jahn I. (2015). *Structural Deformation of a Circular Thin Plate with Combinations of Fixed and Free Edges*. Technical report, The University of Queensland, Australia.

Rajapakse and Selvadurai. (1991). Response of Circular Footings and Anchor Plates in Non-Homogenous Elastic Soils. *International Journal for Numerical and Analytical Methods In Geomechanics*, *Vol.* 15, 457-470.

Reddy, J.N. (2007). *Theory and Analysis of Elastic Plates and Shells*, Second Edition, London New York.

Reissner, E. (1958): A Note on Deflections of Plates on a Viscoelastic Foundation. *Journal of Applied Mechanics*, ASME, 25 (80): 144-145

Selvadurai, A.P.S. (1979). *Elastic Analysis of Soil-Foundation Interaction*. Elsevier Scientific Publishing Company, New York

Straughan, W.T. (1990). Analysis of Plates on Elastic Foundation, Texas Tech University.

Szilard, R.(2004), *Theories and Applications of Plate Analysis; Classical, Numerical and Engineering Methods*. Canada.

Tanahashi, H. (2004). Formulas for an Infinitely Long Bernoullii-Euler Beam on the Pasternak Model. *Soils and Foundations, Japanese Geotechnical Society*, 2004, 44 (5): 109-118

Tanahashi, H. (2007). Pasternak Model Formulation of Elastic Displacements in the Case of a Rigid Circular Foundation. *Journal of Asian Architecture and Building Engineering*, 6 (1): 167-173.

Timoshenko SP. and Woinowsky-Krieger S. (1959). *Theory of Plates and Shells*, New York: McGraw-Hill.

Vallabhan CVG & Das YC. (1991) . Analysis of circular tank foundations. *Journal of Engineering Mechanics*, 117(4): 789–797.

Ventsel, E & Krauthammer, T. (2001). *Thin Plates and Shells: Theory, Analysis, and Applications*. CRC Press, Boca Raton, FL, 1st ed., pp. 197–199.

Vlasov, V.Z. and Leont'ev, N.N. (1966). *Beams, Plates, and Shells on Elastic Foundations*. Israel Program for Scientific Translations, Jerusalem, 1966 (Translated from Russian)

Wang, H., Tham, L. G., and Cheung, Y. K. (2005). Beams and plates on elastic foundations: A review, *Prog. Struct.Eng.Mater*.,7(4),174–182.

Worku, A. (2010). Part I: A Generalized Formulation of Continuum Models for Elastic Foundations. *Advances in Analysis, Modeling & Design*, GeoFlorida.

Worku, A. (2013). Calibrated Analytical Formulas for Foundation Model Parameters. *International Journal of Geomechanics*, *Vol. 13, No. 4*.

Worku, A. (2014). Development of a Calibrated Pasternak Foundation Model for Practical Use. *International Journal of Geotechnical Engineering*, *Vol. 8, No. 1.*

Worku, A. and Degu Y. (2010). Part II: Application of Newly Derived and Calibrated Subgrade Models in the Analysis of Beams on Elastic Foundations. *Journal of Eng. Mechanics*, GeoFlorida.

Zhaohua F & Cook RD. (1983). Beam element on two-parameter elastic foundations. *Journal of Engineering Mechanics* (ASCE), 109(6):1390–1402.

Appendix A

General Solution of the partial differential equation

The governing homogeneous differential equation for the deflection of the foundation outside the domain of plate is given by

$$k_p w_F(x,y) - G_p \nabla^2 w_F(x,y) = 0 \qquad \text{(A.1)}$$

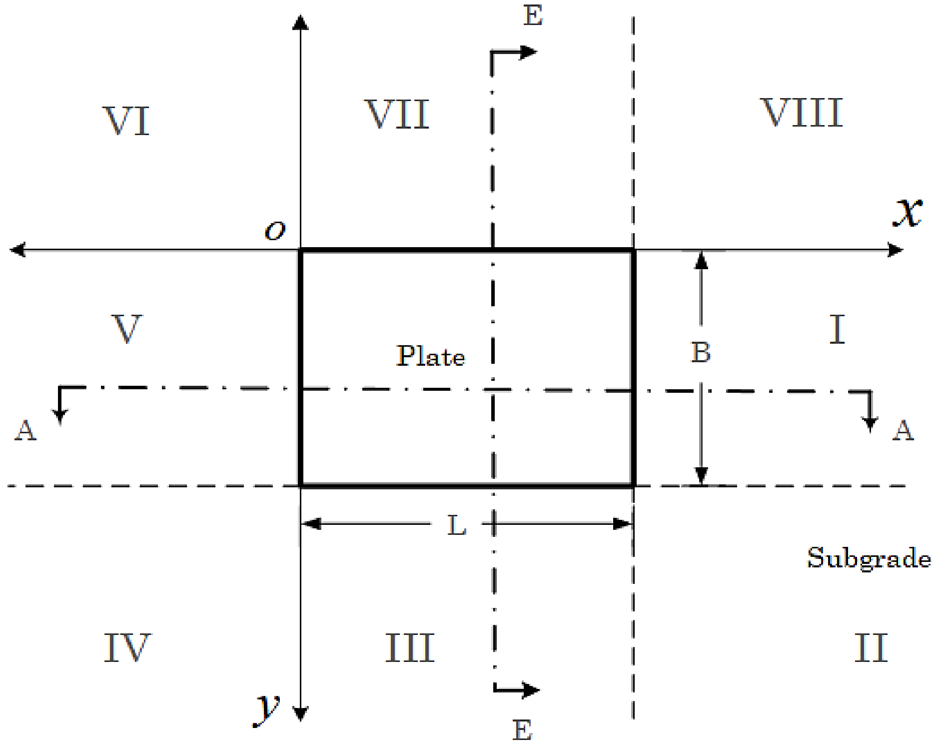

Figure A1: Rectangular plate-soil surface divided into regions.

The required separation solution of the partial differential equations is then exposed as a product

$$w_F(x,y) = X(x)Y(y) \qquad \text{(A.2)}$$

Where X (x) and Y (y) are functions of x and y, respectively and are continuously differentiable.

$$\frac{\partial^2 w}{\partial x^2} = \left[\frac{\partial^2}{\partial x^2}\left(X(x)\right)\right]Y(y)$$
$$\frac{\partial^2 w}{\partial y^2} = \left[\frac{\partial^2}{\partial y^2}\left(Y(y)\right)\right]X(x) \tag{A.3}$$

Substituting Equations (A.3) into the Equation (A.2) to obtain

$$\left(\left[\frac{\partial^2}{\partial x^2}\left(X(x)\right)\right]Y(y) + \left[\frac{\partial^2}{\partial y^2}\left(Y(y)\right)\right]X(x)\right) - \frac{k_p}{G_p}X(x)Y(y) = 0 \tag{A.4}$$

This can also be expressed in the form

$$\left(\left[\frac{\partial^2}{\partial x^2}\left(X(x)\right)\right]Y(y)\right) - \frac{k_p}{G_p}X(x)Y(y) = -\left[\frac{\partial^2}{\partial y^2}\left(Y(y)\right)\right]X(x)$$

(A.5)

$$\frac{\left[\frac{\partial^2}{\partial x^2}\left(X(x)\right)\right] - \frac{k_p}{G_p}X(x)}{X(x)} = \frac{-\left[\frac{\partial^2}{\partial y^2}\left(Y(y)\right)\right]}{Y(y)} \tag{A.6}$$

Since the left-hand side of this equation is a function of x only and the right-hand is a function of y only, it follows that Equation (A.6) can be true if both sides are equal to the same constant value k which is called an arbitrary separation constant.

$$\frac{\left[\frac{\partial^2}{\partial x^2}\left(X(x)\right)\right] - \frac{k_p}{G_p}X(x)}{X(x)} = \frac{-\left[\frac{\partial^2}{\partial y^2}\left(Y(y)\right)\right]}{Y(y)} = k \tag{A.7}$$

Consequently, Equation (A.8) gives two ordinary differential equations

$$\left[\frac{\partial^2}{\partial x^2}\left(X(x)\right)\right] - \frac{k_p}{G_p}X(x) = kX(x) \tag{A.8}$$

$$-\left[\frac{\partial^2}{\partial y^2}\left(Y(y)\right)\right] = kY(y) \tag{A.9}$$

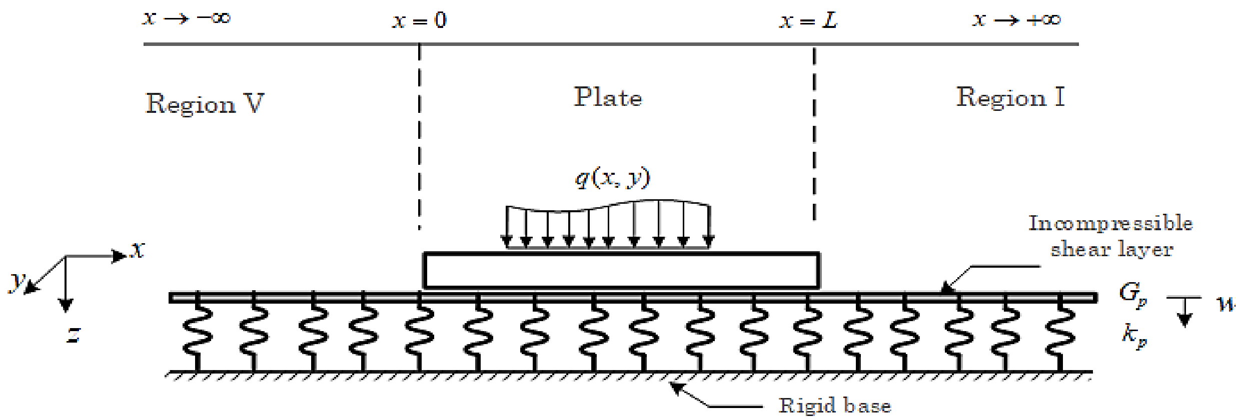

Figure A2: Section A-A of plate on resting on Pasternak foundation

The arbitrary separation constant could be zero, negative, or positive. By taking the first case ($k = 0$) Equations (A.8) and (A.9) expressed in the form

$$\left[\frac{\partial^2}{\partial x^2}\left(X(x)\right)\right] - \frac{k_p}{G_p} X(x) = 0 \tag{A.10}$$

$$-\left[\frac{\partial^2}{\partial y^2}\left(Y(y)\right)\right] = 0 \tag{A.11}$$

For region I and V, respectively, the general solution of Equation (A.10) is given by

$$X(x) = C_1 e^{\lambda(x-L)} + C_2 e^{-\lambda(x-L)} \tag{A.12a}$$

$$X(x) = A_1 e^{\lambda x} + A_2 e^{-\lambda x} \tag{A.12b}$$

Where A_1, A_2, C_1 and C_2 are open constants and $\lambda = \sqrt{\frac{k_p}{G_p}}$

From the plate shown the figure the following boundary conditions are drawn

For region I

1. At $x = 0$, $w_f(0, y) = w_L$
2. At $x \to \infty$, $w_f(x, y) = 0$

For region V

1. At $x = L$, $w_f(L, y) = w_{L,}$
2. At $x \to -\infty$, $w_f(x, y) = 0$

For region I, applying the second boundary on Equation (A.12a) eliminate C_1 thus, Equation (A.12a) becomes

$$X(x) = C_2 e^{-\lambda(x-L)} \quad \text{(A.13)}$$

From the first boundary condition

$$w(L, y) = X(L)Y(y) \quad \text{(A.14)}$$

$$X(L) = \frac{w(L, y)}{Y(y)} = \frac{w_L}{Y(y)} \qquad \text{Where } Y(y) \neq 0 \quad \text{(A.15)}$$

Substituting Equation (A.15) to equation (A.13) the second constant becomes

$$C_2 = \frac{w_L}{Y(y)} \qquad Y(y) \neq 0$$

Hence, $X(x) = \dfrac{w_L}{Y(y)} e^{-\lambda(x-L)}$

Therefore, the final solution becomes

$$w_F(x, y) = X(x)Y(y) = w_L e^{-\lambda(x-L)}, \text{ for } L \geq x > \infty \text{ and } 0 \leq y \leq B \quad \text{(A.16)}$$

Likewise, for region v applying the boundary conditions and substituting the open constants the final solution becomes

$$w_F(x, y) = w_L e^{\lambda x}, \text{ for } -\infty < x \leq 0 \text{ and } 0 \leq y \leq B \quad \text{(A.17)}$$

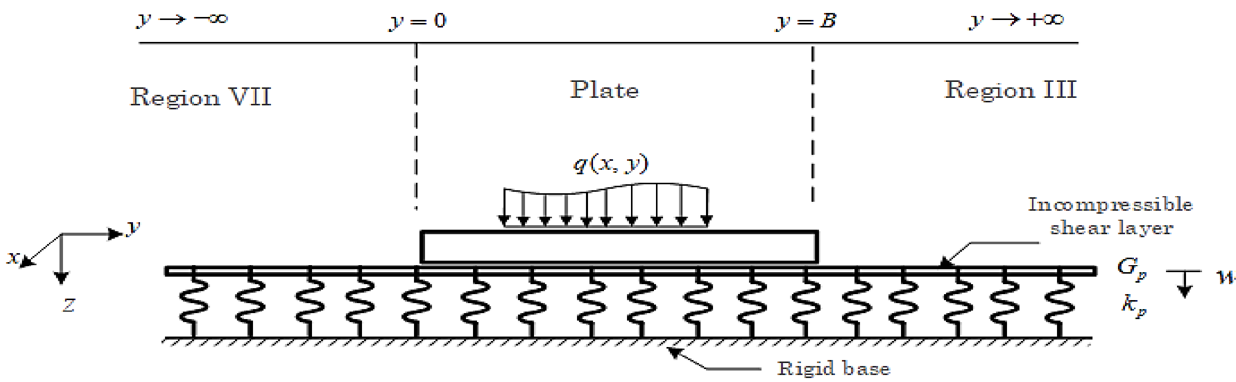

Figure A3: Section E-E of plate on resting on Pasternak foundation

In the case of regions III and VII, Equations A5 can also be expressed in the form

$$\left(\left[\frac{\partial^2}{\partial x^2}\big(X(x)\big)\right]Y(y)\right)-\frac{k_p}{G_p}X(x)Y(y)=-\left[\frac{\partial^2}{\partial y^2}\big(Y(y)\big)\right]X(x) \tag{A.18}$$

$$\frac{\left[\frac{\partial^2}{\partial y^2}\big(Y(y)\big)\right]-\frac{k_p}{G_p}Y(y)}{Y(y)}=\frac{-\left[\frac{\partial^2}{\partial x^2}\big(X(x)\big)\right]}{X(x)} \tag{A.19}$$

Equating Equation (A.19) to a constant k, Equation (A.19) gives two ordinary differential equations

$$\left[\frac{\partial^2}{\partial y^2}\big(Y(y)\big)\right]-\frac{k_p}{G_p}Y(y)=\kappa Y(y) \tag{A.20}$$

$$-\left[\frac{\partial^2}{\partial x^2}\big(X(x)\big)\right]=\kappa X(x) \tag{A.21}$$

The arbitrary separation constant could be zero, negative, or positive. By taking the first case ($\kappa=0$) Equations (A.20) and (A.21) expressed in the form

$$\left[\frac{\partial^2}{\partial x^2}\big(X(x)\big)\right]-\frac{k_p}{G_p}X(x)=0 \tag{A.22}$$

$$-\left[\frac{\partial^2}{\partial y^2}\big(Y(y)\big)\right]=0 \tag{A.23}$$

For region III and VII, respectively, the general solution of Equation (A.22) is given by

$$Y(y) = C_1 e^{\lambda(y-B)} + C_2 e^{-\lambda(y-B)} \tag{A.24a}$$

$$Y(y) = A_1 e^{\lambda y} + A_2 e^{-\lambda y} \tag{A.24b}$$

Where A_1, A_2, C_1 and C_2 are open constants and $\lambda = \sqrt{\frac{k_p}{G_p}}$

The boundary conditions are (Figure A3)

For region III

1. At $y = 0$, $w_f(x, 0) = w_{B,}$
2. At $y \to \infty$, $w_f(x, y) = 0$

For region VII

1. At $y = B$, $w_f(x, B) = w_{B,}$
2. At $y \to -\infty$, $w_f(x, y) = 0$

For region III, applying the second boundary on Equation (A.24a) eliminate C_1 thus, Equation (A.24a) becomes

$$Y(y) = C_2 e^{-\lambda(y-B)} \tag{A.25}$$

From the first boundary condition

$$w(x, B) = X(x)Y(B) \tag{A.26}$$

$$Y(B) = \frac{w(x, B)}{X(x)} = \frac{w_B}{X(x)} \qquad \text{Where } Y(y) \neq 0 \tag{A.27}$$

Substituting Equation (A.27) to Equation (A.25) the second constant becomes

$$C_2 = \frac{w_B}{X(x)} \qquad Y(y) \neq 0$$

Hence, $$Y(y) = \frac{w_B}{X(x)} e^{-\lambda(y-B)} \tag{A.28}$$

Therefore, the final solution becomes

$$w_F(x,y) = X(x)Y(y) = w_B e^{-\lambda(y-B)}, \text{ for } B \geq y > \infty \text{ and } 0 \leq x \leq L \tag{A.29}$$

Likewise for region VII applying the boundary conditions and substituting the open constants the final solution becomes

$$w_F(x,y) = w_B e^{\lambda y}, \text{ for } -\infty < y \leq 0 \text{ and } 0 \leq x \leq L \tag{A.30}$$

For regions II, IV, VI, and VIII, from the plate shown in the Figure (A1) the following boundary conditions are drawn

Region II

1. At $x = L$ and $y = B$, $w_F(L,B) = w_{c,}$
2. At $x = L$, $w_F(L,y) = w_c e^{-\lambda(y-B)}$
3. At $x \to \infty$ and $y \to \infty$, $w_F(x,y) = 0$

Region IV

1. At $x = 0$ and $y = B$, $w_F(0,B) = w_{c,}$
2. At $x = 0$, $w_F(L,y) = w_c e^{-\lambda(y-B)}$
3. At $x \to \infty$ and $y \to \infty$, $w_F(x,y) = 0$

Region VI

1. At $x = 0$ and $y = 0$, $w_F(L,B) = w_{c,}$
2. At $x = 0$, $w_F(0,y) = w_c e^{\lambda y}$
3. At $x \to \infty$ and $y \to \infty$, $w_F(x,y) = 0$

Region VIII

1. At $x = L$ and $y = 0$, $w_F(L,0) = w_{c,}$
2. At $x = L$, $w_F(L,y) = w_c e^{\lambda y}$
3. At $x \to \infty$ and $y \to \infty$, $w_F(x,y) = 0$

In the case of region II, the general solution of Equation (A.10) is given by

$$X(x) = C_1 e^{\lambda(x-L)} + C_2 e^{-\lambda(x-L)} \tag{A.31}$$

Where C_1 and C_2 are open constants and $\lambda = \sqrt{\frac{k_p}{G_p}}$

Applying the third boundary on Equation (A.31) eliminate C_1 thus equation (A.31) becomes

$$X(x) = C_2 e^{-\lambda(x-L)} \tag{A.32}$$

From the first and second boundary conditions

$$w(L, y) = X(L)Y(y) = w_c e^{-\lambda(y-B)} \tag{A.33}$$

$$X(L) = \frac{w_c e^{-\lambda(y-B)}}{Y(y)} \qquad \text{Where } Y(y) \neq 0 \tag{A.34}$$

Substituting Equation (A.34) into Equation (A.32) the second constant becomes

$$C_2 = \frac{w_c e^{-\lambda(y-B)}}{Y(y)} \qquad \text{Where } Y(y) \neq 0$$

Hence, $$X(x) = \frac{w_c}{Y(y)} e^{-\lambda(x-L)} e^{-\lambda(y-B)} \tag{A.35}$$

Therefore, the final solution becomes

$$w_F(x, y) = X(x)Y(y) = w_c e^{-\lambda(x-L)} e^{-\lambda(y-B)}, \text{ for } L \geq x > \infty \text{ and } B \geq y > \infty \tag{A.36}$$

Similarly For regions IV, VI, and VIII, applying the boundary conditions and substituting the open constants the final solutions become

$$w_F(x, y) = w_c e^{-\lambda(x-L)} e^{\lambda y}, \text{ for } L \geq x > \infty \text{ and } 0 \leq y < -\infty \tag{A.37}$$

$$w_F(x, y) = w_c e^{\lambda x} e^{\lambda y}, \text{ for } 0 \leq x < -\infty \text{ and } 0 \leq y < -\infty \tag{A.38}$$

$$w_F(x, y) = w_c e^{\lambda x} e^{-\lambda(y-B)}, \text{ for } 0 \leq x < -\infty \text{ and } B \geq y > \infty \tag{A.39}$$

Appendix B

Deflection relation for a rectangular plate on an elastic foundation with free edge boundary condition

1. Point inside

$$\begin{pmatrix} c11\left(w_{m,n}\right)+c12\left(w_{m-1,n}+w_{m+1,n}+\alpha^2(w_{m,n-1}+w_{m,n+1})\right)+ \\ \alpha^4(w_{m,n-2}+w_{m,n+2})+w_{m-2,n}+w_{m+2,n}+ \\ 2\alpha^2\left(w_{m-1,n-1}+w_{m+1,n-1}+w_{m-1,n+1}+w_{m+1,n+1}\right) \end{pmatrix}=\left(\frac{q(x,y)\iota^4}{D}\right)_{m,n} \tag{B.1}$$

Where

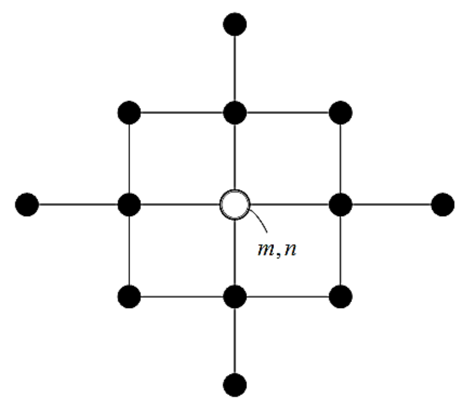

$$c11=6+8\alpha^2+6\alpha^4+2(1+\alpha^2)\hat{G}_p+\hat{k}_p$$
$$c12=-4(1+\alpha^2)-\hat{G}_p$$
$$\hat{G}_p=\frac{G_p\iota^2}{D}$$
$$\hat{k}_p=\frac{k_p\iota^4}{D}$$
$$\iota=\Delta x=\alpha\Delta y$$

2. Point adjacent to free edge x-axis

$$\begin{pmatrix} c11\left(w_{m,n}\right)+c12\left(w_{m-1,n}+w_{m+1,n}+\alpha^2 w_{m,n+1}\right)+c21\left(w_{m,n-1}\right)+ \\ c22\left(w_{m-1,n-1}+w_{m+1,n-1}\right)+2\alpha^2\left(w_{m-1,n+1}+w_{m+1,n+1}\right)+ \\ \left(w_{m-2,n}+w_{m+2,n}\right)+\alpha^4 w_{m,n+2} \end{pmatrix}=\left(\frac{q(x,y)\iota^4}{D}\right)_{m,n} \tag{B.2}$$

Where

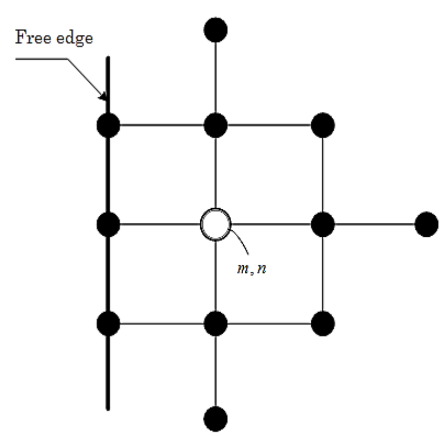

$$c11=6+8\alpha^2+5\alpha^4+2(1+\alpha^2)\hat{G}_p+\hat{k}_p$$
$$c12=-4(1+\alpha^2)-\hat{G}_p$$
$$c21=\alpha^2\left(-4-2\alpha^2+2\nu_p-\hat{G}_p\right)$$
$$c22=\alpha^2(2-\nu_p)$$

3. Point adjacent to free edge y-axis

$$\begin{pmatrix} c11\left(w_{m,n}\right)+c12\left(w_{m-1,n}\right)+c21\left(w_{m+1,n}+\alpha^2(w_{m,n-1}+w_{m,n+1})\right)+ \\ c22\left(w_{m-1,n-1}+w_{m+1,n-1}\right)+2\alpha^2\left(w_{m-1,n+1}+w_{m+1,n+1}\right)+w_{m+2,n}+ \\ \alpha^4\left(w_{m,n-2}+w_{m,n+2}\right) \end{pmatrix}=\left(\frac{q(x,y)\iota^4}{D}\right)_{m,n} \quad \text{(B.3)}$$

Where

$$c11=5+8\alpha^2+6\alpha^4+2(1+\alpha^2)\hat{G}_p+\hat{k}_p$$

$$c12=-2-4\alpha^2+2\nu_p\alpha^2-\hat{G}_p$$

$$c21=-4(1+\alpha^2)-\hat{G}_p$$

$$c22=\alpha^2(2-\nu_p)$$

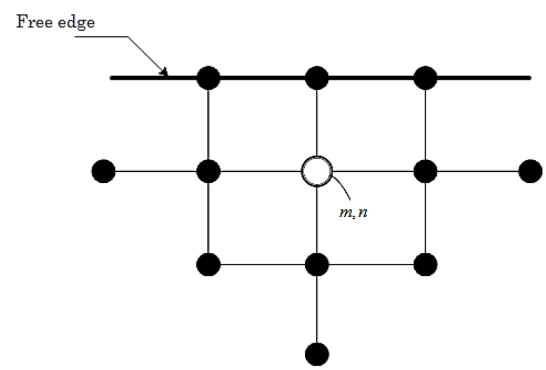

4. A point inside free corner

$$\begin{pmatrix} c11\left(w_{m,n}\right)+c12\left(w_{m-1,n}\right)+c21\left(w_{m+1,n}+\alpha^2 w_{m,n+1}\right)+ \\ c211 w_{m,n-1}+c22\left(w_{m-1,n+1}+w_{m+1,n-1}\right)+ \\ c221\left(w_{m-1,n-1}\right)+2\alpha^2\left(w_{m+1,n+1}\right)+w_{m+2,n}+\alpha^4 w_{m,n+2} \end{pmatrix}=\left(\frac{q(x,y)\iota^4}{D}\right)_{m,n} \quad \text{(B.4)}$$

Where

$$c11=5+8\alpha^2+5\alpha^4+2(1+\alpha^2)\hat{G}_p+\hat{k}_p$$

$$c12=-2-4\alpha^2+2\nu_p\alpha^2-\hat{G}_p$$

$$c21=-4(1+\alpha^2)-\hat{G}_p$$

$$c211=\alpha^2\left(-4-2\alpha^2+2\nu_p\alpha^2-\hat{G}_p\right)$$

$$c22=\alpha^2(2-\nu_p)$$

$$c221=2\alpha^2(1-\nu_p)$$

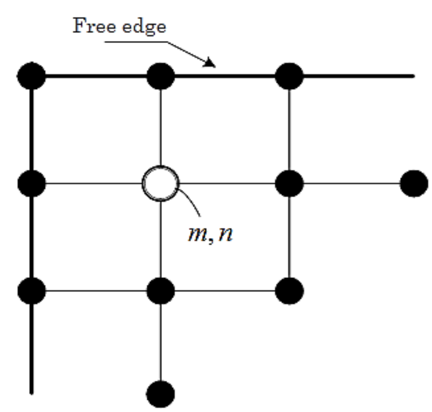

5. Point on free edge x-axis

$$\begin{pmatrix} c11\left(w_{m,n}\right)+c12\left(w_{m-1,n}+w_{m+1,n}\right)+ \\ c13\left(w_{m-2,n}+w_{m+2,n}\right)+c21\left(w_{m,n+1}\right)+ \\ c22\left(w_{m-1,n+1}+w_{m+1,n+1}\right)+2\alpha^4 w_{m,n+2} \end{pmatrix}=\left(\frac{q(x,y)\lambda^4}{D}\right)_{m,n} \tag{B.5}$$

Where

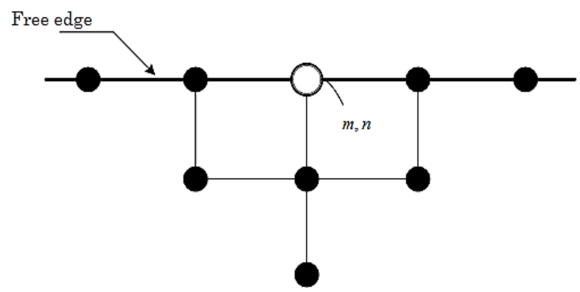

$$c11=\begin{pmatrix} 6+8\alpha^2+2\alpha^4-8\nu_p\alpha^2-6\nu_p^2+2(1+\alpha^2)\hat{G}_p+ \\ \hat{k}_p+\dfrac{2\iota^3\alpha\sqrt{k_pG_p}}{D} \end{pmatrix}$$

$$c12=-4(1+\alpha^2)+4\nu_p\alpha^2+4\nu_p^2-\hat{G}_p$$

$$c13=1-\nu_p^2$$

$$c21=-4\alpha^2\left(2+\alpha^2-\nu_p\right)-2\alpha^2\hat{G}_p$$

$$c22=2\alpha^2\left(2-\nu_p\right)$$

6. Point adjacent to free corner on free edge x-axis

$$\begin{pmatrix} c11\left(w_{m,n}\right)+c12\left(w_{m+1,n}\right)+c121\left(w_{m-1,n}\right)+c13\left(w_{m+2,n}\right)+ \\ c21\left(w_{m,n+1}\right)+c22\left(w_{m-1,n+1}+w_{m+1,n+1}\right)+2\alpha^4 w_{m,n+2} \end{pmatrix}=\left(\frac{q(x,y)\lambda^4}{D}\right)_{m,n} \tag{B.6}$$

Where

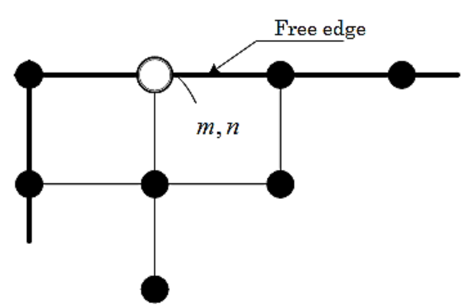

$$c11=\begin{pmatrix} 5+8\alpha^2+2\alpha^4-8\nu_p\alpha^2-5\nu_p^2+2(1+\alpha^2)\hat{G}_p+ \\ \hat{k}_p+\dfrac{2\iota^3\alpha\sqrt{k_pG_p}}{D} \end{pmatrix}$$

$$c12=-4(1+\alpha^2)+4\nu_p\alpha^2+4\nu_p^2-\hat{G}_p$$

$$c121=-2(1+2\alpha^2)+4\nu_p\alpha^2+2\nu_p^2-\hat{G}_p$$

$$c13=1-\nu_p^2$$

$$c21=-4\alpha^2\left(2+\alpha^2-\nu_p\right)-2\alpha^2\hat{G}_p$$

$$c22=2\alpha^2\left(2-\nu_p\right)$$

7. A point on free edge y-axis

$$\begin{pmatrix} c11\left(w_{m,n}\right)+c21\left(w_{m,n-1}+w_{m,n+1}\right)+c31\left(w_{m,n-2}+w_{m,n+2}\right)+ \\ c12\left(w_{m+1,n}\right)+c22\left(w_{m+1,n-1}+w_{m+1,n+1}\right)+2w_{m+2,n} \end{pmatrix}=\left(\frac{q(x,y)\lambda^4}{D}\right)_{m,n} \tag{B.7}$$

Where

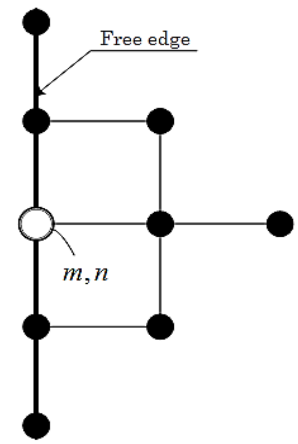

$$c11=\begin{pmatrix} 2+8\alpha^2+6\alpha^4-8\nu_p\alpha^2-6\nu_p^2\alpha^4+ \\ 2(1+\alpha^2)\hat{G}_p+\hat{k}_p+\dfrac{2\iota^3\sqrt{k_pG_p}}{D} \end{pmatrix}$$

$$c21=-4\alpha^2(1+\alpha^2)+4\nu_p\alpha^2+4\nu_p^2\alpha^4-\hat{G}_p$$

$$c31=\alpha^4\left(1-\nu_p^2\right)$$

$$c12=-4-8\alpha^2+4\nu_p\alpha^2-2\hat{G}_p$$

$$c22=2\alpha^2\left(2-\nu_p\right)$$

8. Point adjacent to free corner on free edge y-axis

$$\begin{pmatrix} c11\left(w_{m,n}\right)+c21\left(w_{m,n+1}\right)+c211\left(w_{m,n-1}\right)+c31\left(w_{m,n-2}+w_{m,n+2}\right) \\ +c12\left(w_{m+1,n}\right)+c22\left(w_{m+1,n-1}+w_{m+1,n+1}\right)+2w_{m+2,n} \end{pmatrix}=\left(\frac{q(x,y)\lambda^4}{D}\right)_{m,n} \tag{B.8}$$

Where

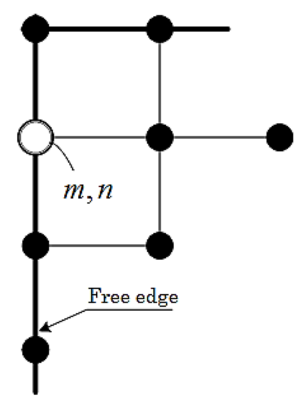

$$c11=\begin{pmatrix} 2+8\alpha^2+6\alpha^4-8\nu_p\alpha^2-6\nu_p^2\alpha^4 \\ +2(1+\alpha^2)\hat{G}_p+\hat{k}_p+\dfrac{2\iota^3\sqrt{k_pG_p}}{D} \end{pmatrix}$$

$$c21=-4\alpha^2(1+\alpha^2)+4\nu_p\alpha^2+4\nu_p^2\alpha^4-\hat{G}_p$$

$$c211=-2\alpha^2(2+\alpha^2)+4\nu_p\alpha^2+2\nu_p^2\alpha^4-\hat{G}_p$$

$$c31=\alpha^4\left(1-\nu_p^2\right)$$

$$c12=-4-8\alpha^2+4\nu_p\alpha^2-2\hat{G}_p$$

$$c22=2\alpha^2\left(2-\nu_p\right)$$

9. A point on the free corner

$$\begin{pmatrix} c11\left(w_{m,n}\right)+c12\left(w_{m+1,n}\right)+c13\left(w_{m+2,n}\right)+c21\left(w_{m,n+1}\right)+ \\ c22\left(w_{m+1,n+1}\right)+c31\left(w_{m,n+2}\right) \end{pmatrix} = \left(\frac{q(x,y)\iota^4}{D}\right)_{m,n} \tag{B.9}$$

Where

$$c11 = \begin{pmatrix} 2+8\alpha^2+2\alpha^4-8\nu_p\alpha^2-2\nu_p^2\left(1+\alpha^2\right)+ \\ (1+\alpha)\hat{G}_p+\hat{k}_p+\dfrac{2\iota^3(1+\alpha)\sqrt{k_pG_p}}{D} \end{pmatrix}$$

$$c12 = -4-8\alpha^2+8\nu_p\alpha^2+4\nu_p^2-\hat{G}_p$$

$$c13 = 2\left(1-\nu_p^2\right)$$

$$c21 = -8\alpha^2-4\alpha^4+8\nu_p\alpha^2+4\nu_p^2\alpha^4-\alpha\hat{G}_p$$

$$c22 = 8\alpha^2\left(1-\nu_p\right)$$

$$c31 = 2\alpha^4\left(1-\nu_p^2\right)$$

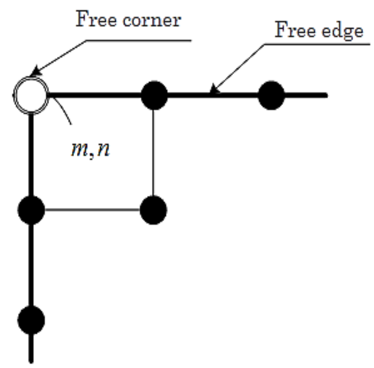

Appendix C

Expressions for Moment, shears, and subgrade reactions

1. Point inside

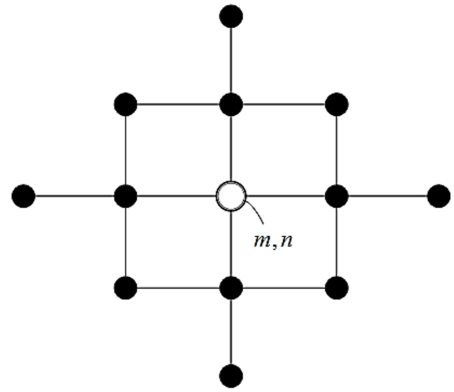

$$\left(M_x\right)_{m,n} = -\frac{D}{\iota^2}\begin{bmatrix} -2(1+\nu_p\alpha^2)w_{m,n} + \nu_p\alpha^2(w_{m,n-1}+w_{m,n+1}) + \\ w_{m-1,n}+w_{m+1,n} \end{bmatrix}$$

$$\left(M_y\right)_{m,n} = -\frac{D}{\iota^2}\begin{bmatrix} -2(\nu_p+\alpha^2)w_{m,n} + \alpha^2(w_{m,n-1}+w_{m,n+1}) + \\ \nu_p(w_{m-1,n}+w_{m+1,n}) \end{bmatrix}$$

$$\left(M_{xy}\right)_{m,n} = -\frac{D(1-\nu_p)\alpha}{4\iota^2}\left(w_{m-1,n-1}-w_{m+1,n-1}-w_{m-1,n+1}+w_{m+1,n+1}\right)$$

$$\left(V_x\right)_{m,n} = -\frac{D}{2\iota^3}\begin{bmatrix} \left(2(1+\alpha^2)+\hat{G}_p\right)(w_{m-1,n}-w_{m+1,n}) - \alpha^2(w_{m-1,n-1} \\ +w_{m-1,n+1}) + \alpha^2(w_{m+1,n-1}+w_{m+1,n+1}) - w_{m-2,n}+w_{m+2,n} \end{bmatrix} \tag{C.1}$$

$$\left(V_y\right)_{m,n} = -\frac{D}{2\iota^3}\begin{bmatrix} \left(2(1+\alpha^2)-\hat{G}_p\right)\left(w_{m,n-1}-w_{m,n+1}\right) - w_{m-1,n-1} - \\ w_{m+1,n-1}+w_{m-1,n+1}+w_{m+1,n+1}+\alpha^2(-w_{m,n-2}+w_{m,n+2}) \end{bmatrix}$$

$$\left(p(x,y)\right)_{m,n} = -\frac{G_p}{\iota^2}\left[\left(-2(1+\alpha^2)+\frac{k_p\iota^2}{G_p}\right)w_{m,n} + \alpha^2\left(w_{m,n-1}+w_{m,n+1}\right) + w_{m+1,n}+w_{m-1,n}\right]$$

2. Point adjacent to free edge x-axis

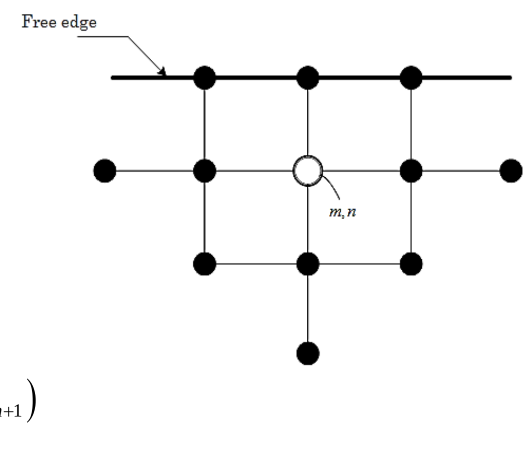

$$\left(M_x\right)_{m,n} = -\frac{D}{\iota^2}\begin{bmatrix} -2(1+\nu_p\alpha^2)w_{m,n} + \nu_p\alpha^2(w_{m,n-1}+w_{m,n+1}) + \\ w_{m-1,n}+w_{m+1,n} \end{bmatrix}$$

$$\left(M_y\right)_{m,n} = -\frac{D}{\iota^2}\begin{bmatrix} -2(\nu_p+\alpha^2)w_{m,n} + \alpha^2(w_{m,n-1}+w_{m,n+1}) + \\ \nu_p(w_{m-1,n}+w_{m+1,n}) \end{bmatrix}$$

$$\left(M_{xy}\right)_{m,n} = -\frac{D(1-\nu_p)\alpha}{4\iota^2}\left(w_{m-1,n-1}-w_{m+1,n-1}-w_{m-1,n+1}+w_{m+1,n+1}\right)$$

$$\left(V_x\right)_{m,n} = -\frac{D}{2\iota^3}\begin{bmatrix} \left(2(1+\alpha^2)+\hat{G}_p\right)(w_{m-1,n}-w_{m+1,n})-\alpha^2(w_{m-1,n-1}+w_{m-1,n+1})+ \\ \alpha^2(w_{m+1,n-1}+w_{m+1,n+1})-w_{m-2,n}+w_{m+2,n} \end{bmatrix} \tag{C.2}$$

$$\left(V_y\right)_{m,n} = -\frac{D}{2\iota^3}\begin{bmatrix} \left(2(1+\alpha^2)+\hat{G}_p\right)(w_{m,n-1}-w_{m,n+1})-(1-\nu_p)(w_{m-1,n-1}+w_{m+1,n-1}) \\ +w_{m-1,n+1}+w_{m+1,n+1}+\alpha^2(w_{m,n}+w_{m,n+2}) \end{bmatrix}$$

$$\left(p(x,y)\right)_{m,n} = -\frac{G_p}{\iota^2}\left[\left(-2(1+\alpha^2)+\frac{k_p\iota^2}{G_p}\right)w_{m,n}+\alpha^2\left(w_{m,n-1}+w_{m,n+1}\right)+w_{m+1,n}+w_{m-1,n}\right]$$

3. Point adjacent to free edge y-axis

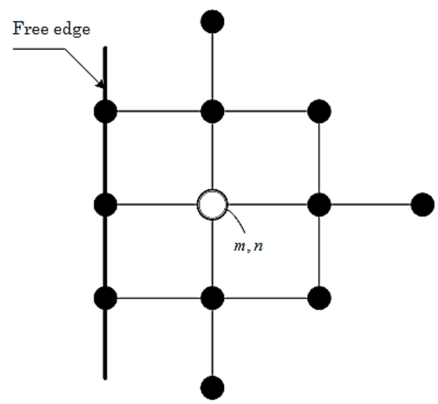

$$\left(M_x\right)_{m,n} = -\frac{D}{\iota^2}\begin{bmatrix} -2(1+\nu_p\alpha^2)w_{m,n}+\nu_p\alpha^2(w_{m,n-1}+w_{m,n+1})+ \\ w_{m-1,n}+w_{m+1,n} \end{bmatrix}$$

$$\left(M_y\right)_{m,n} = -\frac{D}{\iota^2}\begin{bmatrix} -2(\nu_p+\alpha^2)w_{m,n}+\alpha^2(w_{m,n-1}+w_{m,n+1})+ \\ \nu_p(w_{m-1,n}+w_{m+1,n}) \end{bmatrix}$$

$$\left(M_{xy}\right)_{m,n} = -\frac{D(1-\nu_p)\alpha}{4\iota^2}\left(w_{m-1,n-1}-w_{m+1,n-1}-w_{m-1,n+1}+w_{m+1,n+1}\right)$$

$$\left(V_x\right)_{m,n} = -\frac{D}{2\iota^3}\begin{bmatrix} -2\left(1+\alpha^2\right)w_{m+1,n}-\hat{G}_p\left(w_{m-1,n}-w_{m+1,n}\right)+\alpha^2(w_{m+1,n-1}+w_{m+1,n+1})- \\ \alpha^2\left(1-\nu_p\right)\left(w_{m-1,n-1}+w_{m-1,n+1}-w_{m-1,n}\right)+w_{m+2,n} \end{bmatrix} \tag{C.3}$$

$$\left(V_y\right)_{m,n} = -\frac{D}{2\iota^3}\begin{bmatrix} \left(2(1+\alpha^2)-\hat{G}_p\right)\left(w_{m,n-1}-w_{m,n+1}\right)-w_{m-1,n-1}-w_{m+1,n-1}+ \\ w_{m-1,n+1}+w_{m+1,n+1}+\alpha^2(-w_{m,n-2}+w_{m,n+2}) \end{bmatrix}$$

$$\left(p(x,y)\right)_{m,n} = -\frac{G_p}{\iota^2}\left[\left(-2(1+\alpha^2)+\frac{k_p\iota^2}{G_p}\right)w_{m,n}+\alpha^2\left(w_{m,n-1}+w_{m,n+1}\right)+w_{m+1,n}+w_{m-1,n}\right]$$

4. Point inside free corner

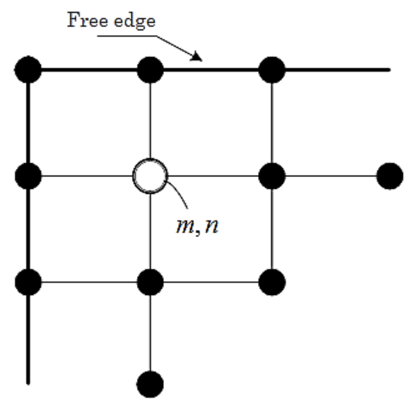

$$\left(M_x\right)_{m,n} = -\frac{D}{\iota^2}\begin{bmatrix} -2(1+\nu_p\alpha^2)w_{m,n} + \nu_p\alpha^2(w_{m,n-1} + w_{m,n+1}) + \\ w_{m-1,n} + w_{m+1,n} \end{bmatrix}$$

$$\left(M_y\right)_{m,n} = -\frac{D}{\iota^2}\begin{bmatrix} -2(\nu_p+\alpha^2)w_{m,n} + \alpha^2(w_{m,n-1} + w_{m,n+1}) + \\ \nu_p(w_{m-1,n} + w_{m+1,n}) \end{bmatrix}$$

$$\left(M_{xy}\right)_{m,n} = -\frac{D(1-\nu_p)\alpha}{4\iota^2}\left(w_{m-1,n-1} - w_{m+1,n-1} - w_{m-1,n+1} + w_{m+1,n+1}\right)$$

$$\left(V_x\right)_{m,n} = -\frac{D}{2\iota^3}\begin{bmatrix} -2\left(1+\alpha^2\right)w_{m+1,n} - \hat{G}_p\left(w_{m-1,n} - w_{m+1,n}\right) + \alpha^2(w_{m+1,n-1} + w_{m+1,n+1}) - \\ \alpha^2\left(1-\nu_p\right)\left(w_{m-1,n-1} + w_{m-1,n+1} - w_{m-1,n}\right) + w_{m+2,n} \end{bmatrix} \tag{C.4}$$

$$\left(V_y\right)_{m,n} = -\frac{D}{2\iota^3}\begin{bmatrix} \left(2(1+\alpha^2) - \hat{G}_p\right)(w_{m,n-1} - w_{m,n+1}) - (1-\nu_p)(w_{m-1,n-1} + w_{m+1,n-1}) + \\ w_{m-1,n+1} + w_{m+1,n+1} + \alpha^2(w_{m,n} + w_{m,n+2}) \end{bmatrix}$$

$$\left(p(x,y)\right)_{m,n} = -\frac{G_p}{\iota^2}\left[\left(-2(1+\alpha^2) + \frac{k_p\iota^2}{G_p}\right)w_{m,n} + \alpha^2\left(w_{m,n-1} + w_{m,n+1}\right) + w_{m+1,n} + w_{m-1,n}\right]$$

5. Point on free edge x-axis

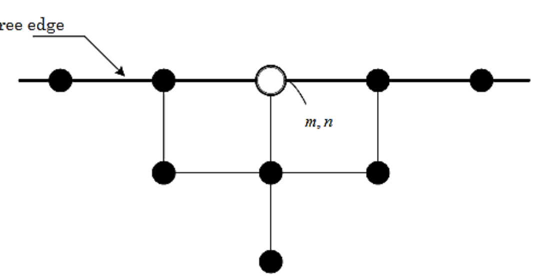

$$\left(M_x\right)_{m,n} = -\frac{D\left(1-\nu_p^2\right)}{\iota^2}\left[-2w_{m,n} + w_{m-1,n} + w_{m+1,n}\right]$$

$$\left(M_y\right)_{m,n} = 0$$

$$\left(V_x\right)_{m,n} = -\frac{D}{2\iota^3}\left[\hat{G}_p\left(w_{m+1,n} - w_{m-1,n}\right) + \left(1-\nu_p\right)\left(2\left(w_{m-1,n} - w_{m+1,n}\right) - w_{m-2,n} + w_{m+2,n}\right)\right] \tag{C.5}$$

$$\left(V_y\right)_{m,n} = -\frac{G_p}{2\iota\alpha}\left[\left(-2(\nu_p+\alpha^2) + 2\iota\alpha\sqrt{\frac{k_p}{G_p}}\right)w_{m,n} + \nu_p\left(w_{m-1,n} + w_{m+1,n}\right) + 2\alpha^2 w_{m,n+1}\right]$$

$$\left(p(x,y)\right)_{m,n} = -\frac{G_p}{\iota^2}\left[\left(-2(1-\nu_p) - \frac{k_p\iota^2}{G_p}\right)w_{m,n} + (1-\nu_p)\left(w_{m+1,n} + w_{m-1,n}\right)\right]$$

6. Point adjacent to free corner on free edge x-axis

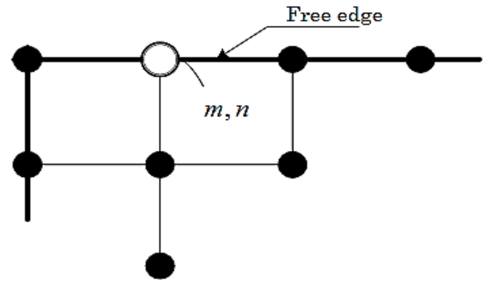

$$\left(M_x\right)_{m,n} = -\frac{D\left(1-\nu_p^2\right)}{\iota^2}\left[-2w_{m,n} + w_{m-1,n} + w_{m+1,n}\right]$$

$$\left(M_y\right)_{m,n} = 0$$

$$\left(V_x\right)_{m,n} = -\frac{D}{2\iota^3}\left[\hat{G}_p\left(w_{m+1,n} - w_{m-1,n}\right) + \left(1-\nu_p\right)\left(2w_{m+1,n} - w_{m-1,n} + w_{m+2,n}\right)\right] \qquad \text{(C.6)}$$

$$\left(V_y\right)_{m,n} = -\frac{G_p}{2\iota\alpha}\left[\left(-2(\nu_p+\alpha^2) + 2\iota\alpha\sqrt{\frac{k_p}{G_p}}\right)w_{m,n} + \nu_p\left(w_{m-1,n} + w_{m+1,n}\right) + 2\alpha^2 w_{m,n+1}\right]$$

$$\left(p(x,y)\right)_{m,n} = -\frac{G_p}{\iota^2}\left[\left(-2(1-\nu_p) - \frac{k_p\iota^2}{G_p}\right)w_{m,n} + (1-\nu_p)\left(w_{m+1,n} + w_{m-1,n}\right)\right]$$

7. Point on free edge y-axis

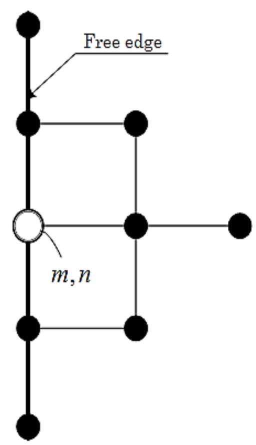

$$\left(M_x\right)_{m,n} = 0$$

$$\left(M_y\right)_{m,n} = -\frac{D\left(1-\nu_p^2\right)\alpha^2}{\iota^2}\left[-2w_{m,n} + w_{m,n-1} + w_{m,n+1}\right]$$

$$\left(V_x\right)_{m,n} = -\frac{G_p}{2\iota}\left[\left(-2(1+\nu_p\alpha^2) + 2\iota\sqrt{\frac{k_p}{G_p}}\right)w_{m,n} + \nu_p\alpha^2\left(w_{m,n-1} + w_{m,n+1}\right) + 2w_{m+1,n}\right] \qquad \text{(C.7)}$$

$$\left(V_y\right)_{m,n} = -\frac{D}{2\iota^3}\left[\hat{G}_p\left(w_{m,n+1} - w_{m,n-1}\right) + \alpha^2\left(1-\nu_p\right)\left(2(w_{m,n-1} - w_{m,n+1}) - w_{m,n-2} + w_{m,n+2}\right)\right]$$

$$\left(p(x,y)\right)_{m,n} = -\frac{G_p}{\iota^2}\left[\left(-2(1-\nu_p)\alpha^2 - \frac{k_p\iota^2}{G_p}\right)w_{m,n} + \alpha^2(1-\nu_p)\left(w_{m,n+1} + w_{m,n-1}\right)\right]$$

8. Point adjacent to free corner on free edge y-axis

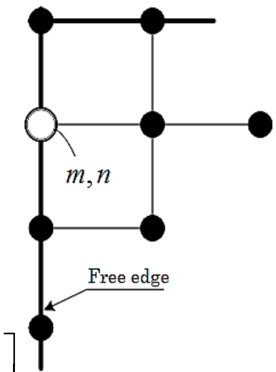

$$(M_x)_{m,n} = 0$$

$$(M_y)_{m,n} = -\frac{D\left(1-\nu_p^2\right)\alpha^2}{\iota^2}\left[-2w_{m,n} + w_{m,n-1} + w_{m,n+1}\right]$$

$$(V_x)_{m,n} = -\frac{G_p}{2\iota}\left[\left(-2(1+\nu_p\alpha^2)+2\iota\sqrt{\frac{k_p}{G_p}}\right)w_{m,n} + \nu_p\alpha^2\left(w_{m,n-1}+w_{m,n+1}\right)+2w_{m+1,n}\right] \tag{C.8}$$

$$(V_y)_{m,n} = -\frac{D}{2\iota^3}\left[\hat{G}_p\left(w_{m,n+1}-w_{m,n-1}\right)+\alpha^2\left(1-\nu_p\right)\left(-2w_{m,n+1}+w_{m,n}+w_{m,n+2}\right)\right]$$

$$\left(p(x,y)\right)_{m,n} = -\frac{G_p}{\iota^2}\left[\left(-2(1-\nu_p)\alpha^2 - \frac{k_p\iota^2}{G_p}\right)w_{m,n} + \alpha^2(1-\nu_p)\left(w_{m,n+1}+w_{m,n-1}\right)\right]$$

9. Point on free corner

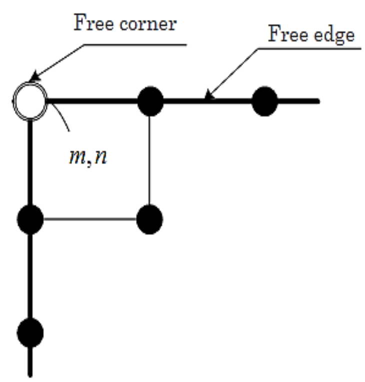

$$(M_x)_{m,n} = 0$$

$$(M_y)_{m,n} = 0$$

$$(V_x)_{m,n} = -\frac{G_p}{\iota}\left[\left(-1+\iota\sqrt{\frac{k_p}{G_p}}\right)w_{m,n} + w_{m+1,n}\right]$$

$$(V_y)_{m,n} = -\frac{G_p}{\iota}\left[\left(-\alpha+\iota\sqrt{\frac{k_p}{G_p}}\right)w_{m,n} + \alpha w_{m,n+1}\right] \tag{C.9}$$

$$\left(p(x,y)\right)_{m,n} = k_p\left[w_{m,n}\right]$$

Appendix D

Numerical comparison for rectangular plates

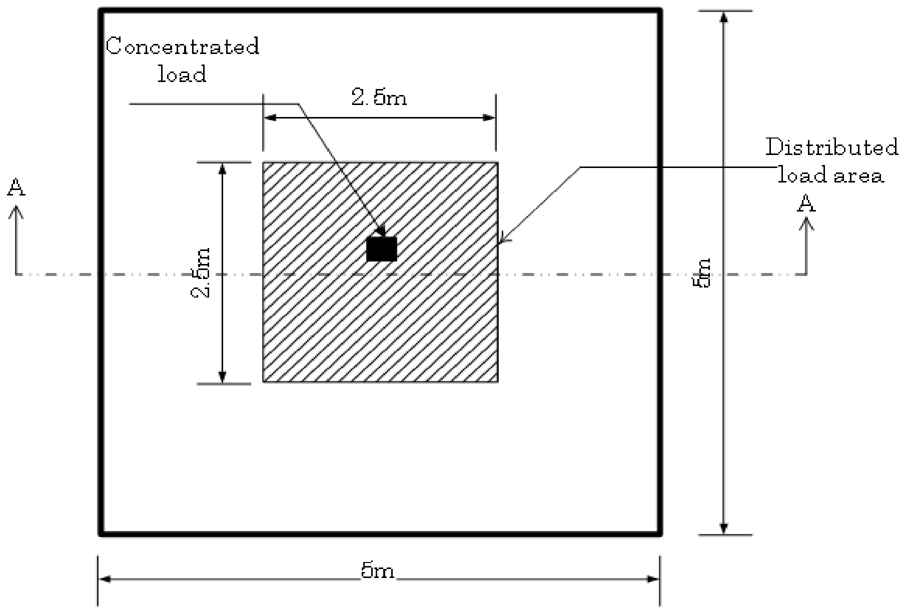

a)

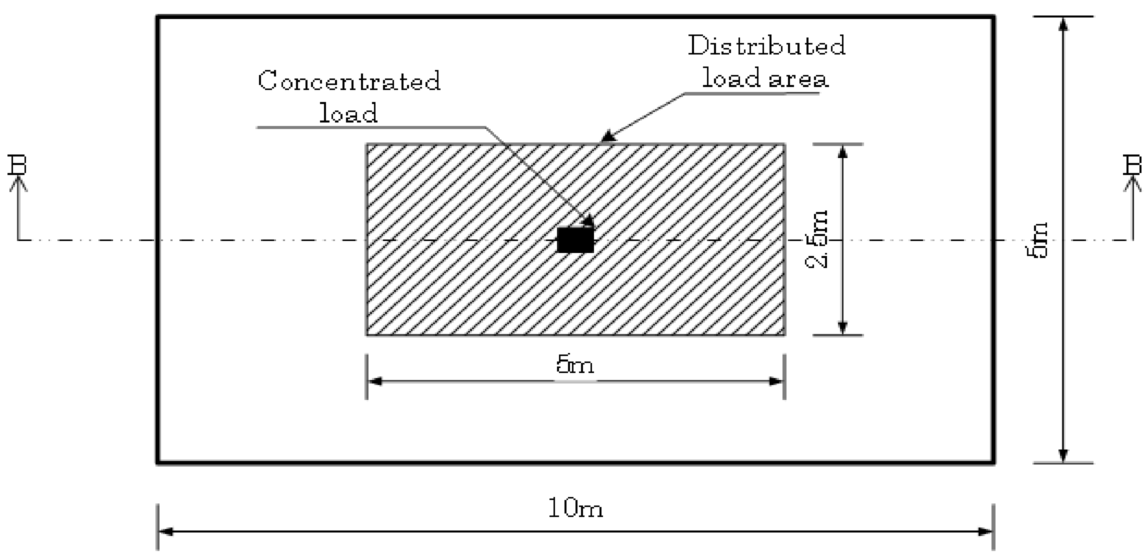

b)

Figure D1: Rectangular plate with a) L/B=1 b) L/B=2

D1.1. Concentrated load (L/B=1)

Worku's Pasternak type model (FDM)

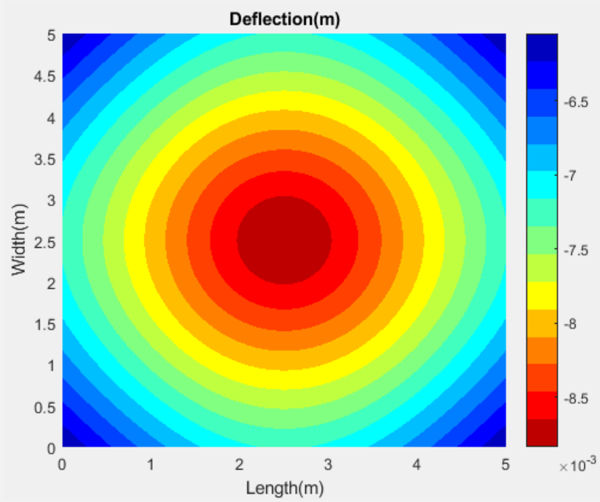

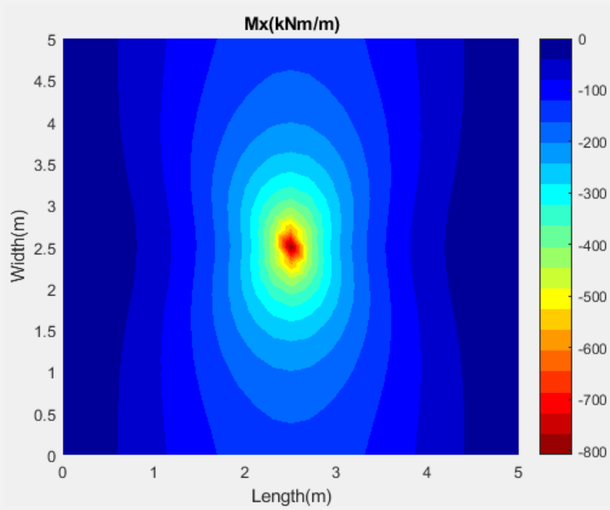

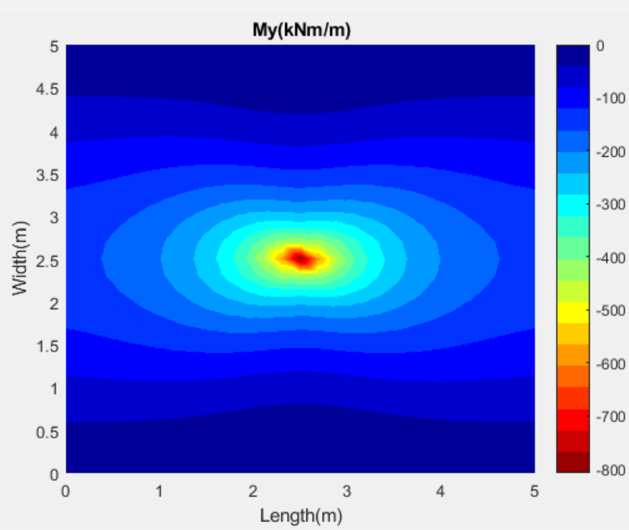

Plaxis 3D

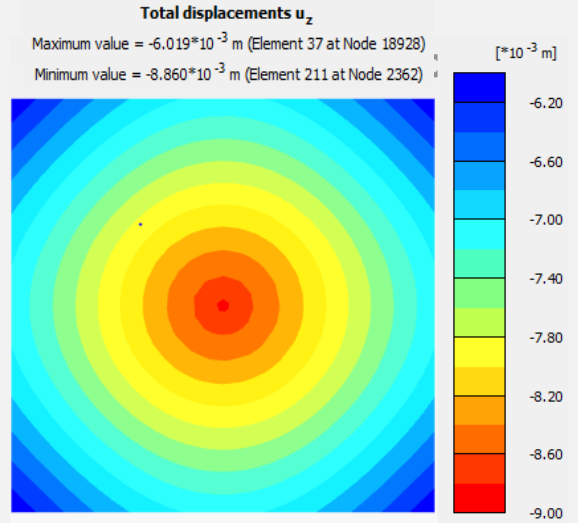

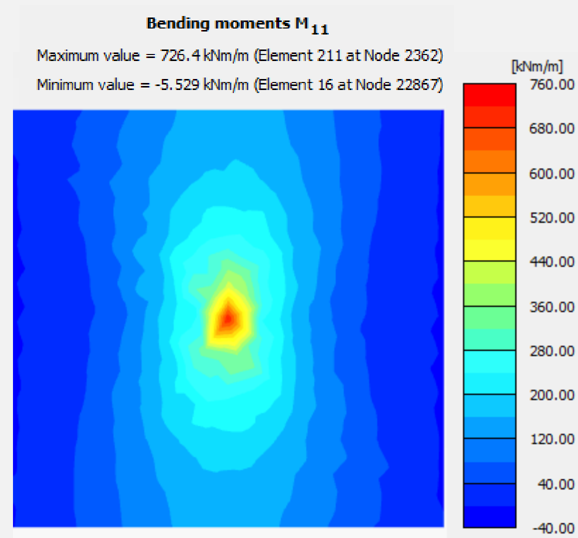

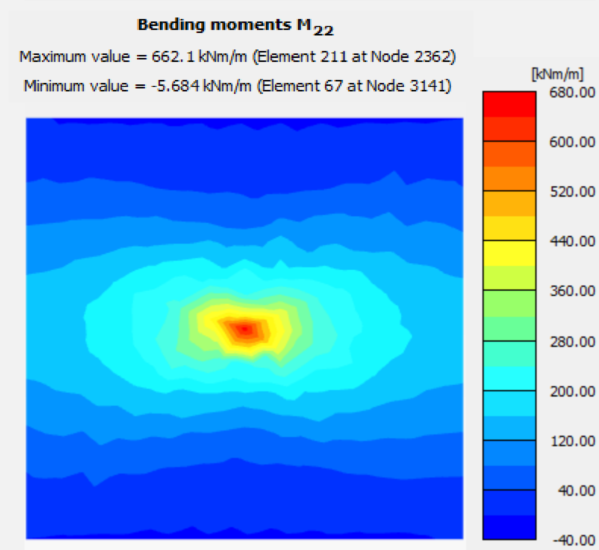

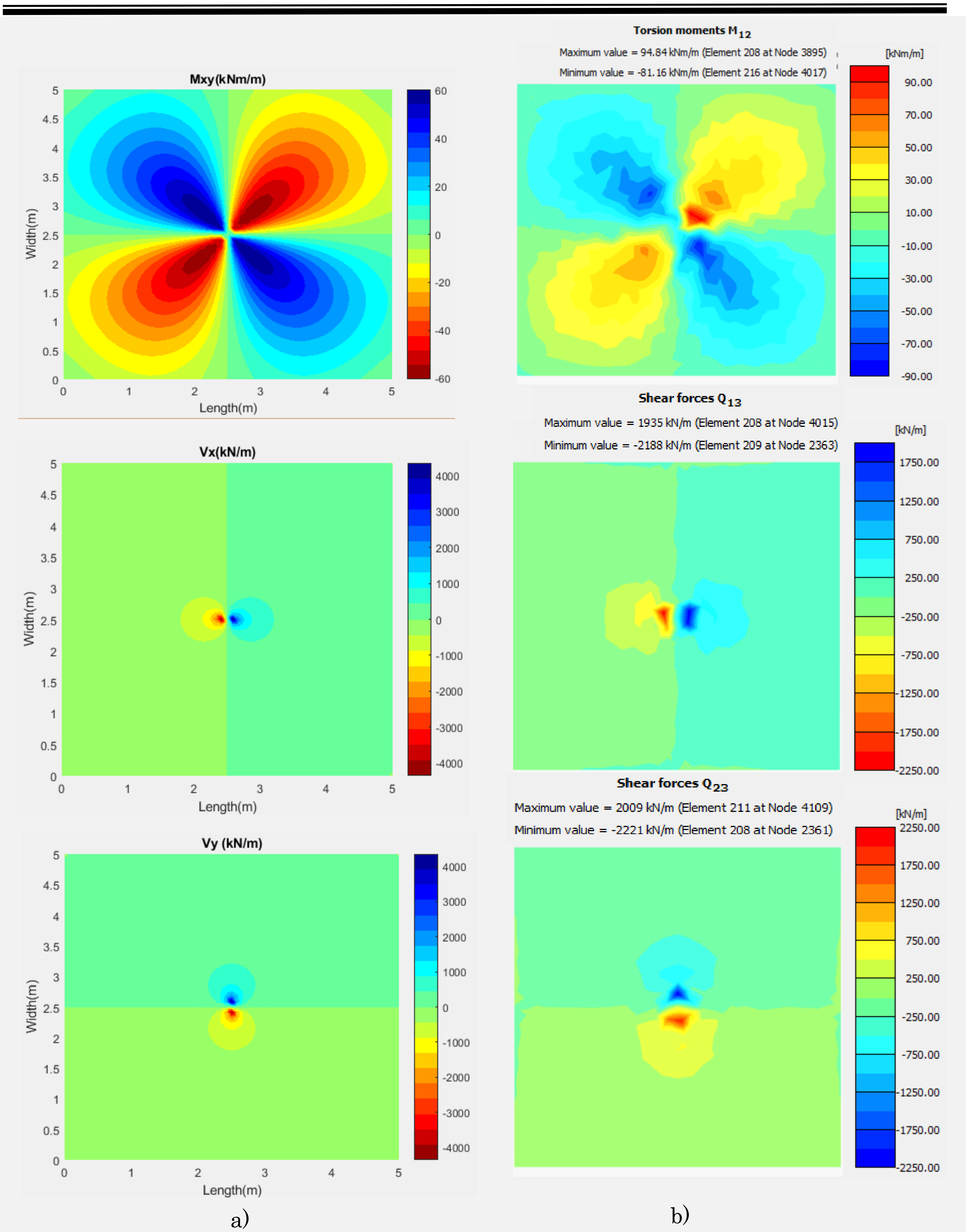

Figure D2: Deflection and internal action of Rectangular plate (L/B=1) resting on Medium strength soil subjected to a vertical concentrated load based on; a) Worku's Pasternak type model (FDM) b) Plaxis 3D.

D.1.2. Uniformly distributed load(L/B=1)

Worku's Pasternak type model (FDM)

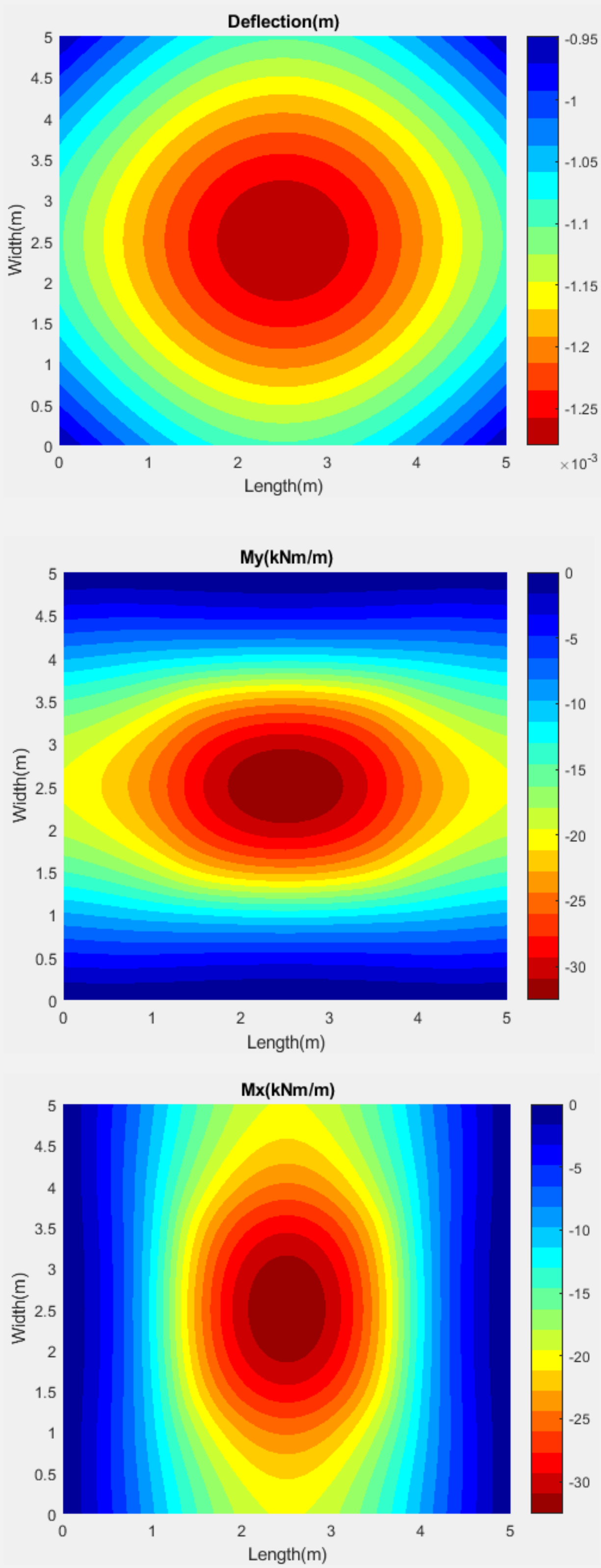

Plaxis 3D

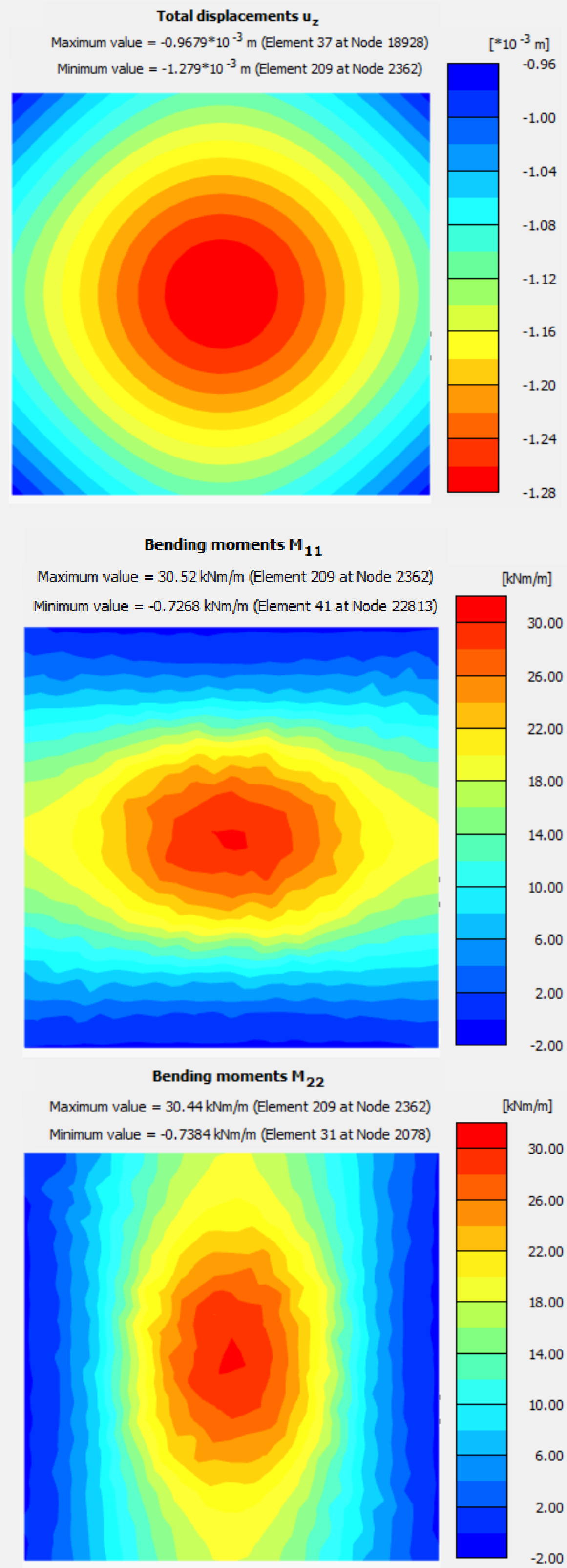

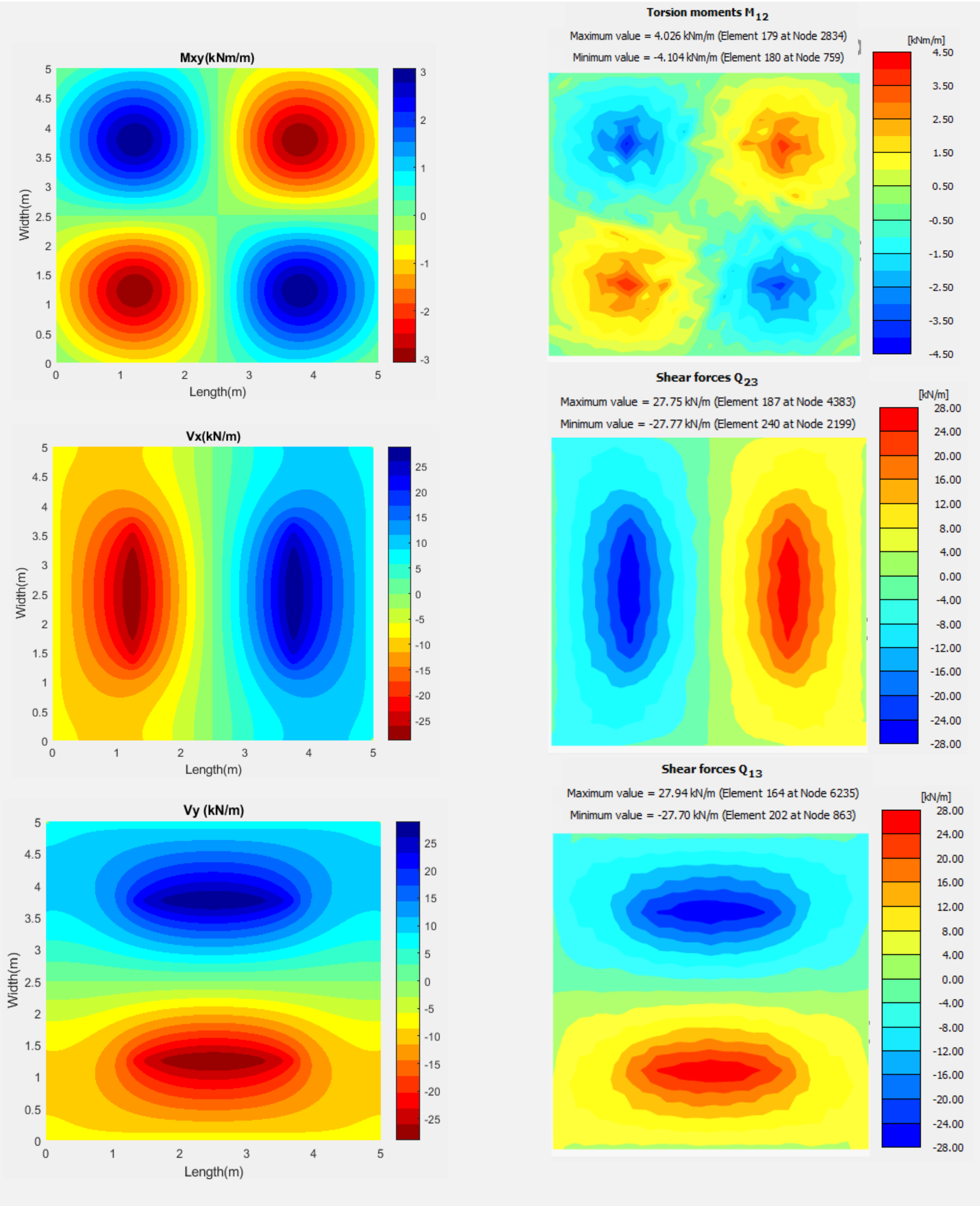

a) b)

Figure D3: Deflection and internal action of Rectangular plate (L/B=1) resting on Medium strength soil subjected to a uniformly distributed load based on; a) Worku's Pasternak type model (FDM), b) Plaxis 3D

D.1.3. Combined load

Worku's Pasternak type model (FDM)

Plaxis 3D

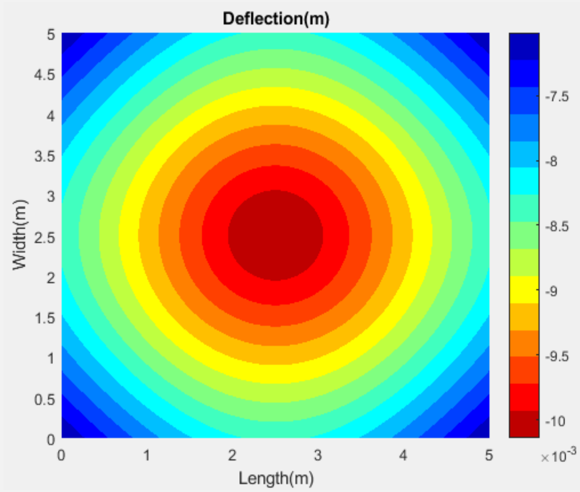

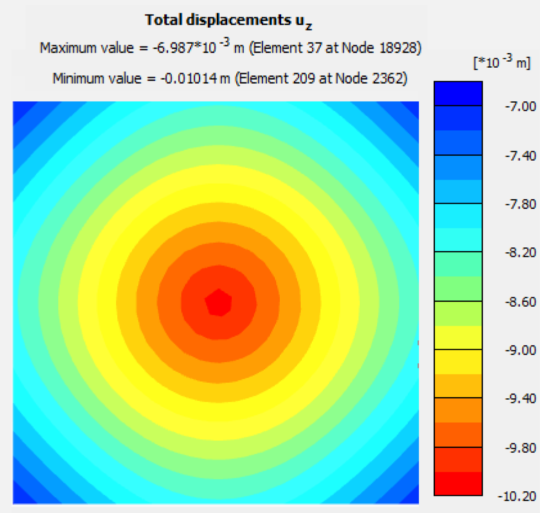

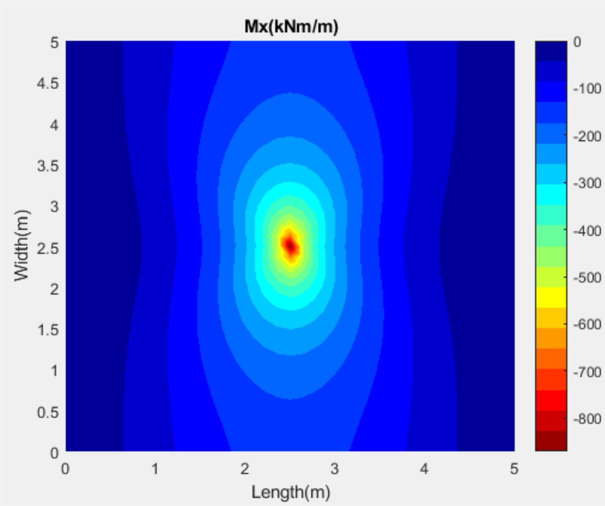

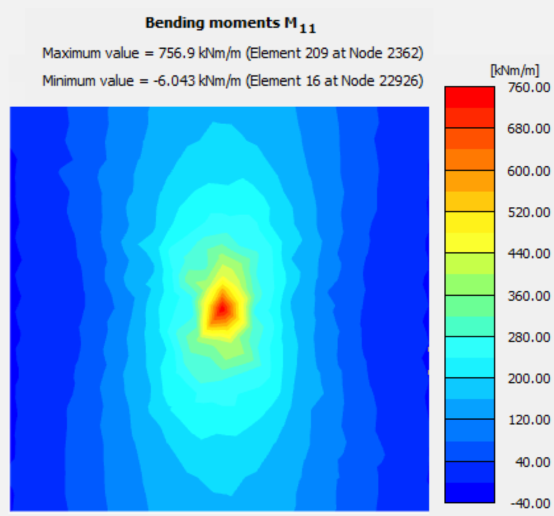

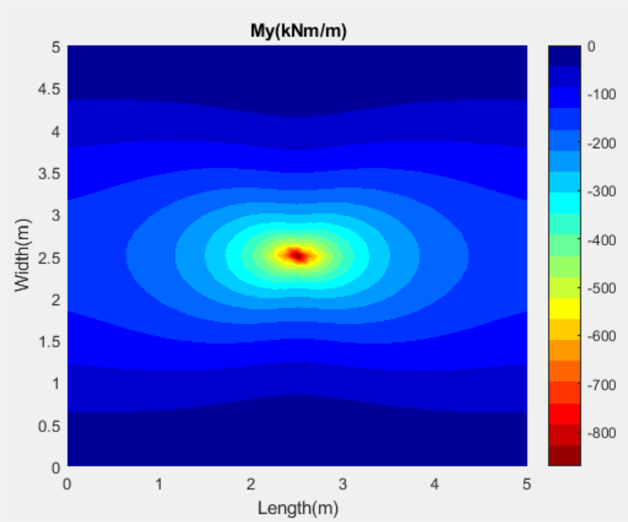

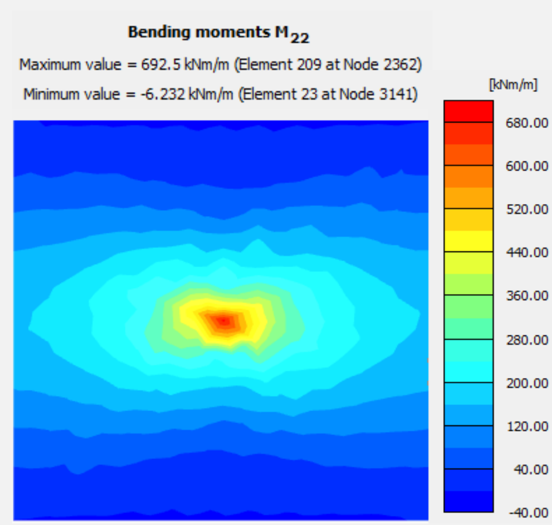

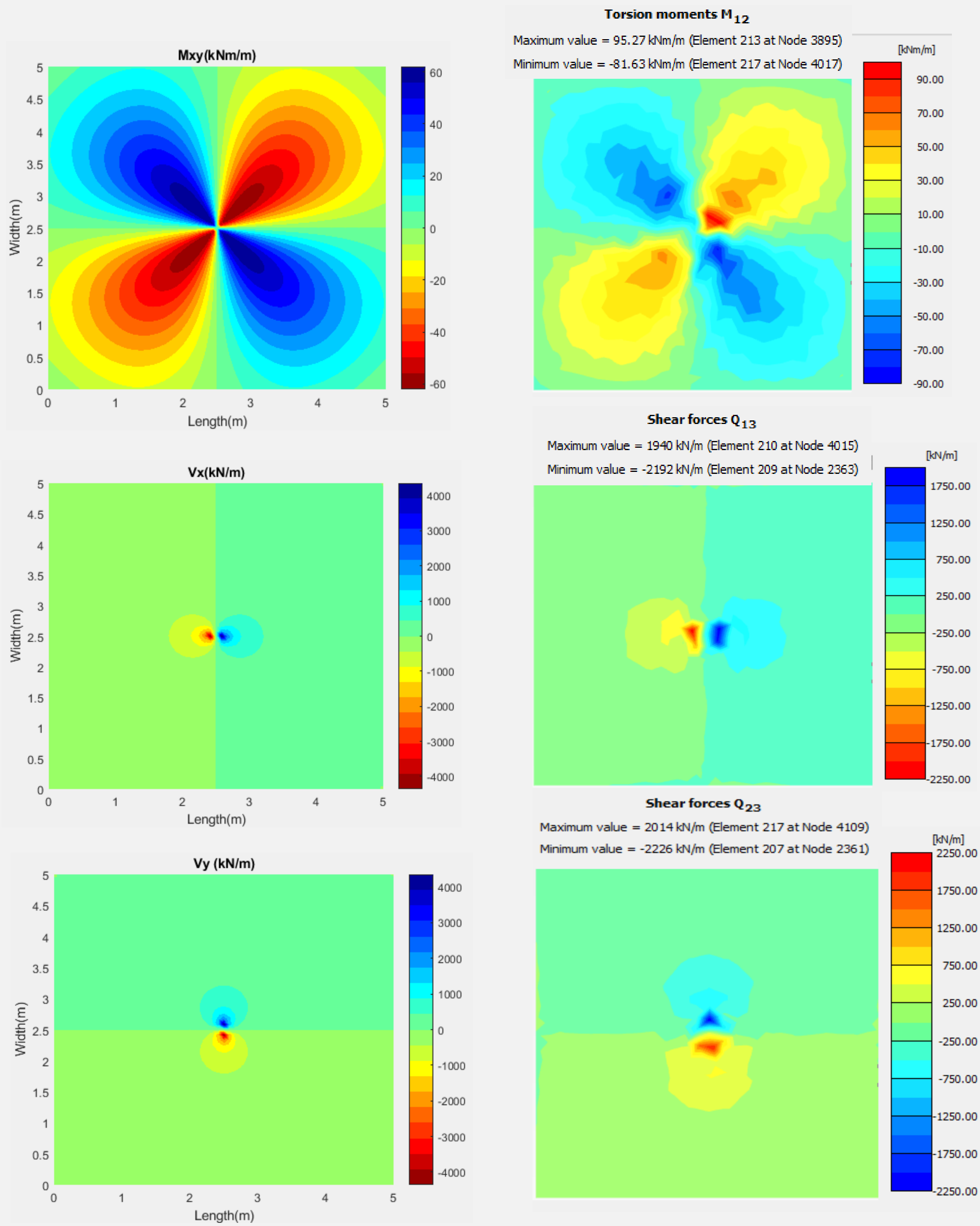

a) b)

Figure D4: Deflection and internal action of Rectangular plate (L/B=1) resting on Medium strength soil subjected to a combined load based on; a) Worku's Pasternak type model (FDM), b) Plaxis 3D

D2.1. Concentrated load (L/B=2)

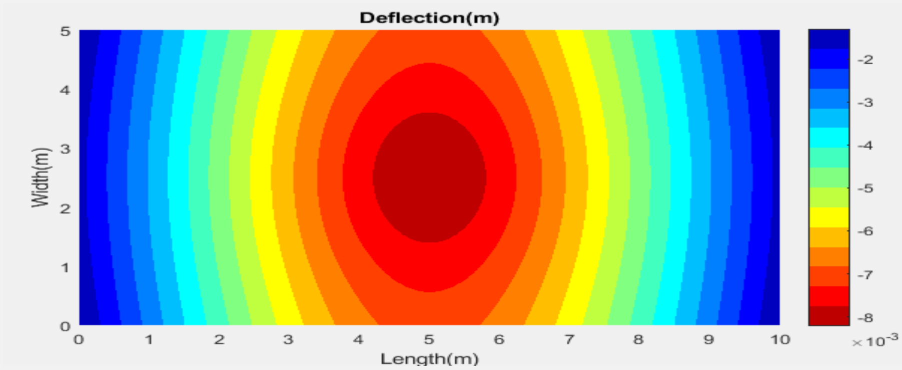

Worku's Pasternak type model (FDM)

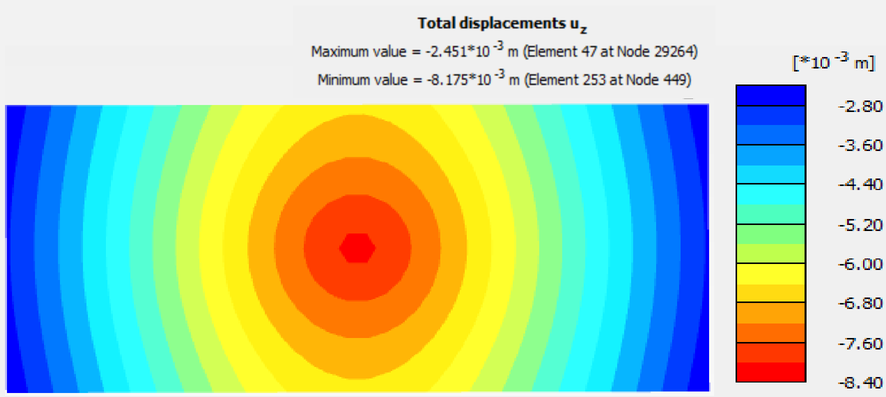

Plaxis 3D

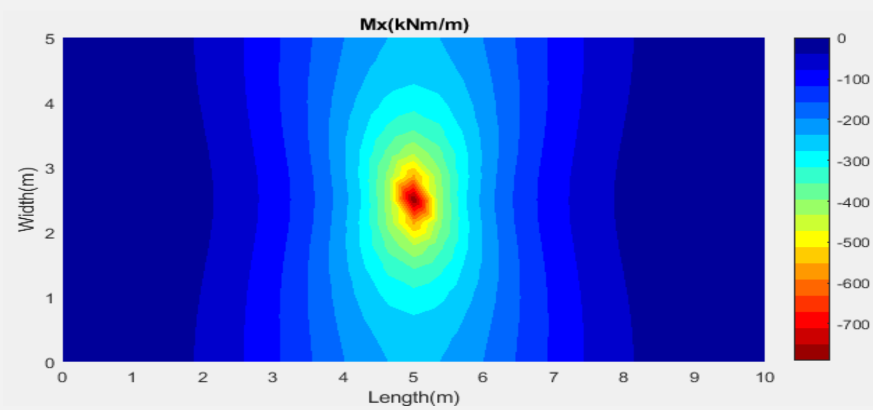

Worku's Pasternak type model (FDM)

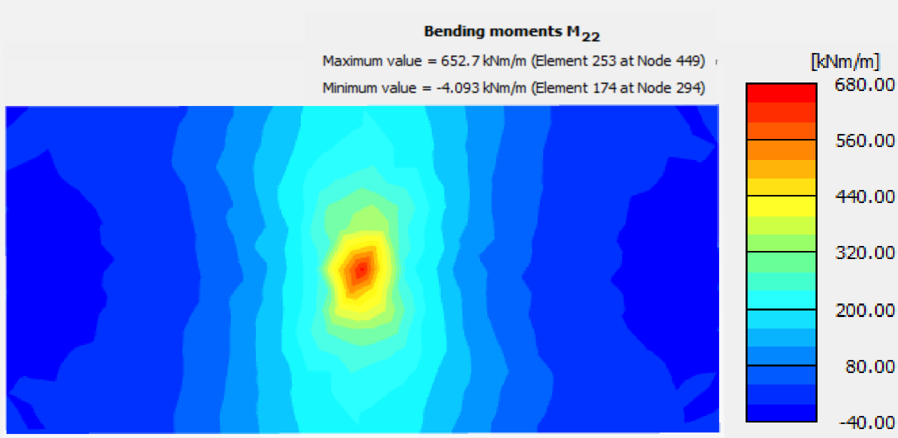

Plaxis 3D

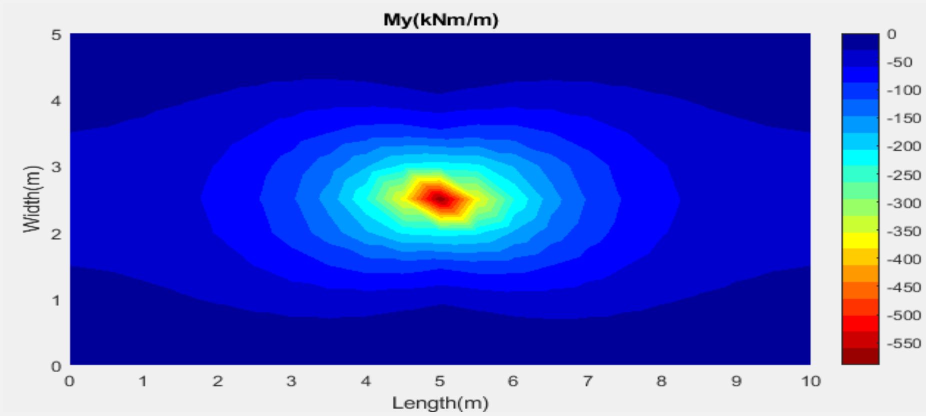

Worku's Pasternak type model (FDM)

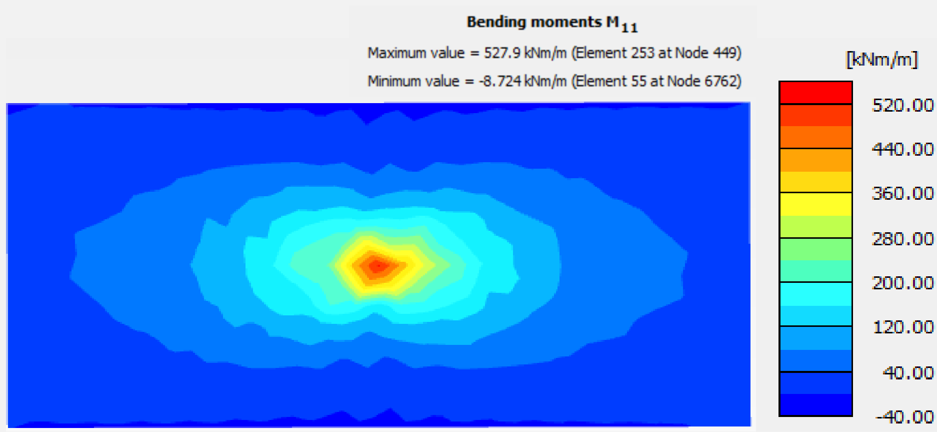

Plaxis 3D

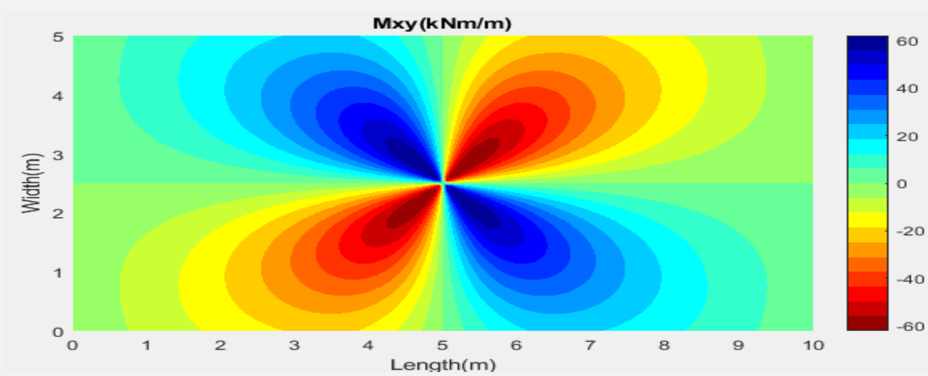

Worku's Pasternak type model (FDM)

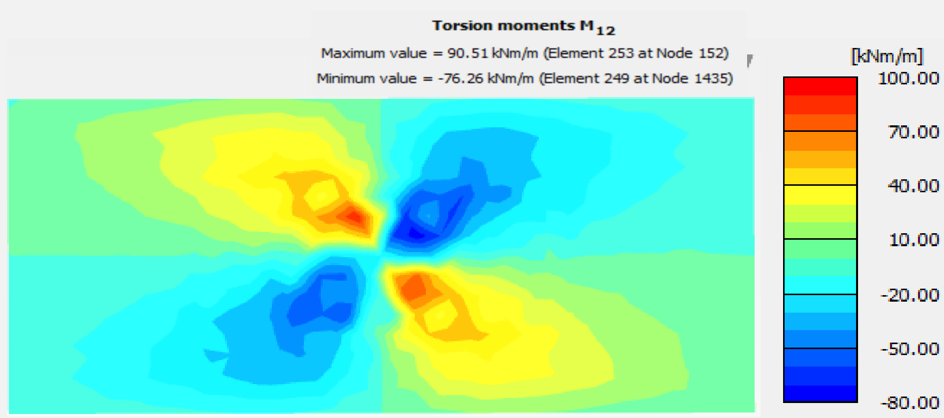

Plaxis 3D

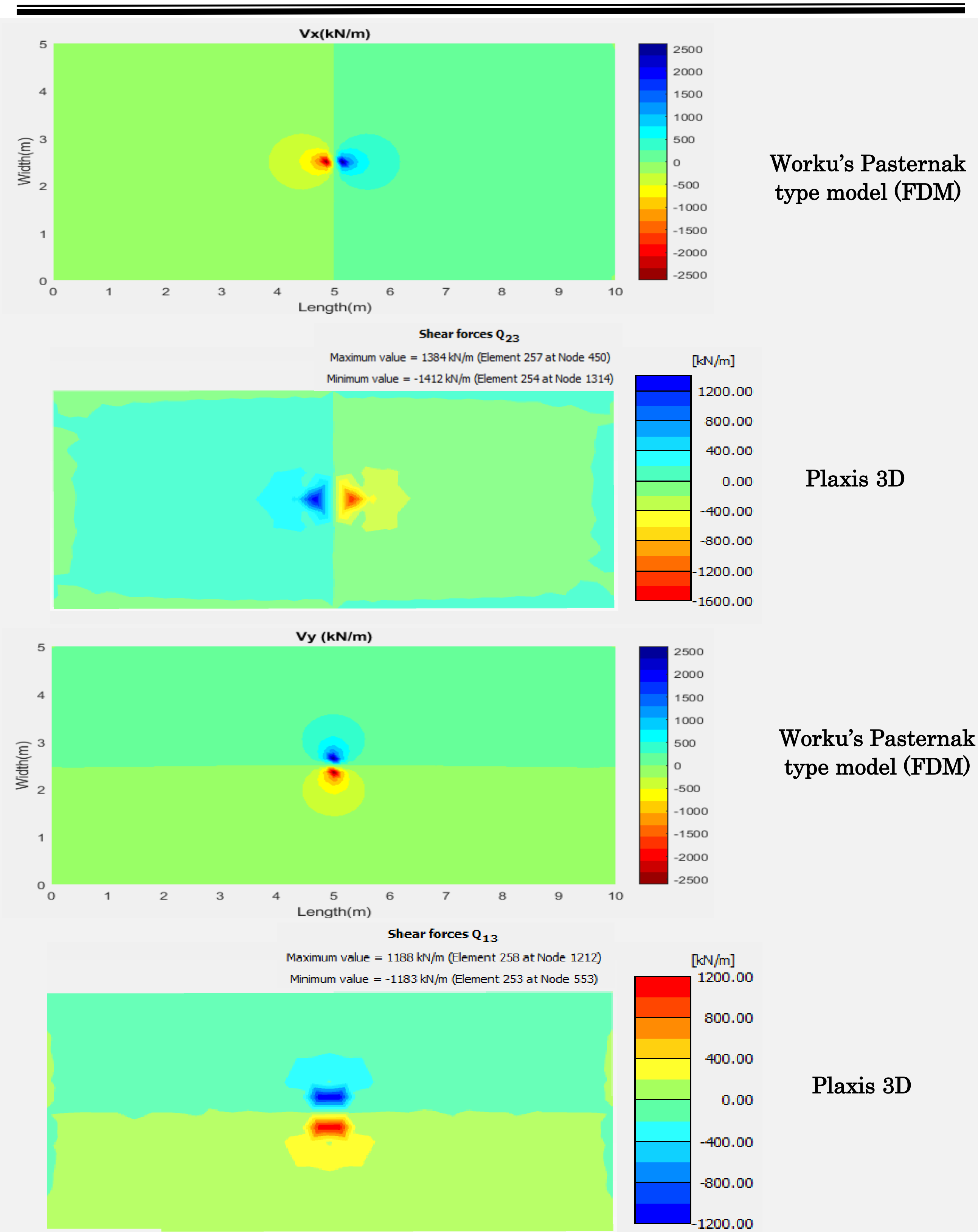

Figure D5: Deflection and internal action of Rectangular plate (L/B=2) resting on Medium strength soil subjected to a concentrated load

D2.1.2. Uniformly distributed load L/B=2

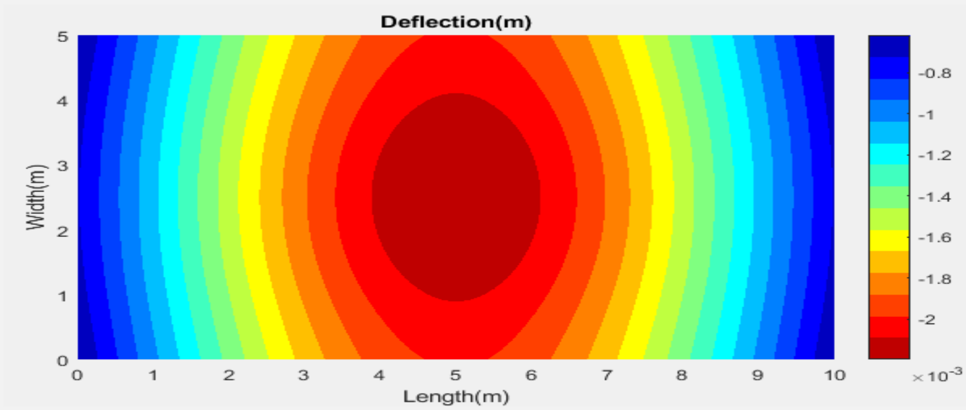

Worku's Pasternak type model (FDM)

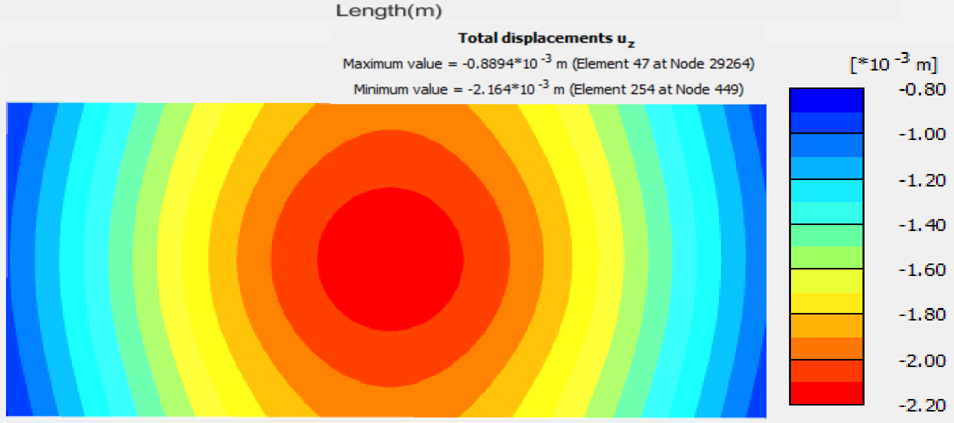

Plaxis 3D

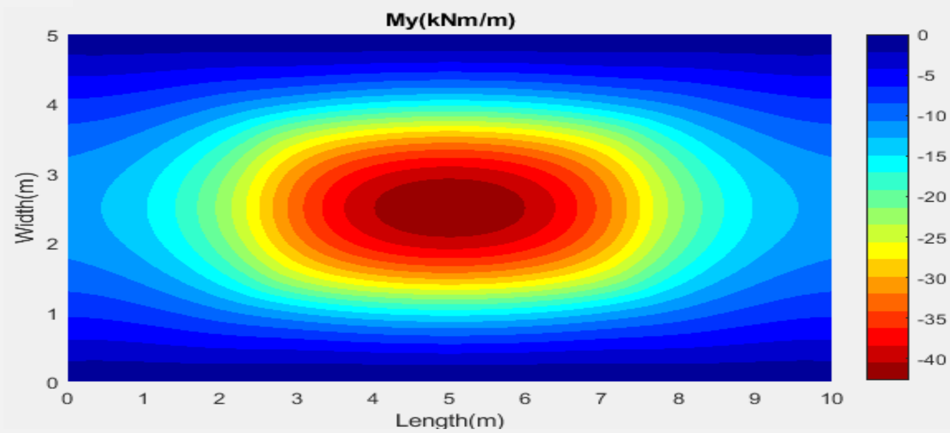

Worku's Pasternak type model (FDM)

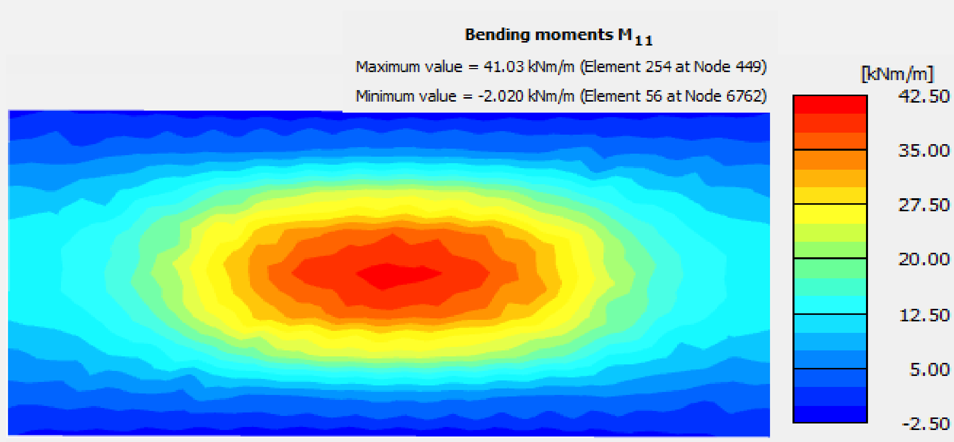

Plaxis 3D

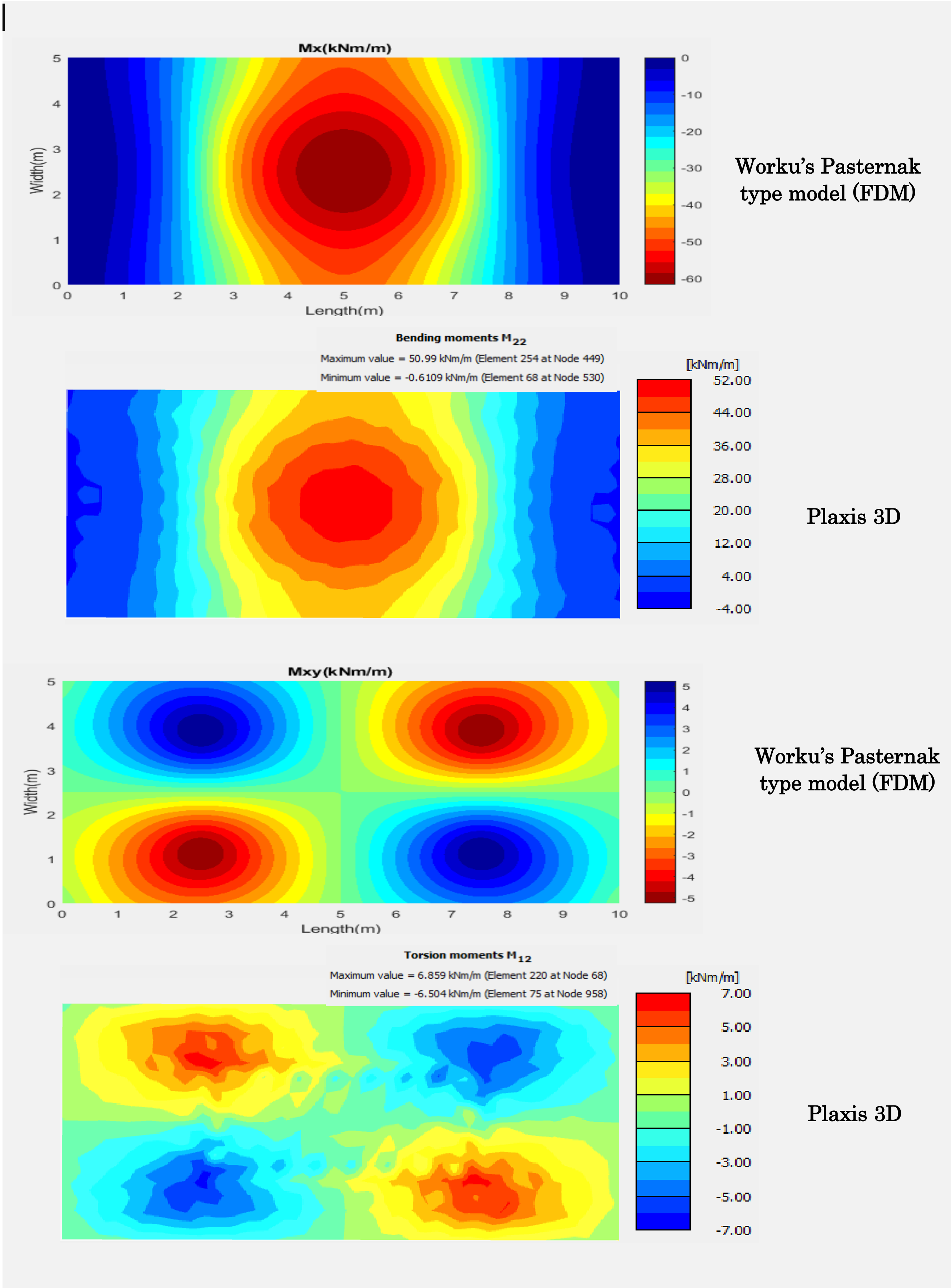
Mx(kNm/m)
Width(m)
Length(m)
Worku's Pasternak type model (FDM)
Bending moments M22
Maximum value = 50.99 kNm/m (Element 254 at Node 449)
Minimum value = -0.6109 kNm/m (Element 68 at Node 530)
[kNm/m]
52.00
44.00
36.00
28.00
20.00
12.00
4.00
-4.00
Plaxis 3D
Mxy(kNm/m)
Width(m)
Length(m)
Worku's Pasternak type model (FDM)
Torsion moments M12
Maximum value = 6.859 kNm/m (Element 220 at Node 68)
Minimum value = -6.504 kNm/m (Element 75 at Node 958)
[kNm/m]
7.00
5.00
3.00
1.00
-1.00
-3.00
-5.00
-7.00
Plaxis 3D

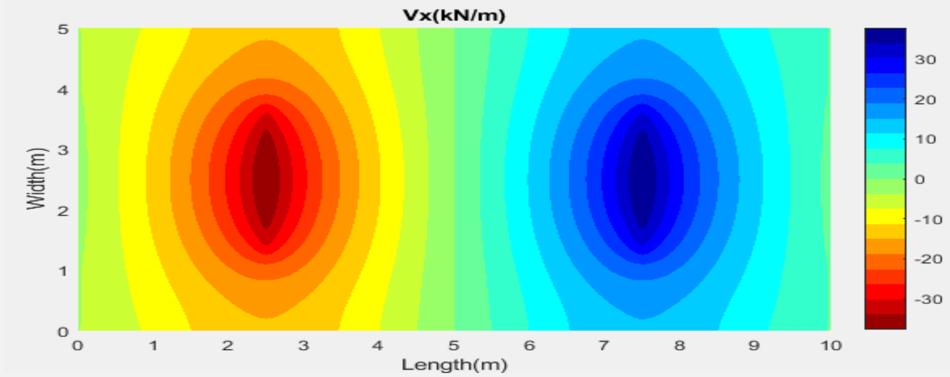

Worku's Pasternak type model (FDM)

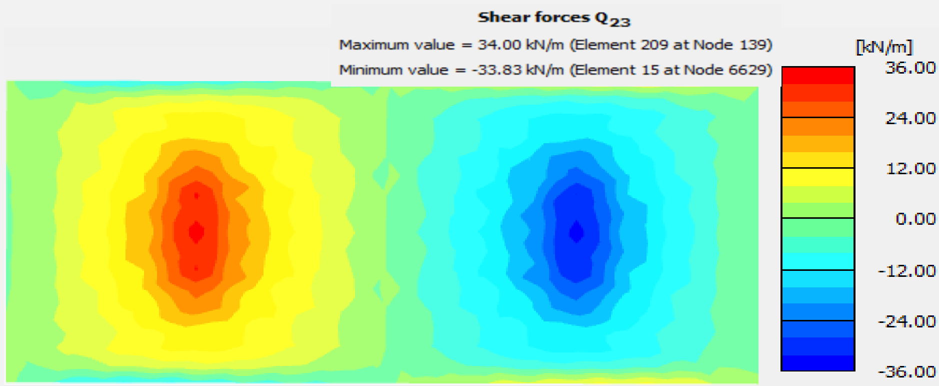

Plaxis 3D

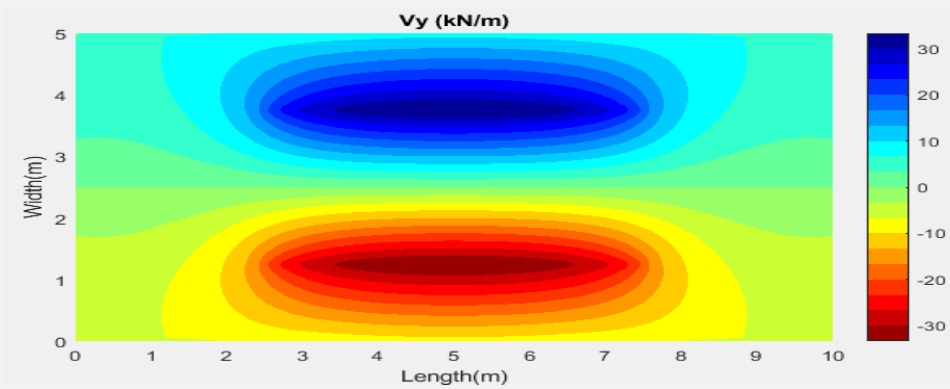

Worku's Pasternak type model (FDM)

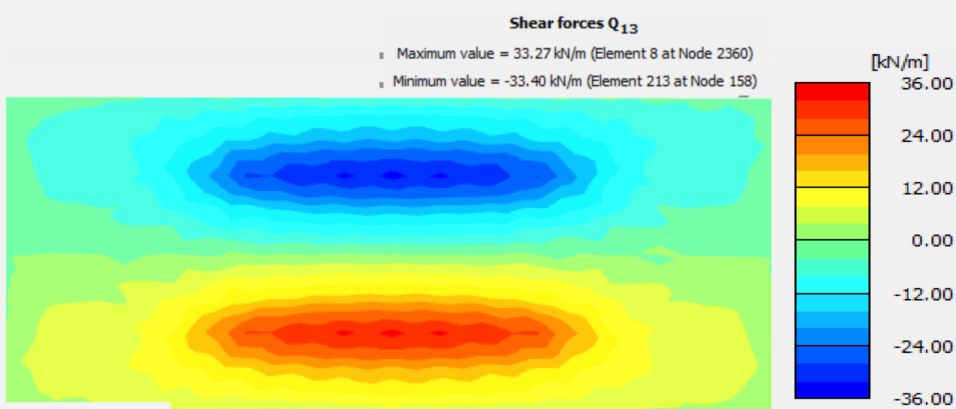

Plaxis 3D

Figure D6: Deflection and internal action of Rectangular plate (L/B=2) resting on Medium strength soil subjected to uniformly distributed load

D2.3. Combined load (L/B)

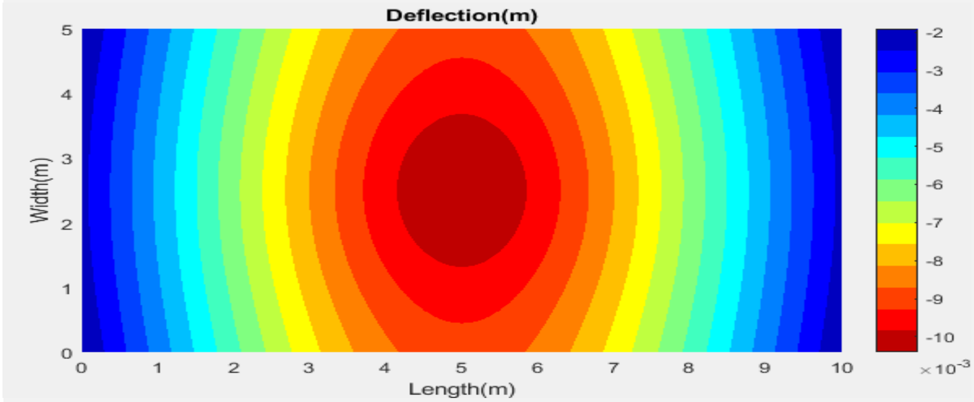

Worku's Pasternak type model (FDM)

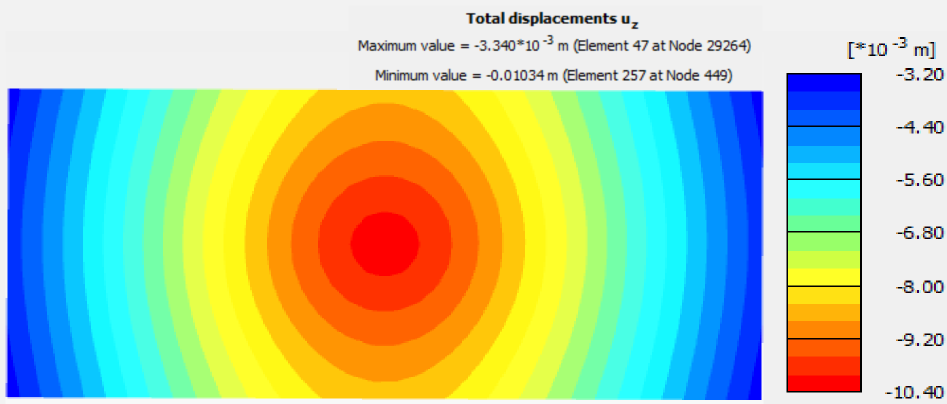

Plaxis 3D

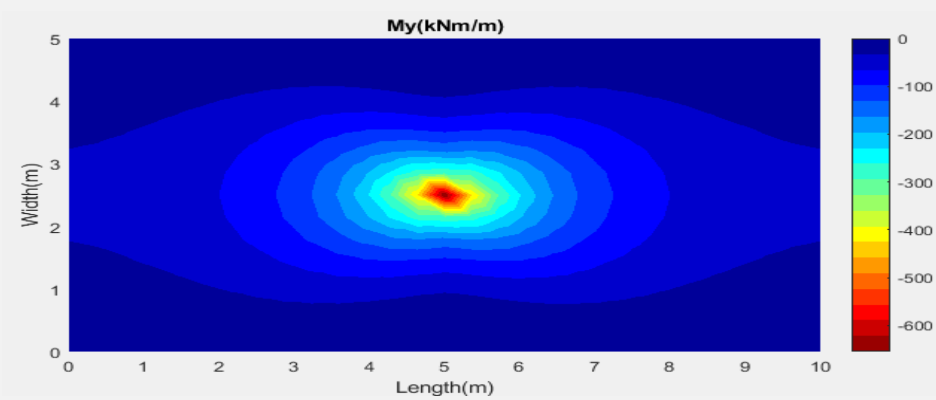

Worku's Pasternak type model (FDM)

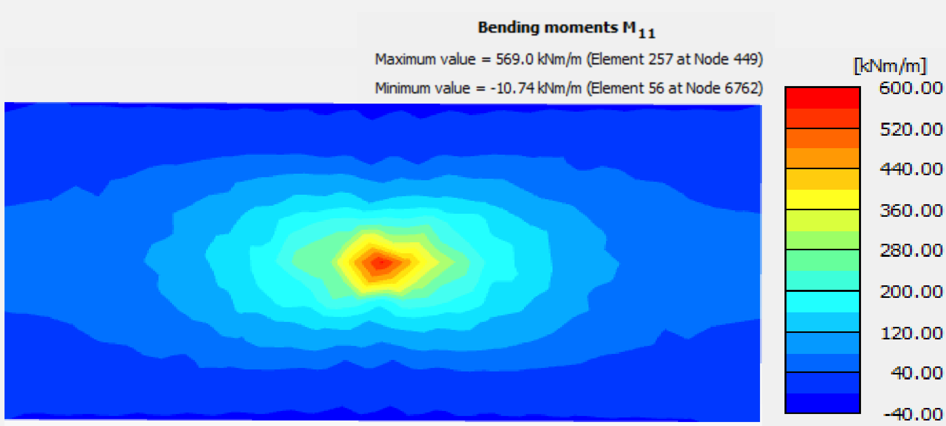

Plaxis 3D

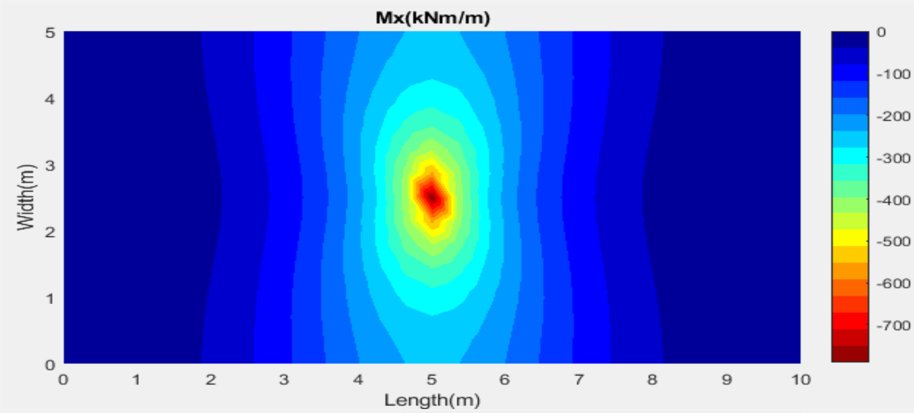

Worku's Pasternak type model (FDM)

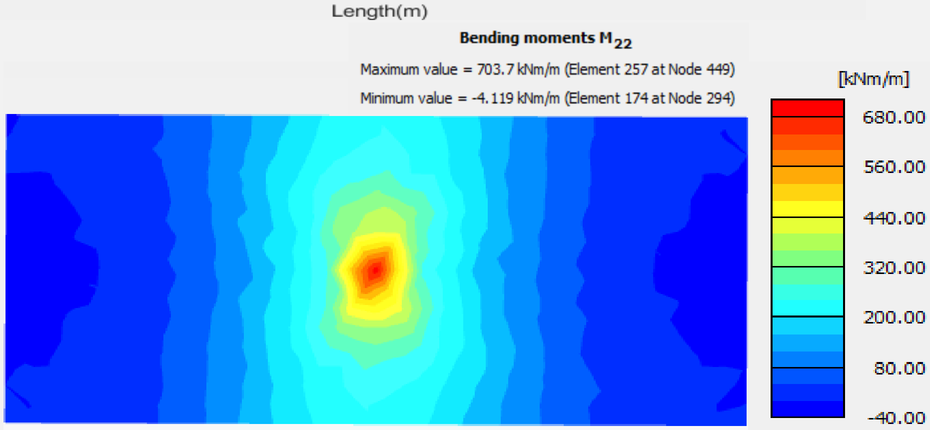

Plaxis 3D

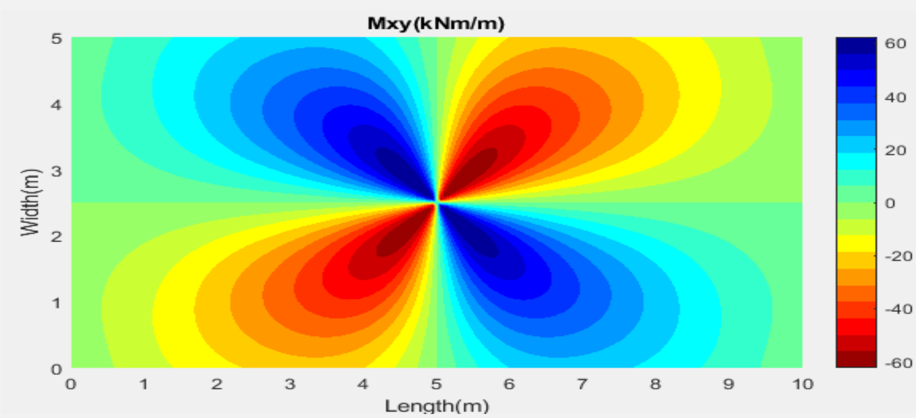

Worku's Pasternak type model (FDM)

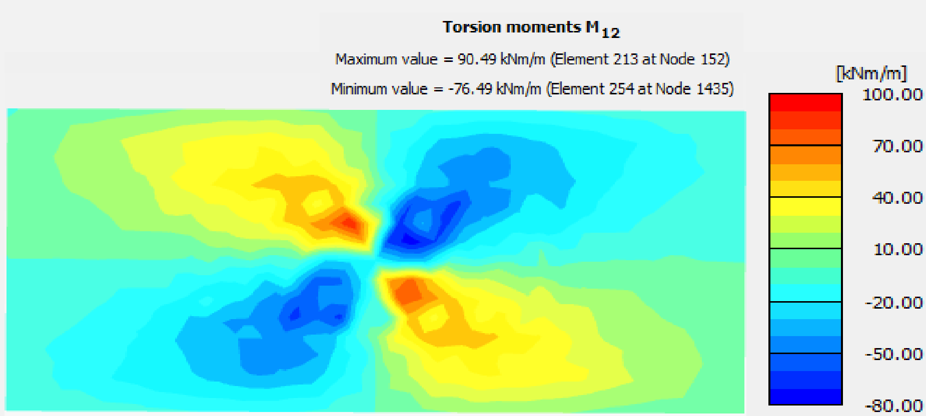

Plaxis 3D

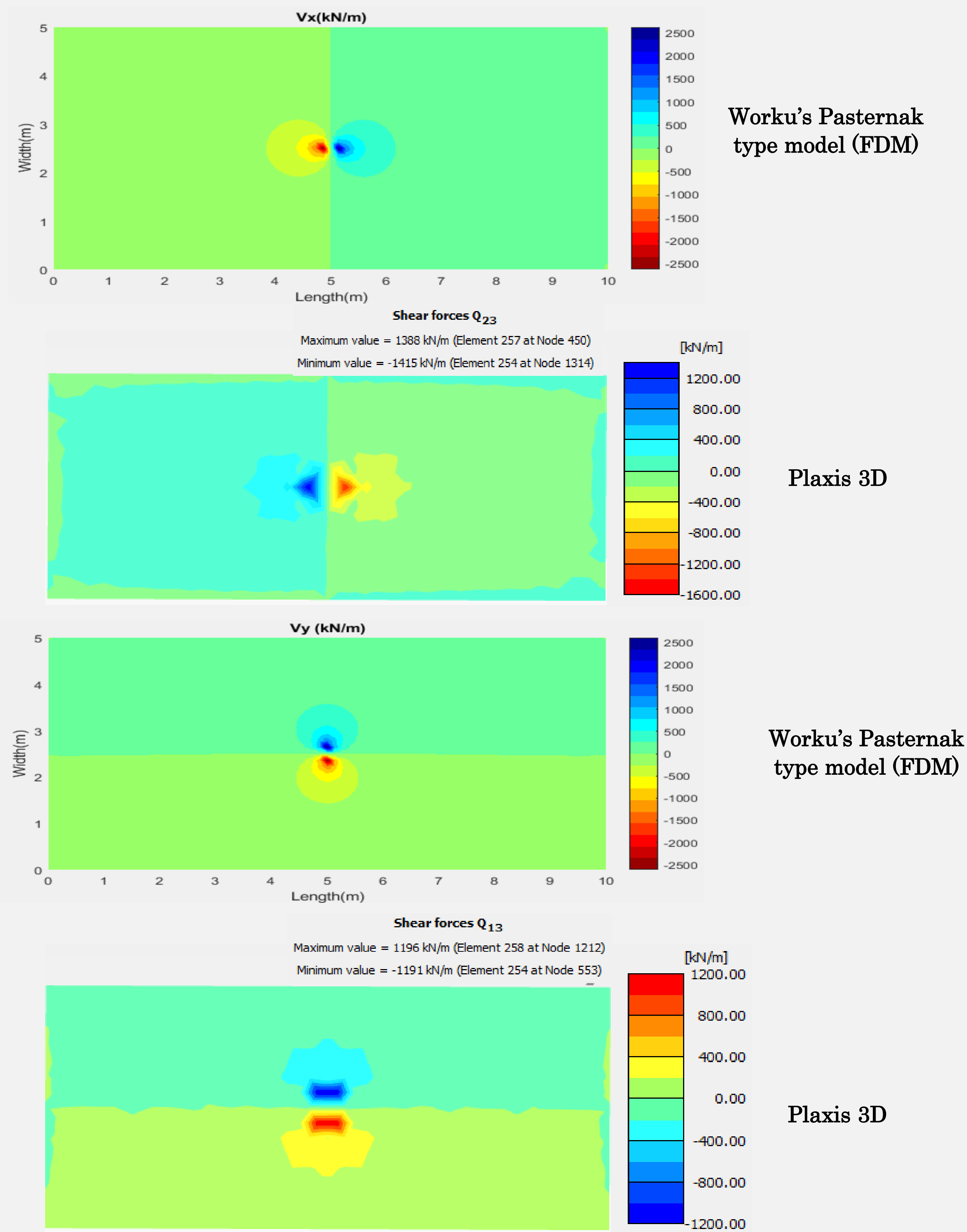

Figure D7: Deflection and internal action of Rectangular plate (L/B=2) resting on Medium strength soil subjected to the combined load

Appendix F

MATLAB® FDM Program

FDM program based on MATLAB® has been developed and provided here for the analysis of rectangular plates on an elastic foundation. The program file is MATLAB® script file (.m file) and can be executed in all versions of MATLAB®. Though to generate graphical output, the full version is required.

General program

```
%==========================================================================
%  Application of a Rigorous Subgrade Model in the Analysis of Rectangular
%       Plates on an Elastic Foundation Using Finite Difference Method
%                        by Tofik seid
%                  Advisor: Dr.-Ing Asrat Worku
%              Addis Ababa institute of Technology
%==========================================================================
clc % Clear screen
clear % Clear all variables in memory

tic;
disp('**********************************************')
disp('********** S T A R T I N G R U N ***************')
disp('**********************************************')
disp('COMPUTATION TIME(sec)       TASK ')
disp([num2str(round(toc,4)),'       START'])
%  +-------------------------------------------+-----> x
%  |           (xw1,yw1)                       |
%  |                 +------------------|       |
%  |      +          |||||||||||||||||||        |
%  |   (x1,y1)       ||||Distributed |||        | B
%  | Concentrated    |||||||Load|||||||        |
%  |     Loads       |||||||||||||||||||        |
%  |                 |------------------+       |
%  |                              (xw2,yw2)    |
%  +--------------------L----------------------+
%  |
% \/  y
% ========================================================================
% ************************** I N P U T **********************************
%=========================================================================
% soil parameters
Es=40000;    % Elastic modulus of the soil in kPa
vs=0.3;      % Poisson's ratio of the soil
H=100;        % Soil layer thickness in m
%=========================================================================
% Plate properties
L=5;         % Plate length in m(x-axis)
B=5;         % Plate width in m(y-axis)
hp=0.5;      % Thickness of the plate m
Ep=30e6;     % Elastic modulus of the plate in kPa
vp=0.2;      % Poisson's ratio of the plate
%  Mesh generation
no_ele=50;   % Number of elements in one direction
```

```
mm=no_ele;   % Number of elements in the y-direction
nn=B*no_ele/L; % Number of elements in the x-direction
%=========================================================================
% Applied loads
% Concentrated load (for 4 loads)
%load(kN)            location coordinate in meter
F1=0*1000;              x1=1.2;          y1=1.2;
F2=0*1000;             x2=1.2;            y2=3.8;
F3=0*1000;             x3=3.8;            y3=1.2;
F4=0*1000;             x4=3.8;            y4=3.8;
% Distributed load(uniform)
%load(kN/m2)        location  (first corner)     (second  corner)
Fw=1*100;             xw1=0;  yw1=0;         xw2=L;      yw2=B;
%=========================================================================
% Plot type
plott=1; % 1 on the plot else off
p2D_3D=2;  % 1 for 3D(surface) view 2 for 2D(Shaded)view
%=========================================================================

% ************************************************************************
% ******************** P R E - P R O C E S S I N G **********************
% ************************************************************************
D=Ep*hp^3/(12*(1-vp^2)); % Flexural rigidity of the plate
Kr=pi*Es*L^2*B/(8*D*(1-vs^2));
r=L/B; A=(L*B);
% Adjustment factor for the model sensitivity to the stratum thickness
if H <= B
    x=H/B;
elseif H > B
        if Es <=30000
x=(((-0.0002*Kr^2 +0.0045*Kr + 1.1106)*((F1+F2+F3+F4)~=0)+(-0.0001*Kr^2+...
0.0034*Kr+1.0948)*(Fw~=0))*((((F1+F2+F3+F4)~=0)+(Fw~=0))==1)+...
(-0.0002*Kr^2+.0048*Kr+1.0996)*((((F1+F2+F3+F4)~=0)+(Fw~=0))==2))*(r==1)...
+(((-3E-07*Kr^3+9E-05*Kr^2-0.0118*Kr+1.6036)*((F1+F2+F3+F4)~=0)...
+(-2E-7*Kr^3+6E-05*Kr^2-0.0089*Kr+1.5613)*(Fw~=0))*((((F1+F2+F3+F4)~=0)+...
(Fw~=0))==1)+(3E-05*Kr^2-0.008*Kr+1.5719)*((((F1+F2+F3+F4)~=0)+...
(Fw~=0))==2))*(r==2)+((( 4E-06*Kr^2-.0028*Kr+1.5985)*((F1+F2+F3+F4)~=0)...
+(6E-6*Kr^2-.0026*Kr+1.6849)*(Fw~=0))*((((F1+F2+F3+F4)~=0)+(Fw~=0))==1)+...
  ( 5E-06*Kr^2-0.0029*Kr+1.813)*((((F1+F2+F3+F4)~=0)+(Fw~=0))==2))*(r==4);
        elseif Es >=30000 && Es <=80000
x=(((-7E-05*Kr^2-0.0004*Kr+1.3072)*((F1+F2+F3+F4)~=0)+(-5E-5*Kr^2-...
   0.0005*Kr+1.2718)*(Fw~=0))*((((F1+F2+F3+F4)~=0)+(Fw~=0))==1)+...
(-6E-05*Kr^2+0.0001*Kr+1.2915)*((((F1+F2+F3+F4)~=0)+(Fw~=0))==2))*(r==1)...
+(((-1E-7*Kr^3+6E-5*Kr^2-.0097*Kr+1.651)*((F1+F2+F3+F4)~=0)+(-1E-7*Kr^3+...
5E-05*Kr^2-0.0088*Kr+1.6927)*(Fw~=0))*((((F1+F2+F3+F4)~=0)+(Fw~=0))==1)+...
 (1E-05*Kr^2-0.0058*Kr+1.6573)*((((F1+F2+F3+F4)~=0)+(Fw~=0))==2))*(r==2)...
+(((1E-06*Kr^2-0.0017*Kr+1.6249)*((F1+F2+F3+F4)~=0)...
+(1E-6*Kr^2-.0013*Kr+1.6981)*(Fw~=0))*((((F1+F2+F3+F4)~=0)+(Fw~=0))==1)+...
  (-1E-05*Kr^2+0.0069*Kr+0.753)*((((F1+F2+F3+F4)~=0)+(Fw~=0))==2))*(r==4);
        elseif Es >=80000
x=(((1E-05*Kr^2-0.0069*Kr+1.5371)*((F1+F2+F3+F4)~=0)+(2E-05*Kr^2-...
  .0063*Kr+1.459)*(Fw~=0))*((((F1+F2+F3+F4)~=0)+(Fw~=0))==1)+(9E-6*Kr^2-...
  0.0055*Kr+1.4997)*((((F1+F2+F3+F4)~=0)+(Fw~=0))==2))*(r==1)...
+(((-1E-8*Kr^3+1E-5*Kr^2-.0048*Kr+1.624)*((F1+F2+F3+F4)~=0)+(-8E-9*Kr^3+...
9E-06*Kr^2-0.004*Kr+1.5824)*(Fw~=0))*((((F1+F2+F3+F4)~=0)+(Fw~=0))==1)+...
(2E-06*Kr^2-0.0026*Kr+1.571)*((((F1+F2+F3+F4)~=0)+(Fw~=0))==2))*(r==2)...
+(((4E-07*Kr^2-0.0011*Kr+1.6327)*((F1+F2+F3+F4)~=0)+( 2E-07*Kr^2-...
```

```
0.0005*Kr+1.6337)*(Fw~=0))*((((F1+F2+F3+F4)~=0)+(Fw~=0))==1)+...
( 3E-07*Kr^2-0.0009*Kr+2.32)*((((F1+F2+F3+F4)~=0)+(Fw~=0))==2))*(r==4);
         end
end

n=nn+1; m=mm+1;% number of nodes in the x and y-direction
dx=L/(m-1); dy=B/(n-1);% space length between nodes in the y & x-direction
a=dx/dy; l=dx; % Ratios
% Ker-equivalent Pasternak parameters based on Generalized continuum model
kp=(0.4*vs+0.67)*Es/(B*x);
Gp=(1.36*vs+2.28)*Es*x*B/(2*(1+vs)*A);
% Relations of Pasternak parameters with plate properties
kpp=kp*l^4/D;
Gpp=Gp*l^2/D;

% Load vector
% Concentrated load
P11=sparse(1,m*n);  % First concentrated load
P12=spalloc(1,n*m,1); % First concentrated load
P13=spalloc(1,n*m,1); % First concentrated load
P14=spalloc(1,n*m,1); % First concentrated load
ep11=(x1/dx-floor(x1/dx))*dx; ep12=dx-ep11;
fp11=(y1/dy-floor(y1/dy))*dy; fp12=dy-fp11;
kp11=ceil(y1/dy)*m+ceil(x1/dx)+1; k11=floor(y1/dy)*m+floor(x1/dx)+1;
k12=k11+1; k13=k11+m; k14=k11+(m+1);
% Concentrated load 1
if kp11==k11
P11(k11)=4*F1*l^4/(dx*dy*D);
else
if fp11==0
P11(k11)=ep12*fp12*a^2*F1/(D); P11(k12)=ep11*fp12*F1*a^2/D;
elseif ep11==0
P11(k11)=ep12*fp12*a^2*F1/(D); P11(k13)=ep12*fp11*F1*a^2/D;
elseif fp12==0
P11(k13)=ep12*fp11*F1*a^2/D; P11(k14)=ep11*fp11*F1*a^2/D;
elseif ep12==0
P11(k12)=ep11*fp12*F1*a^2/D; P11(k14)=ep11*fp11*F1*a^2/D;
else
P11(k11)=ep12*fp12*a^2*F1/(D); P11(k12)=ep11*fp12*F1*a^2/D;
P11(k13)=ep12*fp11*F1*a^2/D; P11(k14)=ep11*fp11*F1*a^2/D;
end
end

% Concentrated load 2
ep21=(x2/dx-floor(x2/dx))*dx; ep22=dx-ep21;
fp21=(y2/dy-floor(y2/dy))*dy; fp22=dy-fp21;
kp21=ceil(y2/dy)*m+ceil(x2/dx)+1; k21=floor(y2/dy)*m+floor(x2/dx)+1;
k22=k21+1; k23=k21+m; k24=k21+m+1;
if kp21==k21
P12(k21)=4*F2*l^4/(dx*dy*D);
else
if fp21==0
P12(k21)=ep22*fp22*a^2*F2/(D); P12(k22)=ep21*fp22*F2*a^2/D;
elseif ep21==0
P12(k21)=ep22*fp22*a^2*F2/(D); P12(k23)=ep22*fp21*F2*a^2/D;
elseif fp22==0
P12(k23)=ep22*fp21*F2*a^2/D; P12(k24)=ep21*fp21*F2*a^2/D;
```

```
elseif ep22==0
P12(k22)=ep21*fp22*F2*a^2/D; P12(k24)=ep21*fp21*F2*a^2/D;
else
P12(k21)=ep22*fp22*a^2*F2/(D); P12(k22)=ep21*fp22*F2*a^2/D;
P12(k23)=ep22*fp21*F2*a^2/D; P12(k24)=ep21*fp21*F2*a^2/D;
end
end

% Concentrated load 3
ep31=(x3/dx-floor(x3/dx))*dx; ep32=dx-ep31;
fp31=(y3/dy-floor(y3/dy))*dy; fp32=dy-fp31;
kp31=ceil(y3/dy)*m+ceil(x3/dx)+1; k31=floor(y3/dy)*m+floor(x3/dx)+1;
k32=k31+1; k33=k31+m; k34=k31+m+1;
P13(k31)=ep32*fp32*F3*a^2/D; P13(k32)=ep31*fp32*F3*a^2/D;
P13(k33)=ep32*fp31*F3*a^2/D; P13(k34)=ep31*fp31*F3*a^2/D;
if kp31==k31
P13(k31)=4*F3*l^4/(dx*dy*D);
else
if fp31==0
P13(k31)=ep32*fp32*F3*a^2/D; P13(k32)=ep31*fp32*F3*a^2/D;
elseif ep31==0
P13(k31)=ep32*fp32*F3*a^2/D; P13(k33)=ep32*fp31*F3*a^2/D;
elseif fp32==0
P13(k33)=ep32*fp31*F3*a^2/D; P13(k34)=ep31*fp31*F3*a^2/D;
elseif ep32==0
P13(k32)=ep31*fp32*F3*a^2/D; P13(k34)=ep31*fp31*F3*a^2/D;
else
P13(k31)=ep32*fp32*F3*a^2/D; P13(k32)=ep31*fp32*F3*a^2/D;
P13(k33)=ep32*fp31*F3*a^2/D; P13(k34)=ep31*fp31*F3*a^2/D;
end
end

% Concentrated load 4
ep41=(x4/dx-floor(x4/dx))*dx; ep42=dx-ep41;
fp41=(y4/dy-floor(y4/dy))*dy; fp42=dy-fp41;
kp41=ceil(y4/dy)*m+ceil(x4/dx)+1; k41=floor(y4/dy)*m+floor(x4/dx)+1;
k42=k41+1; k43=k41+m; k44=k41+m+1;
P14(k41)=ep42*fp42*F4*a^2/D; P14(k42)=ep41*fp42*F4*a^2/D;
P14(k43)=ep42*fp41*F4*a^2/D; P14(k44)=ep41*fp41*F4*a^2/D;
if kp41==k41
P14(k41)=4*F4*l^4/(dx*dy*D);
else
if fp41==0
P14(k41)=ep42*fp42*F4*a^2/D; P14(k42)=ep41*fp42*F4*a^2/D;
elseif ep41==0
P14(k41)=ep42*fp42*F4*a^2/D; P14(k43)=ep42*fp41*F4*a^2/D;
elseif fp42==0
P14(k43)=ep42*fp41*F4*a^2/D; P14(k44)=ep41*fp41*F4*a^2/D;
elseif ep42==0
P14(k42)=ep41*fp42*F4*a^2/D; P14(k44)=ep41*fp41*F4*a^2/D;
else
P14(k41)=ep42*fp42*F4*a^2/D; P14(k42)=ep41*fp42*F4*a^2/D;
P14(k43)=ep42*fp41*F4*a^2/D; P14(k44)=ep41*fp41*F4*a^2/D;
end
end

%Distributed load
```

```
P21=sparse(1,m*n); % preallocation for the load
%k=(i-1)*m+j;(y1-1)*m+x1 global node numbering
ew11=(xw1/dx-floor(xw1/dx))*dx; ew22=(xw2/dx-floor(xw2/dx))*dx;
ew12=dx-ew11; ew21=dx-ew22; xx1=dx/2-ew12; xx2=dx/2-ew21;
fw11=(yw1/dy-floor(yw1/dy))*dy; fw22=(yw2/dy-floor(yw2/dy))*dy;
fw12=dy-fw11; fw21=dy-fw22; yy1=dy/2-fw12; yy2=dy/2-fw21;

kc111=floor(yw1/dy)*m+floor(xw1/dx)+1; kc14=ceil(yw1/dy)*m+ceil(xw1/dx)+1;
kc11=kc14-m-1; kc12=kc14-m; kc13=kc14-1;

kc222=floor(yw1/dy)*m+ceil(xw2/dx)+1; kc23=ceil(yw1/dy)*m+floor(xw2/dx)+1;
kc21=kc23-m; kc22=kc23-m+1; kc24=kc23+1;

kc333=ceil(yw2/dy)*m+floor(xw1/dx)+1; kc32=floor(yw2/dy)*m+ceil(xw1/dx)+1;
kc31=kc32-1;  kc33=kc32+m-1; kc34=kc32+m;

kc444=ceil(yw2/dy)*m+ceil(xw2/dx)+1;kc41=floor(yw2/dy)*m+floor(xw2/dx)+1;
kc42=kc41+1;  kc43=kc41+m; kc44=kc41+m+1;

% corner 1 of the distributed load
if kc14==kc111
    kc1=(yw1/dy)*m+xw1/dx+1;
    P21(kc1)=Fw*l^4/(4*D);
elseif kc14~=kc111
    if fw11==0
        P21(kc13)=(dy*(dx/2-ew11)/(dx*dy)*(xx1<0&& yy1<0)...
            +(dx/2-ew11)*(dy/2+fw12)/(dx*dy)*((xx1<0&& yy1>0)))*Fw*l^4/D;
        P21(kc14)=(1*(xx1<0 && yy1<0)+(dx/2+ew12)*(dy/2+fw12)/(dx*dy)*...
            ((xx1>0&& yy1>0)))*Fw*l^4/D;
    elseif ew11==0
        P21(kc12)=(dx*(dy/2-fw11)/(dx*dy)*(xx1<0&& yy1 <0)+...
            (dx/2+ew12)*(dy/2-fw11)/(dx*dy)*(xx1> 0&& yy1<0))*Fw*l^4/D;
        P21(kc14)=(1*(xx1<0 && yy1<0)+(dx/2+ew12)*(dy/2+fw12)/(dx*dy)*...
            ((xx1>0&& yy1>0)))*Fw*l^4/D;
    else
    P21(kc11)=((dx/2-ew11)*(dy/2-fw11)/(dx*dy)*(xx1<0&& yy1<0))*Fw*l^4/D;
    P21(kc12)=(dx*(dy/2-fw11)/(dx*dy)*(xx1<0&& yy1 <0)+...
        (dx/2+ew12)*(dy/2-fw11)/(dx*dy)*(xx1> 0&& yy1<0))*Fw*l^4/D;
    P21(kc13)=(dy*(dx/2-ew11)/(dx*dy)*(xx1<0&& yy1<0)...
        +(dx/2-ew11)*(dy/2+fw12)/(dx*dy)*((xx1<0&& yy1>0)))*Fw*l^4/D;
    P21(kc14)=(1*(xx1<0 && yy1<0)+(dx/2+ew12)*(dy/2+fw12)/(dx*dy)*...
        ((xx1>0&& yy1>0)))*Fw*l^4/D;
    end
end
% corner 2 of the distributed load
if kc23==kc222
    kc2=(yw1/dy)*m+xw2/dx+1;
    P21(kc2)=Fw*l^4/(4*D);
elseif kc23~=kc222
    if fw11==0
        P21(kc23)=(1*(xx2<0 && yy1<0)+(dx/2+ew21)*(dy/2+fw12)/(dx*dy)*...
        ((xx2>0&& yy1>0)))*Fw*l^4/D;
        P21(kc24)=(dy*(dx/2-ew22)/(dx*dy)*(xx2<0&& yy1<0)...
        +(dx/2-ew22)*(dy/2+fw12)/(dx*dy)*((xx2<0&& yy1>0)))*Fw*l^4/D;
    elseif ew22==0
    P21(kc21)=(dx*(dy/2-fw11)/(dx*dy)*(xx2 <0&& yy1 <0)+...
```

```
        (dx/2+ew21)*(dy/2-fw11)/(dx*dy)*(xx2> 0&& yy1<0))*Fw*l^4/D;
    P21(kc23)=(1*(xx2<0 && yy1<0)+(dx/2+ew21)*(dy/2+fw12)/(dx*dy)*...
        ((xx2>0&& yy1>0)))*Fw*l^4/D;
    else
    P21(kc21)=(dx*(dy/2-fw11)/(dx*dy)*(xx2 <0&& yy1 <0)+...
        (dx/2+ew21)*(dy/2-fw11)/(dx*dy)*(xx2> 0&& yy1<0))*Fw*l^4/D;
    P21(kc22)=((dx/2-ew22)*(dy/2-fw11)/(dx*dy)*(xx2< 0 && yy1<0))*Fw*l^4/D;
    P21(kc23)=(1*(xx2<0 && yy1<0)+(dx/2+ew21)*(dy/2+fw12)/(dx*dy)*...
        ((xx2>0&& yy1>0)))*Fw*l^4/D;
    P21(kc24)=(dy*(dx/2-ew22)/(dx*dy)*(xx2<0&& yy1<0)...
        +(dx/2-ew22)*(dy/2+fw12)/(dx*dy)*((xx2<0&& yy1>0)))*Fw*l^4/D;
    end
end
% corner 3 of the distributed load
if kc32==kc333
    kc3=(yw2/dy)*m+xw1/dx+1;
    P21(kc3)=Fw*l^4/(4*D);
elseif kc32~=kc333
    if fw22==0
    P21(kc31)=(dy*(dx/2-ew12)/(dx*dy)*(xx1 <0&& yy2 <0)+...
        (dx/2-ew12)*(dy/2+fw21)/(dx*dy)*(xx1< 0&& yy2>0))*Fw*l^4/D;
    P21(kc32)=(1*(xx1<0 && yy2<0)+(dx/2+ew12)*(dy/2+fw21)/(dx*dy)*...
        ((xx1>0&& yy2>0)))*Fw*l^4/D;
    elseif ew11==0
    P21(kc32)=(1*(xx1<0 && yy2<0)+(dx/2+ew12)*(dy/2+fw21)/(dx*dy)*...
        ((xx1>0&& yy2>0)))*Fw*l^4/D;
    P21(kc34)=(dx*(dy/2-fw22)/(dx*dy)*(xx1<0&& yy2<0)...
        +(dx/2+ew12)*(dy/2-fw22)/(dx*dy)*((xx1>0&& yy2<0)))*Fw*l^4/D;
    else
    P21(kc31)=(dy*(dx/2-ew12)/(dx*dy)*(xx1 <0&& yy2 <0)+...
        (dx/2-ew12)*(dy/2+fw21)/(dx*dy)*(xx1< 0&& yy2>0))*Fw*l^4/D;
    P21(kc32)=(1*(xx1<0 && yy2<0)+(dx/2+ew12)*(dy/2+fw21)/(dx*dy)*...
        ((xx1>0&& yy2>0)))*Fw*l^4/D;
    P21(kc33)=((dx/2-ew11)*(dy/2-fw22)/(dx*dy)*(xx1< 0 && yy2<0))*Fw*l^4/D;
    P21(kc34)=(dx*(dy/2-fw22)/(dx*dy)*(xx1<0&& yy2<0)...
        +(dx/2+ew12)*(dy/2-fw22)/(dx*dy)*((xx1>0&& yy2<0)))*Fw*l^4/D;
    end
end
% corner 4 of the distributed load
if kc41==kc444
    kc4=(yw2/dy)*m+xw2/dx+1;
    P21(kc4)=Fw*l^4/(4*D);
elseif kc41~=kc444
    if fw22==0
    P21(kc41)=(1*(xx2<0 && yy2<0)+(dx/2+ew21)*(dy/2+fw21)/(dx*dy)*...
        ((xx2>0&& yy2>0)))*Fw*l^4/D;
    P21(kc42)=(dy*(dx/2-ew22)/(dx*dy)*(xx2<0&& yy2<0)...
        +(dx/2-ew22)*(dy/2+fw21)/(dx*dy)*((xx2<0&& yy2>0)))*Fw*l^4/D;
    elseif ew22==0
    P21(kc41)=(1*(xx2<0 && yy2<0)+(dx/2+ew21)*(dy/2+fw21)/(dx*dy)*...
        ((xx2>0&& yy2>0)))*Fw*l^4/D;
    P21(kc43)=(dx*(dy/2-fw22)/(dx*dy)*(xx2<0&& yy2 <0)+...
        (dx/2+ew21)*(dy/2-fw22)/(dx*dy)*(xx2> 0&& yy2<0))*Fw*l^4/D;
    else
    P21(kc41)=(1*(xx2<0 && yy2<0)+(dx/2+ew21)*(dy/2+fw21)/(dx*dy)*...
        ((xx2>0&& yy2>0)))*Fw*l^4/D;
    P21(kc42)=(dy*(dx/2-ew22)/(dx*dy)*(xx2<0&& yy2<0)...
```

```
        +(dx/2-ew22)*(dy/2+fw21)/(dx*dy)*((xx2<0&& yy2>0)))*Fw*l^4/D;
    P21(kc43)=(dx*(dy/2-fw22)/(dx*dy)*(xx2<0&& yy2 <0)+...
        (dx/2+ew21)*(dy/2-fw22)/(dx*dy)*(xx2> 0&& yy2<0))*Fw*l^4/D;
    P21(kc44)=((dx/2-ew11)*(dy/2-fw11)/(dx*dy)*(xx2<0&& yy2<0))*Fw*l^4/D;
    end
end
% inside points of the distributed load
x11=ceil(xw1/dx)+1;   x12=floor(xw2/dx)+1;
y11=ceil(yw1/dy)+1;   y12=floor(yw2/dy)+1;
for j=x11+1:x12-1
    for i=y11+1:y12-1
    k=(i-1)*m+j;
    P21(k)=(Fw*l^4/(D));
    end
end
% side 1 (y-axis) of the distributed load
if ew11==0
    for j=x11
        for i=y11+1:y12-1
    k=(i-1)*m+j;
    P21(k)=(Fw*l^4/(2*D));
        end
    end
else
    for j=x11
        for i=y11+1:y12-1
    k=(i-1)*m+j;
    P21(k)=(1*(xx1<0)+(dx/2+ew12)/dx*(xx1>0))*(Fw*l^4/(D));
    P21(k-1)=(dx/2-ew11)/dx*(xx1<0)*(Fw*l^4/(D));
        end
    end
end

% side 2 (y-axis) of the distributed load
if ew22==0
    for j=x12
        for i=y11+1:y12-1
    k=(i-1)*m+j;
    P21(k)=(Fw*l^4/(2*D));
        end
    end
else
    for j=x12
        for i=y11+1:y12-1
    k=(i-1)*m+j;
    P21(k)=(1*(xx2<0)+(dx/2+ew21)/dx*(xx2>0))*(Fw*l^4/(D));
    P21(k+1)=(dx/2-ew22)/dx*(xx2<0)*(Fw*l^4/(D));
        end
    end
end
% side 1 (x-axis) of the distributed load
if fw11==0
    for i=y11
        for j=x11+1:x12-1
        k=(i-1)*m+j;
        P21(k)=(Fw*l^4/(2*D));
        end
```

```
    end
else
    for i=y11
        for j=x11+1:x12-1
        k=(i-1)*m+j;
        P21(k)=(1*(yy1<0)+(dy/2+fw12)/dy*(yy1>0))*(Fw*l^4/(D));
        P21(k-m)=(dy/2-fw11)/dy*(yy1<0)*(Fw*l^4/(D));
        end
    end
end
% side 2 (x-axis) of the distributed load
if fw22==0
    for i=y12
        for j=x11+1:x12-1
        k=(i-1)*m+j;
        P21(k)=(Fw*l^4/(2*D));
        end
    end
else
    for i=y12
        for j=x11+1:x12-1
        k=(i-1)*m+j;
        P21(k)=(1*(yy2<0)+(dy/2+fw21)/dy*(yy2>0))*(Fw*l^4/(D));
        P21(k+m)=(dy/2-fw22)/dy*(yy2<0)*(Fw*l^4/(D));
        end
    end
end
P=P11+P12+P13+P14+P21;
%**************************************************************************
%***                      P R O C E S S I N G                          ***
%**************************************************************************
disp([num2str(round(toc,4)),'       COMPUTING COEFFICIENT MATRIX'])
% Coefficient matrix  'C' formation
%==========================================================================
nzmax=4*6+8*8+44+(2*(m-4)+2*(n-4))*9+(2*(m-4)+2*(n-4))*12+13*(n-4)*(m-4);
C=spalloc(m*n,m*n,nzmax);
%=============================1============================================
%point on inside the plate
%         |
%     ----+----
%         |
c11=6+8*a^2+6*a^4+2*(1+a^2)*Gpp+kpp;
c12=-4*(1+a^2)-Gpp;
c13=1;
c21=-4*(1+a^2)*a^2-Gpp*a^2;
c31=a^4;
c22=2*a^2;
for i=3:n-2
   for j=3:m-2
        k=(i-1)*m+j;
                 C(k,k-2*m)=c31;
                 C(k,k-m-1)=c22;
                 C(k,k-m)=c21;
                 C(k,k-m+1)=c22;
                 C(k,k-2)=c13;
                 C(k,k-1)=c12;
                 C(k,k)=c11;
```

```
                 C(k,k+1)=c12;
                 C(k,k+2)=c13;
                 C(k,k+m-1)=c22;
                 C(k,k+m)=c21;
                 C(k,k+m+1)=c22;
                 C(k,k+2*m)=c31;
    end
end
%=======================================2==================================
% Point inside free corner 1
%       ____
%      | +
cic11=c11-1-a^4;
cic21=-4*a^2-2*a^4+2*a^2*vp-Gpp*a^2;
cic12=-2-4*a^2+2*vp*a^2-Gpp;
cic221=2*a^2*(1-vp);
cic222=a^2*(2-vp);
%k=m+2; i=2,j=2
C(m+2,1)=cic221;
C(m+2,2)=cic21;
C(m+2,3)=cic222;
C(m+2,m+1)=cic12;
C(m+2,m+2)=cic11;
C(m+2,m+3)=c12;
C(m+2,m+4)=c13;
C(m+2,2*m+1)=cic222;
C(m+2,2+2*m)=c21;
C(m+2,2*m+3)=c22;
C(m+2,2+3*m)=c31;
%=============================3============================================
% Point inside free corner (2)
%         _____
%           +  |
%for j=m-1 k=m+j; i=2 k=2*m-1
C(2*m-1,m-2)=cic222;
C(2*m-1,m-1)=cic21;
C(2*m-1,m)=cic221;
C(2*m-1,2*m-3)=c13;
C(2*m-1,2*m-2)=c12;
C(2*m-1,2*m-1)=cic11;
C(2*m-1,2*m)=cic12;
C(2*m-1,3*m-2)=c22;
C(2*m-1,3*m-1)=c21;
C(2*m-1,3*m)=cic222;
C(2*m-1,4*m-1)=c31;
%===================================4====================================
% point inside free corner (3)
%       | +
%       -----
% k=(n-2)*m+2; for i=n-1 j=2
C((n-2)*m+2,(n-2)*m-2*m+2)=c31;
C((n-2)*m+2,(n-2)*m-m+1)=cic222;
C((n-2)*m+2,(n-2)*m-m+2)=c21;
C((n-2)*m+2,(n-2)*m-m+3)=c22;
C((n-2)*m+2,(n-2)*m+1)=cic12;
C((n-2)*m+2,(n-2)*m+2)=cic11;
C((n-2)*m+2,(n-2)*m+3)=c12;
```

```
C((n-2)*m+2,(n-2)*m+4)=c13;
C((n-2)*m+2,(n-2)*m+m+1)=cic221;
C((n-2)*m+2,(n-2)*m+m+2)=cic21;
C((n-2)*m+2,(n-2)*m+m+3)=cic222;
%==================================5=====================================
% point inside free corner (4)
%        +  |
%        ----
%for j=m-1 i=n-1 k=(n-2)*m+m-1
cip4=(n-2)*m+m-1;
C(cip4,cip4-m*2)=c31;
C(cip4,(n-2)*m-2)=c22;
C(cip4,(n-2)*m-1)=c21;
C(cip4,(n-2)*m)=cic222;
C(cip4,cip4-2)=c13;
C(cip4,cip4-1)=c12;
C(cip4,cip4)=cic11;
C(cip4,cip4+1)=cic12;
C(cip4,n*m-2)=cic222;
C(cip4,n*m-1)=cic21;
C(cip4,n*m)=cic221;
%================================6========================================
% points inside free edge (x-axis(1)) top
%        -------
%           +
cifx11=c11-a^4;
cifx12=-4*a^2-2*a^4+2*a^2*vp-Gpp*a^2;
cifx22=a^2*(2-vp);
for j=3:m-2 %for i=2
   k=m+j;
   C(k,k-m-1)=cifx22;
   C(k,k-m)=cifx12;
   C(k,k-m+1)=cifx22;
   C(k,k-2)=c13;
   C(k,k-1)=c12;
   C(k,k)=cifx11;
   C(k,k+1)=c12;
   C(k,k+2)=c13;
   C(k,k+m-1)=c22;
   C(k,k+m)=c21;
   C(k,k+m+1)=c22;
   C(k,k+m*2)=c31;
end
%==================================7======================================
% points inside free edge (x-axis (2)) bottom
%                 +
%              -------
for j=3:m-2 %for i=n-1
   k=(n-2)*m+j;
   C(k,k-m*2)=c31;
   C(k,k-m-1)=c22;
   C(k,k-m)=c21;
   C(k,k-m+1)=c22;
   C(k,k-2)=c13;
   C(k,k-1)=c12;
   C(k,k)=cifx11;
   C(k,k+1)=c12;
```

```
   C(k,k+2)=c13;
   C(k,k+m-1)=cifx22;
   C(k,k+m)=cifx12;
   C(k,k+m+1)=cifx22;
end
%================================8=======================================
%points inside free edge (Y-axis (1)) left
%                  |
%                  | +
%                  |
cfeiy11=c11-1;
cfeiy12=-2-4*a^2+2*vp*a^2-Gpp;
cfeiy22=a^2*(2-vp);
for i=3:n-2 %for j=2
   k=(i-1)*m+2;
   C(k,k-2*m)=c31;
   C(k,k-m-1)=cfeiy22;
   C(k,k-m)=c21;
   C(k,k-m+1)=c22;
   C(k,k-1)=cfeiy12;
   C(k,k)=cfeiy11;
   C(k,k+1)=c12;
   C(k,k+2)=c13;
   C(k,k+m-1)=cfeiy22;
   C(k,k+m)=c21;
   C(k,k+m+1)=c22;
   C(k,k+m*2)=c31;
end
%================================9=======================================
% points on free edge (Y-axis (2)) right
%                  |
%                + |
%                  |

for i=3:n-2 %for j=m-1
   k=(i-1)*m+m-1;
   C(k,k-2*m)=c31;
   C(k,k-m-1)=c22;
   C(k,k-m)=c21;
   C(k,k-m+1)=cfeiy22;
   C(k,k-2)=c13;
   C(k,k-1)=c12;
   C(k,k)=cfeiy11;
   C(k,k+1)=cfeiy12;
   C(k,k+m-1)=c22;
   C(k,k+m)=c21;
   C(k,k+m+1)=cfeiy22;
   C(k,k+m*2)=c31;
end
% Edge reaction coefficients
srx11=2*l^3*(sqrt(kp*Gp)+Gp*(a^2+vp)/l)/(D);
srx12=2*l^3*(-Gp*vp/(l*2))/(D);
srx21=2*l^3*(-Gp*a^2/l)/(D);
sry11=2*l^3*(sqrt(kp*Gp)+Gp*(1+a^2*vp)/l)/(D);
sry21=2*l^3*(-Gp*vp*a^2/(l*2))/(D);
sry12=2*l^3*(-Gp/l)/(D);
src11=2*l^3*((1+a)*sqrt(kp*Gp)+Gp*(1+a)/l)/(D);
```

```
src12=2*l^3*(-Gp/l)/(D);
src21=2*l^3*(-Gp*a/l)/(D);
%===================================10=====================================
% points on free edge (x-axis(1)) top
%            ---+---
cfex11=6+8*a^2+2*a^4-8*vp*a^2-6*vp^2+0.5*kpp+(2-2*vp)*Gpp+srx11;%<==
cfex12=-4*(1+a^2)+4*vp*a^2+4*vp^2-(1-vp)*Gpp+srx12;%<==
cfex13=1-vp^2;
cfex21=-8*a^2-4*a^4+4*vp*a^2+srx21;%<==
cfex31=2*a^4;
cfex22=2*(2-vp)*a^2;
for j=3:m-2 %for i=1
   k=j;
   C(k,k-2)=cfex13;
   C(k,k-1)=cfex12;
   C(k,k)=cfex11;
   C(k,k+1)=cfex12;
   C(k,k+2)=cfex13;
   C(k,k+m-1)=cfex22;
   C(k,k+m)=cfex21;
   C(k,k+m+1)=cfex22;
   C(k,k+2*m)=cfex31;
end
%=====================================11====================================
% points on free edge (x-axis (2)) y=B
    %    --+--
for j=3:m-2 %for i=n
   k=(n-1)*m+j;
   C(k,k-m*2)=cfex31;
   C(k,k-m-1)=cfex22;
   C(k,k-m)=cfex21;
   C(k,k-m+1)=cfex22;
   C(k,k-2)=cfex13;
   C(k,k-1)=cfex12;
   C(k,k)=cfex11;
   C(k,k+1)=cfex12;
   C(k,k+2)=cfex13;
end
%============================12=================================
% point adjacent to free corner on free edge (y=0) (1)
%    -+---
%   |
cac11=cfex11+vp^2-1;%<==
cac121=cfex12+2-2*vp^2;%<==
%k=(i-1)*m+j=2;for i=1,for j=2
C(2,1)=cac121;
C(2,2)=cac11;
C(2,3)=cfex12;
C(2,4)=cfex13;
C(2,m+1)=cfex22;
C(2,m+2)=cfex21;
C(2,m+3)=cfex22;
C(2,2+2*m)=cfex31;
%==================================13====================================
% point adjacent to free corner on free edge (x-axis) (2)
%    -+---
%        |
```

```
%for j=m-1 i=1 %k=(i-1)*m+j=m-1
C(m-1,m-3)=cfex13;
C(m-1,m-2)=cfex12;
C(m-1,m-1)=cac11;
C(m-1,m)=cac121;
C(m-1,2*m-2)=cfex22;
C(m-1,2*m-1)=cfex21;
C(m-1,2*m)=cfex22;
C(m-1,3*m-1)=cfex31;
%====================================14=====================================
% point adjacent to free corner on free edge x-axis (3)
%    |
%     -+---
%for j=2 i=n k=(n-1)*m+j=(n-1)*m+2;
C((n-1)*m+2,(n-1)*m+2-2*m)=cfex31;
C((n-1)*m+2,(n-1)*m-m+1)=cfex22;
C((n-1)*m+2,(n-1)*m-m+2)=cfex21;
C((n-1)*m+2,(n-1)*m-m+3)=cfex22;
C((n-1)*m+2,(n-1)*m+1)=cac121;
C((n-1)*m+2,(n-1)*m+2)=cac11;
C((n-1)*m+2,(n-1)*m+3)=cfex12;
C((n-1)*m+2,(n-1)*m+4)=cfex13;
%===================================15======================================
% point adjacent to free corner on free edge (x-axis)(4)
%         |
%    -+---
%for i=n j=m-1 k=(i-1)*m+j=n*m-1;
C(n*m-1,n*m-2*m-1)=cfex31;
C(n*m-1,n*m-m-2)=cfex22;
C(n*m-1,n*m-m-1)=cfex21;
C(n*m-1,n*m-m)=cfex22;
C(n*m-1,n*m-3)=cfex13;
C(n*m-1,n*m-2)=cfex12;
C(n*m-1,n*m-1)=cac11;
C(n*m-1,n*m)=cac121;
%===================================16=======================================
%points on free edge (Y-axis(1)) left
%                  |
%                  +
%                  |
cfey11=2+8*a^2+6*a^4-8*vp*a^2-6*vp^2*a^4+0.5*kpp+2*(1-vp)*a^2*Gpp+sry11;%<=
cfey21=-4*a^2*(1+a^2)+4*vp*a^2+4*vp^2*a^4-Gpp*(1-vp)*a^2+sry21;%<==
cfey31=a^4*(1-vp^2);
cfey12=-4-8*a^2+4*vp*a^2+sry12;%<==
cfey22=2*a^2*(2-vp);
cfey13=2;
for i=3:n-2 %for j=1
   k=(i-1)*m+1;
        C(k,k-2*m)=cfey31;
        C(k,k-m)=cfey21;
        C(k,k-m+1)=cfey22;
        C(k,k)=cfey11;
        C(k,k+1)=cfey12;
        C(k,k+2)=cfey13;
        C(k,k+m)=cfey21;
        C(k,k+m+1)=cfey22;
        C(k,k+2*m)=cfey31;
```

```
end
%====================================17====================================
%points on free edge (Y-axis (2)) right
%                   |
%                   +
%                   |
for i=3:n-2 %for j=m
   k=(i-1)*m+m;
       C(k,k-2*m)=cfey31;
       C(k,k-m-1)=cfey22;
       C(k,k-m)=cfey21;
       C(k,k-2)=cfey13;
       C(k,k-1)=cfey12;
       C(k,k)=cfey11;
       C(k,k+m-1)=cfey22;
       C(k,k+m)=cfey21;
       C(k,k+2*m)=cfey31;
end
%====================================18====================================
% point adjacent to free corner on free edge (y-axis) (1)
%  |-----
%  +
%  |
cacy11=cfey11-a^4*(1-vp^2);%<==
cacy211=cfey21+2*a^4*(1-vp^2);%<==
 %k=(i-1)*m+j=m+1;for j=1 for i=2
C(m+1,1)=cacy211;
C(m+1,2)=cfey22;
C(m+1,m+1)=cacy11;
C(m+1,m+2)=cfey12;
C(m+1,m+3)=cfey13;
C(m+1,2*m+1)=cfey21;
C(m+1,2*m+2)=cfey22;
C(m+1,3*m+1)=cfey31;
%====================================19=====================================
% point adjacent to free corner on free edge (y-axis) (2)
%  -----|
%       +
%       |
%for j=m i=2 %k=(i-1)*m+j=2*m;
C(2*m,m-1)=cfey22;
C(2*m,m)=cacy211;
C(2*m,2*m-2)=cfey13;
C(2*m,2*m-1)=cfey12;
C(2*m,2*m)=cacy11;
C(2*m,3*m-1)=cfey22;
C(2*m,3*m)=cfey21;
C(2*m,4*m)=cfey31;
%===================================20======================================
% point adjacent to free corner on free edge (y-axis) (3)
%  |
%  +
%  |________
%for j=1 i=n-1 k=(n-2)*m+j=(n-2)*m+1;
C((n-2)*m+1,(n-2)*m+1-2*m)=cfey31;
C((n-2)*m+1,(n-2)*m+1-m)=cfey21;
C((n-2)*m+1,(n-2)*m+1-m+1)=cfey22;
```

```
C((n-2)*m+1,(n-2)*m+1)=cacy11;
C((n-2)*m+1,(n-2)*m+1+1)=cfey12;
C((n-2)*m+1,(n-2)*m+1+2)=cfey13;
C((n-2)*m+1,(n-2)*m+1+m)=cacy211;
C((n-2)*m+1,(n-2)*m+1+m+1)=cfey22;
%==================================21=====================================
% point adjacent to free corner on free edge (y-axis) (4)
%      |
%      +
% _____|

%for i=n-1 j=m k=(n-2)*m+m;
C(n*m-m,n*m-3*m)=cfey31;
C(n*m-m,n*m-2*m-1)=cfey22;
C(n*m-m,n*m-2*m)=cfey21;
C(n*m-m,n*m-m-2)=cfey13;
C(n*m-m,n*m-m-1)=cfey12;
C(n*m-m,n*m-m)=cacy11;
C(n*m-m,n*m-1)=cfey22;
C(n*m-m,n*m)=cacy211;
%================================= 22=====================================
%point on free corner (1)
%     +---
%     |
cfc11=2+8*a^2+2*a^4-8*vp*a^2-2*vp^2*(1+a^4)+0.25*kpp+src11; %<==
cfc12=-4-8*a^2+8*vp*a^2+4*vp^2+src12;  %<==
cfc13=2-2*vp^2;
cfc21=-8*a^2-4*a^4+8*vp*a^2+4*vp^2*a^4+src21;%<==
cfc31=2*a^4*(1-vp^2);
cfc22=8*a^2-8*vp*a^2;

C(1,1)=cfc11;
C(1,2)=cfc12;
C(1,3)=cfc13;
C(1,m+1)=cfc21;
C(1,m+2)=cfc22;
C(1,2*m+1)=cfc31;
%==================================23=====================================
%point on free corner 2
%      _____+
%           |
%k=(i-1)*m+j=m; for i=1,for j=m
C(m,m-2)=cfc13;
C(m,m-1)=cfc12;
C(m,m)=cfc11;
C(m,2*m-1)=cfc22;
C(m,2*m)=cfc21;
C(m,3*m)=cfc31;
%==================================24=====================================
%point on free corner 3
%     |
%     +-----
%k=(i-1)*m+j=m*(n-1)+1; for j=1, i=n
C(m*(n-1)+1,m*(n-1)+1-2*m)=cfc31;
C(m*(n-1)+1,m*(n-1)-m+1)=cfc21;
C(m*(n-1)+1,m*(n-1)-m+2)=cfc22;
C(m*(n-1)+1,m*(n-1)+1)=cfc11;
```

```
C(m*(n-1)+1,m*(n-1)+2)=cfc12;
C(m*(n-1)+1,m*(n-1)+3)=cfc13;
%====================================25====================================
%point on free corner 4
%       |
%     --+
%for j=m i=n k=(n-1)*m+j;
C(m*n,m*n-2*m)=cfc31;
C(m*n,m*n-m-1)=cfc22;
C(m*n,m*n-m)=cfc21;
C(m*n,m*n-2)=cfc13;
C(m*n,m*n-1)=cfc12;
C(m*n,m*n)=cfc11;
%==========================================================================
% SOLVE SYSTEM
% Deflection in m
% Function [W,w]=deflection(C,P)
disp([num2str(round(toc,4)),'       SOLVING THE SYSTEM OF EQUATIONS '])
Wf= -C\(P');
W=full(Wf);
w=zeros(n,m);
for i=1:n
    for j=1:m
        k=(i-1)*m+j;
     w(i,j)=W(k);
    end
end
% Moment about y
MX(1:length(W))=0;
mxbi11=D*2*(1+vp*a^2)/l^2;
mxbi12=-D*(vp*a^2)/l^2;
mxbi21=-D/l^2;

for i=2:n-1
    for j=2:m-1
        k=(i-1)*m+j;
        MX(k)=W(k)*mxbi11+mxbi21*(W(k+1)+W(k-1))+(W(k-m)+W(k+m))*mxbi12;
    end
end
for j=2:m-1
        k=j;
        MX(k)=-D*(1-vp^2)*(W(k-1)-2*W(k)+W(k+1))/l^2;
end
for j=2:m-1
        k=(n-1)*m+j;
        MX(k)=-D*(1-vp^2)*(W(k-1)-2*W(k)+W(k+1))/l^2;
end
mx(:,:)=0;
for i=1:n
    for j=1:m
        k=(i-1)*m+j;
       mx(i,j)=MX(k);
    end
end
%==========================================================================
% Moment about x
MY(1:length(W))=0;
```

```
mybi11=D*(2*a^2+2*vp)/(l^2);
mybi12=-D*(a^2)/l^2;
mybi21=-D*vp/l^2;
for i=2:n-1
    for j=2:m-1
        k=(i-1)*m+j;
        MY(k)=W(k)*mybi11+(W(k+1)+W(k-1))*mybi21+(W(k+m)+W(k-m))*mybi12;
    end
end
for i=2:n-1
        k=(i-1)*m+1;
        MY(k)=-D*(1-vp^2)*a^2*(W(k-m)-2*W(k)+W(k+m))/l^2;
end
for i=2:n-1
        k=(i-1)*m+m;
        MY(k)=-D*(1-vp^2)*a^2*(W(k-m)-2*W(k)+W(k+m))/l^2;
end
my(:,:)=0;
for i=1:n
    for j=1:m
        k=(i-1)*m+j;
     my(i,j)=MY(k);
    end
end
%=====================================================================
% Moment in the xy
MXY(1:length(W))=0;
mxybi1=D*(1-vp)*a/(4*l^2);
mxybi12=-D*(1-vp)*a/(4*l^2);

for i=2:n-1
    for j=2:m-1
        k=(i-1)*m+j;
        MXY(k)=(W(k-m-1)+W(k+m+1)-(W(k-m+1)+W(k+m-1)))*mxybi1;
    end
end
mxybe12=D*(1-vp)*2*a*(1+vp*a^2)/(4*l^2);
mxybe13=D*(1-vp)*vp*a^3/(4*l^2);
mxybe21=D*(1-vp)*2*a/(4*l^2);
for i=3:n-2
        k=(i-1)*m+1;
        MXY(k)=mxybe12*(W(k-m)-W(k+m))+mxybe13*(-W(k-2*m)+W(k+2*m))...
            +mxybe21*(-W(k-m+1)+W(k+m+1));
end
for i=3:n-2
        k=(i-1)*m+m;
        MXY(k)=mxybe12*(-W(k-m)+W(k+m))+mxybe13*(W(k-2*m)-W(k+2*m))...
            +mxybe21*(W(k-m-1)-W(k+m-1));
end
mxybe211=D*(1-vp)*2*(a^2+vp)/(4*a*l^2);
mxybe311=D*(1-vp)*vp/(4*a*l^2);
mxybe122=D*(1-vp)*2*a^2/(4*a*l^2);
for j=3:m-2
        k=j;
        MXY(k)=mxybe211*(W(k-1)-W(k+1))+mxybe311*(-W(k-2)+W(k+2))...
            +mxybe122*(-W(k+m-1)+W(k+m+1));
end
```

```
for j=3:m-2 %i=n
    k=(n-1)*m+j;
 MXY(k)=mxybe211*(-W(k-1)+W(k+1))+mxybe311*(W(k-2)-W(k+2))...
     +mxybe122*(W(k-m-1)-W(k-m+1));
end
%k=(i-1)*m+j=2; i=1,j=2
MXY(2)=-mxybe211*W(3)+mxybe311*(W(2)+W(4))+mxybe122*(-W(m+1)+W(m+3)+W(1));
%k=(i-1)*m+j=m-1; i=1 j=m-1
MXY(m-1)=mxybe211*W(m-2)-mxybe311*(W(m-1)+W(m-3))+...
    mxybe122*(-W(2*m-2)+W(2*m)-W(m));
%k=(i-1)*m+j=(n-1)*m+2; i=n,j=2
MXY((n-1)*m+2)=mxybe211*W((n-1)*m+3)+mxybe311*(-W((n-1)*m+2)-...
    W((n-1)*m+4))+mxybe122*(W((n-1)*m-m+1)-W((n-1)*m-m+3)-W((n-1)*m+1));
for i=n
    for j=m-1
        k=(i-1)*m+j;
        MXY(k)=-mxybe211*W(k-1)+mxybe311*(W(k)+W(k-2))...
            +mxybe122*(W(k-m-1)-W(k-m+1)+W(k+1));
    end
end
 % k=(i-1)*m+j=m+1;for i=2 for j=1
MXY(m+1)=-mxybe12*W(2*m+1)+mxybe13*(W(m+1)+W(1+3*m))+...
    mxybe21*(-W(2)+W(2*m+2)+W(1));
for i=2
    for j=m
        k=(i-1)*m+j;
        MXY(k)=mxybe12*W(k+m)+mxybe13*(-W(k)-W(k+2*m))...
            +mxybe21*(W(k-m-1)-W(k+m-1)-W(k-m));
    end
end
for i=n-1
    for j=1
        k=(i-1)*m+j;
       MXY(k)=mxybe12*W(k-m)+mxybe13*(-W(k)-W(k-2*m))+...
           mxybe21*(-W(k-m+1)+W(k+m+1)-W(k+m));
    end
end
for i=n-1
    for j=m
        k=(i-1)*m+j;
        MXY(k)=-mxybe12*W(k-m)+mxybe13*(W(k)+W(k-2*m))+...
            mxybe21*(W(k-m-1)-W(k+m-1)+W(k+m));
    end
end

mxy(:,:)=0;
for i=1:n
    for j=1:m
        k=(i-1)*m+j;
     mxy(i,j)=MXY(k);
    end
end
%==========================================================================
% Shear in the x
VX(1:length(W))=0;

vxi12=-D*(2+2*a^2+Gpp)/(2*l^3);
```

```
vxi13=-D/(2*l^3);
vxi21=-D*a^2/(2*l^3);

for j=3:m-2
    for i=2:n-1
        k=(i-1)*m+j;
  VX(k)=(-W(k+1)+W(k-1))*vxi12+(W(k+2)-W(k-2))*vxi13...
      +(W(k-m+1)+W(k+m+1)-W(k+m-1)-W(k-m-1))*vxi21;
    end
end
for j=3:m-2  %i=1
     k=j;
     VX(k)=-D*(-W(k-2)*(1-vp)+(2*(1-vp)+Gpp)*W(k-1)...
         -(2*(1-vp)+Gpp)*W(k+1)+W(k+2)*(1-vp))/(2*l^3);
end
for j=3:m-2 %i=n
    k=(n-1)*m+j;
    VX(k)=-D*(-W(k-2)*(1-vp)+(2*(1-vp)+Gpp)*W(k-1)...
        -(2*(1-vp)+Gpp)*W(k+1)+W(k+2)*(1-vp))/(2*l^3);
end
%i=1,j=2 % k=2
VX(2)=-D*((W(1)-W(3))*Gpp+(W(2)+W(4)-2*W(3))*(1-vp))/(2*l^3);
%i=1,j=m-1,k=m-1
VX(m-1)=-D*((-W(m)+W(m-2))*Gpp-(W(m-1)+W(m-3)-2*W(m-2))*(1-vp))/(2*l^3);
 %i=n ,j=2 k=(n-1)*m+2;
VX((n-1)*m+2)=-D*((W((n-1)*m+1)-W((n-1)*m+3))*Gpp+...
    (W((n-1)*m+2)+W((n-1)*m+4)-2*W((n-1)*m+3))*(1-vp))/(2*l^3);
%i=n,j=m-1  k=(n-1)*m+m-1
VX(n*m-1)=-D*((-W(n*m)+W(n*m-2))*Gpp-(W(n*m-1)+W(n*m-3)-...
    2*W(n*m-2))*(1-vp))/(2*l^3);
for i=2:n-1 %j=2
        k=(i-1)*m+2;
  VX(k)=-W(k-1)*(2*(1-vp)*a^2+Gpp)*D/(2*l^3)-W(k+1)*vxi12+(W(k+2)+...
      W(k))*vxi13+(W(k-m+1)+W(k+m+1)+(-W(k+m-1)-W(k-m-1))*(1-vp))*vxi21;
end
    for i=2:n-1 %j=m-1
        k=(i-1)*m+m-1;
     VX(k)=-W(k+1)*(-2*(1-vp)*a^2-Gpp)*D/(2*l^3)+W(k-1)*vxi12+(-W(k-2)-...
         W(k))*vxi13+(-W(k-m-1)-W(k+m-1)+(W(k+m+1)+W(k-m+1))*(1-vp))*vxi21;
    end
vxsh11=Gp*(1+vp*a^2)/(l)+sqrt(kp*Gp);
vxsh12=-vp*a^2*Gp/(2*l);
vxsh21=-Gp/l;
for i=2:n-1 %j=1
    k=(i-1)*m+1;
    VX(k)=(vxsh11*W(k)+vxsh12*(W(k-m)+W(k+m))+vxsh21*W(k+1));
end
for i=2:n-1 %j=m
    k=(i-1)*m+m;
    VX(k)=-(vxsh11*W(k)+vxsh12*(W(k-m)+W(k+m))+vxsh21*W(k-1));
end
VX(1)=-Gp*(-W(1)+W(2))/l+((kp*Gp)^0.5)*W(1);
VX(m)=Gp*(W(m)-W(m-1))/l+W(m)*(kp*Gp)^0.5;
VX((n-1)*m+1)=-Gp*(-W((n-1)*m+1)+W((n-1)*m+2))/(l)+...
    W((n-1)*m+1)*(kp*Gp)^0.5;
VX(n*m)=Gp*(W(n*m)-W(n*m-1))/l+W(n*m)*(kp*Gp)^0.5;
vx(:,:)=0;
```

```
for i=1:n
    for j=1:m
        k=(i-1)*m+j;
     vx(i,j)=VX(k);
    end
end
%==========================================================================
% Shear in the y
VY(1:length(W))=0;
vyi12=-D*a*(2+2*a^2+Gpp)/(2*l^3);
vyi13=-D*a^3/(2*l^3);
vyi21=-D*a/(2*l^3);
for j=2:m-1
    for i=3:n-2
  k=(i-1)*m+j;
  VY(k)=(-W(k+m)+W(k-m))*vyi12+(W(k+2*m)-W(k-2*m))*vyi13...
      +(-W(k-m+1)+W(k+1+m)+W(k+m-1)-W(k-m-1))*vyi21;
    end
end

for i=3:n-2 %for j=1
 k=(i-1)*m+1;
VY(k)=-D*a^3*(1-vp)*(-W(k-2*m)+(Gpp/(1-vp)+2)*W(k-m)-...
    (Gpp/(1-vp)+2)*W(k+m)+W(k+2*m))/(2*l^3);
end

for i=3:n-2  %for j=m
 k=(i-1)*m+m;
 VY(k)=-D*(1-vp)*a^3*(-W(k-2*m)+(Gpp/(1-vp)+2)*W(k-m)-...
     (Gpp/(1-vp)+2)*W(k+m)+W(k+2*m))/(2*l^3);
end
%k=m+1; for i=2,j=1
VY(m+1)=-D*(1-vp)*a^3*(-2*W(2*m+1)+W(m+1)+W(3*m+1)...
    +Gpp/((1-vp)*a^2)*(W(1)-W(2*m+1)))/(2*l^3);
% k=(n-2)*m+1 for i=n-1 j=1
VY((n-2)*m+1)=-D*(1-vp)*a^3*(-W((n-2)*m+1-2*m)-W((n-2)*m+1)...
  +2*W((n-2)*m+1-m)+Gpp/((1-vp)*a^2)*(W((n-3)*m+1)-W((n-1)*m+1)))/(2*l^3);
% k=2m; for i=2 j=m
VY(2*m)=-D*(1-vp)*a^3*(-2*W(3*m)+W(2*m)+W(4*m)...
    +Gpp/((1-vp)*a^2)*(W(m)-W(3*m)))/(2*l^3);
%k=(n-2)*m+m; for i=n-1, j=m
VY((n-2)*m+m)=-D*(1-vp)*a^3*(2*W((n-2)*m)-W((n-2)*m+m)-W((n-2)*m-m)...
    +Gpp/((1-vp)*a^2)*(W((n-2)*m)-W(n*m)))/(2*l^3);

for j=2:m-1 %for i=2
        k=m+j;
  VY(k)=-W(k-m)*(2*(1-vp)+Gpp)*a*D/(2*l^3)-W(k+m)*vyi12+(W(k+2*m)+...
      W(k))*vyi13+(W(k+m-1)+W(k+1+m)+(-W(k-m-1)-W(k-m+1))*(1-vp))*vyi21;
end

for j=2:m-1  %for i=n-1
   k=(n-2)*m+j;
VY(k)=W(k+m)*(2*(1-vp)+Gpp)*a*D/(2*l^3)+W(k-m)*vyi12+(-W(k-2*m)...
    -W(k))*vyi13+(-W(k-m+1)-W(k-m-1)+(W(k+m-1)+W(k+m+1))*(1-vp))*vyi21;
end
vysh11=Gp*a*(a^2+vp)/(l*a^2)+sqrt(kp*Gp);
```

```
vysh12=-vp*a*Gp/(2*l*a^2);
vysh21=-2*a*Gp/(2*l);
for j=2:m-1 %i=1
    k=j;
    VY(k)=vysh11*W(k)+vysh12*(W(k-1)+W(k+1))+vysh21*W(k+m);
end
for j=2:m-1 %i=n
    k=(n-1)*m+j;
    VY(k)=-(vysh11*W(k)+vysh12*(W(k-1)+W(k+1))+vysh21*W(k-m));
end
VY(1)=2*Gp*a*(W(1)-W(m+1))/(2*l)+((kp*Gp)^0.5)*W(1);
VY(m)=2*Gp*a*(W(m)-W(2*m))/(2*l)+((kp*Gp)^0.5)*W(m);
VY((n-1)*m+1)=-2*Gp*a*(W((n-1)*m+1)-W((n-1)*m+1-m))/(2*l)...
    +((kp*Gp)^0.5)*W((n-1)*m+1);
VY(n*m)=-2*a*Gp*(W(n*m)-W((n-1)*m))/(2*l)+((kp*Gp)^0.5)*W(m*n);
vy(:,:)=0;
for i=1:n
    for j=1:m
        k=(i-1)*m+j;
     vy(i,j)=VY(k);
    end
end
%============================================================================
% Contact pressure
q(1:length(W))=0;
for i=2:n-1
for j=2:m-1
    k=(i-1)*m+j;
    q(k)=(-Gp/l^2)*(W(k-1)+W(k+1))-Gp*a^2/l^2*(W(k-m)+W(k+m))+...
        (kp+2*(1+a^2)*Gp/l^2)*W(k);
end
end
for j=2:m-1  %for i=1
    k=j;
   q(k)=(Gp*(vp-1)/l^2)*W(k-1)+(kp-2*(vp-1)*Gp/l^2)*W(k)+...
       (Gp*(vp-1)/l^2)*W(k+1);
end
for j=2:m-1 %for i=n
    k=(n-1)*m+j;
    q(k)=(Gp*(vp-1)/l^2)*W(k-1)+(kp-2*(vp-1)*Gp/l^2)*W(k)+...
        (Gp*(vp-1)/l^2)*W(k+1);
end
for i=2:n-1 %for j=1
    k=(i-1)*m+1;
    q(k)=a^2*((Gp*(vp-1)/l^2)*W(k-m)+(kp/a^2-2*(vp-1)*Gp/l^2)*W(k)+...
        (Gp*(vp-1)/l^2)*W(k+m));
end
for i=2:n-1 %for j=m
    k=(i-1)*m+m;
    q(k)=a^2*((Gp*(vp-1)/l^2)*W(k-m)+(kp/a^2-2*(vp-1)*Gp/l^2)*W(k)+...
        (Gp*(vp-1)/l^2)*W(k+m));
end
q(1)=kp*W(1);%k=(i-1)*m+j=1; for j=1,i=1
q((n-1)*m+1)=kp*W((n-1)*m+1);%k=(n-1)*m+1; for j=1,i=n
q(m)=kp*W(m);%k=(i-1)*m+j=m; for j=m,i=1
q((n-1)*m+m)=kp*W((n-1)*m+m);%k=(n-1)*m+m;j=m,i=n
qq(:,:)=0;
```

```
for i=1:n
    for j=1:m
        k=(i-1)*m+j;
     qq(i,j)=q(k);
    end
end
%==========================================================================
%***                  P O S T - P R O C E S S I N G                      **
%==========================================================================
%plots
%  -------W------
disp([num2str(round(toc,4)),'       POST-PROCESSING'])
if plott==1
cont=20;
ele_vecx=1:m;
ele_vecy=1:n;
X_true=(ele_vecx-1)*dx;
Y_true=(ele_vecy-1)*dy;
figure(1)
[Gx1, Gy1]=meshgrid(X_true,Y_true);
if p2D_3D==1
surfc(Gx1,Gy1, w)
else
pcolor(X_true,Y_true,w)
shading interp
end
clm = jet(15);
clm = flipud(clm);
colormap(clm);
colorbar
axis('normal')
title('Deflection(m)')%title of the plot
ylabel('Width(m)')
xlabel('Length(m)')
grid on
%         ----Mx---
figure(2)
[Gx2, Gy2]=meshgrid(X_true,Y_true);
if p2D_3D==1
surfc(Gx2,Gy2, mx)
else
pcolor(X_true,Y_true,mx)
shading interp
end
clm = jet(20);
clm = flipud(clm);
colormap(clm);
colorbar
axis('normal')
title('Mx(kNm/m)')%title of the plot
grid on
ylabel('Width(m)')
xlabel('Length(m)')
%      ------My----
figure(3)
[Gx3, Gy3]=meshgrid(X_true,Y_true);
if p2D_3D==1
```

```
surfc(Gx3,Gy3, my)
else
pcolor(X_true,Y_true,my)
shading interp
end
clm = jet(20);
clm = flipud(clm);
colormap(clm);
colorbar
axis('normal')%title of the plot
title('My(kNm/m)')
grid on
ylabel('Width(m)')
xlabel('Length(m)')
%   -------Mxy--------
figure(4)
[Gx4, Gy4]=meshgrid(X_true,Y_true);
if p2D_3D==1
surfc(Gx4,Gy4, mxy)
else
pcolor(X_true,Y_true,mxy)
shading interp
end
clm = jet(20);
clm = flipud(clm);
colormap(clm);
colorbar
axis('normal')
title('Mxy(kNm/m)')%title of the plot
grid on
ylabel('Width(m)')
xlabel('Length(m)')
%      ----Vx-----
figure(5)
[Gx5, Gy5]=meshgrid(X_true,Y_true);
if p2D_3D==1
surfc(Gx5,Gy5, vx)
else
pcolor(X_true,Y_true,vx)
shading interp
end
clm = jet(20);
clm = flipud(clm);
colormap(clm);
colorbar
title('Vx(kN/m)')%title of the plot
grid on
ylabel('Width(m)')
xlabel('Length(m)')
figure(6)
[Gx6, Gy6]=meshgrid(X_true,Y_true);
if p2D_3D==1
surfc(Gx6,Gy6, vy)
else
pcolor(X_true,Y_true,vy)
shading interp
end
```

```
clm = jet(20);
clm = flipud(clm);
colormap(clm);
colorbar
title('Vy (kN/m)')%title of the plot
grid on
ylabel('Width(m)')
xlabel('Length(m)')

%       ----P(x,y)-----
figure(7)
[Gx7, Gy7]=meshgrid(X_true,Y_true);
if p2D_3D==1
surfc(Gx7,Gy7, qq)
else
pcolor(X_true,Y_true,qq)
shading interp
end
clm = jet(20);
clm = flipud(clm);
colormap(clm);
colorbar
ylabel('Width(m)')
xlabel('Length(m)')
title('Contact Pressure (kN/m2)')%title of the plot
grid on
else
end

disp([num2str(round(toc,4)),'       RUN FINISHED'])
% ********************** E N D O F P R O G R A M  ***********************
disp('************************************************')
disp('***           E N D O F R U N              ***')
disp('************************************************')
%==========================================================================
```